AD-A267 597

...MENTATION PAGE

Form Approved
OMB No. 0704-0188

...AGENCY USE ONLY (Leave blank)	2. REPORT DATE	3. REPORT TYPE AND DATES COVERED
	1 Feb. 93	Final, 1 Nov. 90-31 Jan. 92

4. TITLE AND SUBTITLE
PULSED HYDROGEN FLUORIDE OVERTONE CHEMICAL LASER STUDIES

5. FUNDING NUMBERS
F49620-90-C-0008

6. AUTHOR(S)
W.R. Warren, Jr. and Leo E. Schneider

61102F 2303/A3

7. PERFORMING ORGANIZATION NAME(S) AND ADDRESS(ES)
Pacific Applied Research
6 Crestwind Drive
Rancho Palos Verdes, CA 90274

8. PERFORMING ORGANIZATION REPORT NUMBER
PAR-TM-93-103

9. SPONSORING/MONITORING AGENCY NAME(S) AND ADDRESS(ES)
AFOSR/NC
Bolling AFB
Washington, DC 20332-6448

10. SPONSORING/MONITORING AGENCY REPORT NUMBER

11. SUPPLEMENTARY NOTES

12a. DISTRIBUTION/AVAILABILITY STATEMENT
Approved for public release: distribution is unlimited.

12b. DISTRIBUTION CODE

93-17282

13. ABSTRACT (Maximum 200 words)

An experimental study of HF chemical lasers operating on overtone transitions, OTs, in a photolytically initiated, pulsed laser facility was conducted. The primary objective was to obtain comparisons of the specific energy performance of pulsed HF, chain reaction driven, chemical laser resonators when operating only on fundamental transitions, $\Delta V = 1$, and only on first overtone transitions, $\Delta V = 2$. The initial efforts were the buildup of the experimental test facility with which excellent performance as an FT HF laser was demonstrated. However, attempts to produce OT lasing using λ-variable reflectivity mirror coatings (to promote and suppress, simultaneously, the OT and FT mechanisms) were only marginally successful, even though major facility modifications were made to reduce cavity losses, suppress FT superradiance (ASE), suppress parasitic modes and increase laser pulse duration. Finally, CW OT lasing was demonstrated using the OT optical components in a combustion-driven, blowdown test facility. A specific energy level, $\sigma = 266$ w/gm/sec, was inferred from the measurements.

14. SUBJECT TERMS	15. NUMBER OF PAGES
HF Chemical Lasers, HF Overtone Lasers Pulsed Photolytically Initiated Chemical Lasers	78 16. PRICE CODE

17. SECURITY CLASSIFICATION OF REPORT	18. SECURITY CLASSIFICATION OF THIS PAGE	19. SECURITY CLASSIFICATION OF ABSTRACT	20. LIMITATION OF ABSTRACT
UNCLASSIFIED	UNCLASSIFIED	UNCLASSIFIED	UL

93 8 3 017

DISCLAIMER NOTICE

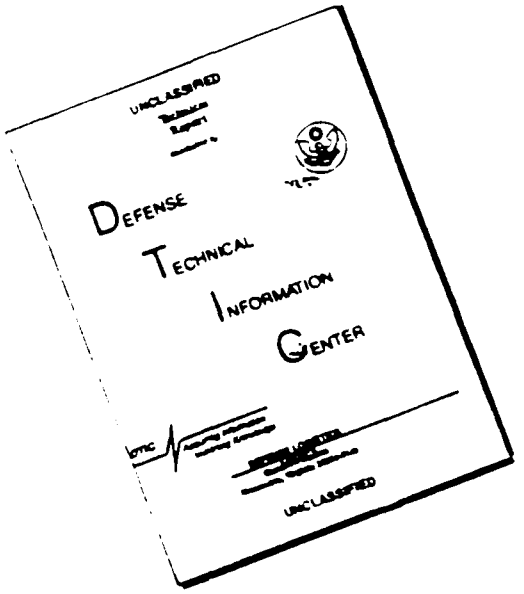

THIS DOCUMENT IS BEST QUALITY AVAILABLE. THE COPY FURNISHED TO DTIC CONTAINED A SIGNIFICANT NUMBER OF PAGES WHICH DO NOT REPRODUCE LEGIBLY.

1. Background

Operation of HF IR chemical lasers on overtone transitions, OTs, between inverted, ground-state vibrational levels has the potential of producing high power laser devices at wavelengths much shorter than now available with single level transitions - fundamental, FTs - operation. Overtone chemical laser devices have been demonstrated several times at the laboratory scale over the past 22 years - see Refs. 1 to 4. However, it was not until the work of Jeffers (Refs. 5 and 6) that the OT laser showed the promise of achieving specific power (mass flow efficiency), σ, levels comparable to that of the FT laser. This is an important property in the context of projected space-based SDI missions, since the brightness potential of systems depends on $A \cdot \sigma \cdot \lambda^{-2}$ (to the first order A = 1; however, system characteristics, such as jitter, will reduce A to somewhat lower values as λ decreases). An important feature of an overtone laser system is that it will allow the use of much of the Alpha Program technology base, hardware, and facility capabilities developed by SDIO for the FT chemical laser. Overtone wavelengths also will allow beam propagation to appreciable depths into the atmosphere which will extend the mission capabilities of a space-based chemical laser and promote ground-based and airborne applications. Current emphasis in the study of the OT laser is on first overtone operation, $\Delta V = 2$; see Ref. 7. Figure 1.a shows the general wavelength regions for fundamental and first and second overtone HF P-branch vibrational transitions; Fig. 1.b gives the numerical values of the transition wavelengths shown in Fig. 1.a.

Current laboratory and scaling studies of the OT mechanism use CW laser devices and are valuable in demonstrating its promise and in studying parts of the mechanism. However, there are complications associated with those test systems. The key property of the OT laser that distinguishes it from the FT laser is the low zero power gain, g_o, levels of its several lasing transitions (factors of 20-30 lower than the useful transitions in the FT laser). Probably the major issue associated with low g_o is the suppression of the FT lasing so that the energy in the inverted HF vibrational

levels can be extracted through the OT mechanism. This has been resolved nicely at the scale used in recent studies - e.g., Refs. 5, 6 and 7 - through the development of resonator mirror coatings with, respectively, very high (> .99) and very low (< .02) reflectivities in the OT and FT wavelength region and through the use of novel optical configurations (e.g., a three-mirror, 4 reflections-per-round-trip resonator which significantly increases the threshold gain for the FT mechanism). However, the suppression of the FT mechanism remains an issue when we consider the development of the large scale devices (up to several meters of gain length) that are of interest to the SDIO. That is, it has to be expected that the residual FT g_os (reduced by OT lasing from their maximum values, but still appreciable) will support a significant superradiant (amplified spontaneous emission, ASE) lasing mechanism at some gain length and this will limit the size of the OT laser resonator - and amplifier - device segments. Fortunately, under this expected limitation, very high power devices still should be feasible through the use of common source MOPA configurations (Ref. 8). However, optimum design should be based on an understanding of this limitation, and current CW experimental studies may not have significant gain length capabilities for its complete study.

A second complication associated with CW laboratory investigation of the OT mechanism is the very complex lasing flow field with strong three-dimensional influences that exists in any type of CW experiment. For example, (1) the small recirculating deactivated (and absorbing) gas flows in the base flow regions in typical supersonic nozzle systems (such as in the Alpha I device) can be expected to have much more significant effects on performance in the low g_o OT mechanism than in the FT mechanism, and (2) the development of an understanding of the new mechanism, its scaling to large device dimensions, and appropriate device modifications will depend on the anchoring of approximate theoretical models of uncertain validity to integrated measurements made through the strongly varying property flows of interest.

A third complication caused by the low g_o OT mechanism is the very high cavity fluxes that are necessary to effectively saturate the laser mechanism. This can be deduced from the information given in Figs. 2 and 3. Shown are approximate power or energy extraction curves for typical high g_o (FT) (Fig. 2) and low g_o (OT) (Fig. 3) mechanisms in stable, two spherical mirror systems. (Also shown in Fig. 2 is the effect on suppression of FT lasing of a 3 mirror/4 reflections per round trip stable cavity modification.) The threshold gain, g_t, expression is given in Fig. 3; the insert shows how the g_o/g_t ratio is related to the power extraction ratio, P/P_o. (Note that the format of Figs. 2 and 3 allows useful comparisons of the two mechanisms but it does not imply that the fully saturated power levels are equal; that is, $P_{oo} \neq P_{of}$. Also, P_{oo} and Pof are proportional to Lg.) Assuming (1) that the absorptivity of the outcoupling element is 0, (2) that the only round trip cavity loss is the power or energy in the main laser beam taken out through one partially transparent mirror, and (3) that an effectively saturated device extracts .9 P_o, the cavity flux Pc for a 75 cm gain length (typical of a "large" CW laboratory experiment) is

$$P_c \approx \frac{P}{1 - R_1R_2} = \frac{P}{1 - 1.0R_2} = \frac{.9P_o}{1 - R_2} \text{ (saturated)}$$

or, at L_g = 75 cm (Fig. 3)

$$\frac{Pc_f}{Po_f} \approx \frac{.9}{1 - R_{2_f}} = \frac{.9}{1 - .667} = 2.70 \qquad \text{FT Laser}$$

$$\frac{Pc_o}{Po_o} \approx \frac{.9}{1 - R_{2_o}} = \frac{.9}{1 - .980} = 45.0 \qquad \text{OT Laser}$$

Therefore,

$$\frac{Pc_o}{Pc_f} \approx \frac{Po_o}{Po_f}\frac{45.0}{2.70} = 16.6\,\frac{Po_o}{Po_f}$$

Thus, we see that if P_{o_o} is an appreciable fraction of P_{o_f} (which it must be for the OT mechanism to be of practical interest), the cavity fluxes required to effectively saturate the OT laser medium

are the order of a factor of 10 higher than for the FT mechanism. For practical power flux levels, this translates into absolute flux values of Pc_o of the order of 100 to a few 100 kilowatts/cm^2. At this point, the development of mirrors with variable reflectivity coatings to survive (and not degrade) in such a severe environment must be assumed (recent experimental results - e.g., Ref. 7 - support this assumption)[1]. The complication that applies to CW testing with limited gain lengths can be seen with the aid of Fig. 3 and the above simple analysis. That is, near-saturation OT operation requires the use of a low transmission outcoupling mirror (e.g., 2% for the L_g = 75 cm example). Thus, if there are unmeasured scattering losses caused by the very high cavity flux, say, of the order of .5% at each mirror surface, the deduced saturation power would be compromised by an uncertainty factor of the order of 50%. However, if the gain length of the experiment were 2 m, the same 1% total scattering loss would result in a Po_o uncertainty factor of only 20% since the outcoupling fraction can be 5% to give the same 90% saturated power level.

The above discussions lead to the thrust of our study: the investigation of the OT mechanism in a pulsed HF Laser device. Our intent was not to work toward the development of pulsed chemical laser systems to replace CW systems for SDI applications but rather to use laboratory scale pulsed experimental techniques that, along with CW studies, would develop a technical base sufficient to support decisions on the future development of large scale OT CW laser devices.

The pulsed approach was seen to have several advantages when the complications of CW experimentation were considered. First, the large maximum gain length of the pulsed medium (up to 4 m) allows the study of the length limit of a single segment caused by superradiance of the FT mechanism. Second, the high cavity fluxes

[1] The same comment applies to grating techniques that might be used to provide the high and low effective reflectivity properties needed to allow the OT mechanism and to suppress FT operation.

needed to saturate the OT mechanism can be obtained primarily by large uninterrupted medium gain lengths and less by small outcoupling fractions or by folding techniques. Thus, the (uncertain) scattering losses from cavity mirrors will be a smaller fraction of the outcoupling fraction which allows a more accurate determination of the maximum extractable power from the OT mechanism than can be achieved in a typical CW experiment. The difference between the outcoupling fraction (or $1-R_2$ values) needed to extract .9 P_o from a typical CW experiment (75 cm) and from a typical pulsed experiment (2 to 4 m) is shown in Fig. 3. Third, as a corollary to the last advantage, our pulsed experimental approach can be configured to drive a single pass amplifier segment (no mirrors and, therefore, no mirror scattering losses) with input fluxes from a resonator segment at levels up to the order of several megawatts. This should be sufficient to obtain true measures of the maximum extractable OT laser relative to that of the FT laser and of the input flux required to efficiently saturate the OT lasing mechanism (the latter being an important input for common source MOPA applications). Fourth, the pulsed chemical laser medium essentially results from a one-dimensional (time) constant volume process in a uniform mixture of reactants and diluents. Thus, measurements integrated over long medium lengths accurately describe conditions at all points in the medium, and a relatively simple thermo-chemical, non-equilibrium code can be used to analyze the data. In contrast to a typical CW experimental situation, complex fluid dynamic effects (e.g., mixing, absorbing recirculation regions) that can prevent a true measure of the potential of the OT mechanism relative to the FT mechanism are not present in the pulsed experimental configuration.

One basic way in which the pulsed OT mechanism differs from the OT mechanism in current CW HF devices is that the former operates on the chain reaction chemical system (most of the initial fluorine is in F_2 molecules) and the latter on the cold reaction system (most fluorine in F atoms). Figures 4, 5, 6, 7, and 8 give, respectively, (1) comparison of the two chemical models (simplified), (2) comparison of the initial vibrational levels

pumped by the cold and hot reactions both of which operate in the chain system, (3) kinetic rates for the cold reaction system, (4) kinetic rates for the chain reaction system, and (5) the development with time of total and partial inversions between HF(v) levels in a typical chain process as predicted by a typical thermo-chemical code (rotational equilibrium assumed). This difference in mechanisms at first can be viewed as a weakness in using the results of a pulsed chemical laser study to support conclusions on CW OT performance. However, it actually may be an advantage; consider the following points. First, as seen in Figs. 4 and 8, the chain reaction system deposits much more chemical energy into the lasing process than does the cold reaction process (130 compared to 65 kcals/mole). Second, this energy initially appears largely in higher vibrational states - Figs. 5 and 8. Indeed, HF FT lasing on transitions as high as V = 6 to 5 has been observed in pulsed chain lasers - see Ref. 9, Fig. 9 (from Ref. 10), and Figs. 10, 21 and 22. On the other hand, significant HF FT lasing for cold reaction lasers occurs only on ΔV = 2 to 1 and 1 to 0 transitions: see Fig. 10. Thus, there are more ΔV = 2 OTs available for lasing and many P-branch cascading paths available in the chain reaction system (e.g., $P_{6-4}(5\text{-}6)$, $P_{4-2}(6\text{-}7)$, $P_{2-0}(7\text{-}8)$).

Third, the Einstein A spontaneous emission coefficients for HF (from Ref. 11) are shown in Fig. 11 for the FT and the 1st and 2nd OTs for upper V levels to 7. We see that there are strong rises in A values for both OT cases with respect to the FT A values as V_1 increases. The low power gain coefficient for a lasing transition is proportional to $A \cdot \lambda^3$; therefore, we have plotted this parameter in Fig. 12 normalized by its value for the P20(4) 1st OT transition (essentially a cross-section ratio). Since the latter is one of the strongest OT lasing transitions observed by Jeffers (Refs. 5 and 6), the solid curve for ΔV = 2 illustrates quantitative tendency towards improved OT lasing conditions at V_1 levels available in a chain reaction system, with respect to an already interesting OT laser demonstration. (Shown in Fig. 12 as the dashed lines is the gain-frequency integral which is proportional to the energy extractable for a given transition; a similar behavior is observed.)

Fourth, pulsed chemical lasers typically are operated at high pressure levels (to initial P levels of the order of 1 atm) compared to the P levels of typical CW chemical lasers (the order of 10 torr). Thus, pressure broadening can be expected to influence the operation and improve the performance of pulsed OT chemical lasers. This issue was described in Ref. 14 and will not be further discussed here.

The above 4 reasons tend to favor OT laser operation on the chain reaction compared to the cold reaction. However, there are two chemical kinetic effects that will tend to reduce these advantages. One is the fact that the "partial inversions" (a concept originally defined by Polanyi; Ref. 12) on which all practical chemical lasers operate are smaller for allowed P-branch OT (J+1) transitions (say V2, J5 to V0, J6) than for those of its corresponding FT cascade (V2, J5 to V1, J6 to V0, J7). The second deleterious kinetic effect is the faster collisional deactivation of the higher V level HF molecules produced in the chain reaction mechanism. Fortunately, the V-V transfer mechanisms are very fast and preferentially pump upward in V level because of the anharmonic vibrational energy level structure; this will alleviate to some degree the deactivation effect. These issues also were described in detail in Ref. 14 and will not be further discussed here.

In summary, compared to an $H+F_2$ cold reaction laser which has already demonstrated attractive OT laser performance (Refs. 5, 6 and 7), four effects imply improved OT performance for an H_2+F_2 chain reaction laser; increased reaction energy, higher initial V level excitation, higher A coefficient at higher V levels, and favorable pressure line width/pressure broadening effects on gain. Two negative effects are the reduced population inversions on P(ΔJ=+1) OT transitions and the increased deactivation rates at higher V levels; however, the former exists already at the 1st OT level which has shown good performance and the latter has been shown to have compensating influences at least at the P20 transition level. Therefore, there is a reasonably probability that the chain reaction mechanism will produce improved OT laser

performance from both the gain and available energy points of view. In support of this conclusion we refer to the results of Refs. 2 and 3. While both of those studies used a "cold" reaction oxidizer (F atoms only), their fuels, HBr and H_2S, produced significantly higher heat releases than does the H_2+F reaction. In both cases, 1st OT lasing from the V_f = 4 and V_f = 3 levels was reported. Coupled with the results of Refs. 5 and 6 in which OT lasing only from the V_f = 2 level was observed, this indicates that OT lasing at higher V levels is enhanced by increased reaction energy. Therefore, it is reasonable to conclude that this enhancement would be increased through the use of the H_2+F_2 chain reaction mechanism which has significantly higher heat release than does either of the F+HBr or F+H_2S reaction.

2. Facilities and Equipment

2.1. Pulsed Laser Facility

The pulsed laser facility used in the program is the latest version of the Pacific Applied Research Model 105 Pulsed Chemical Laser System. This facility is comprised of two single-pulse photolytically-initiated laser heads and their support subsystems: see Figs. 13 to 19. Each head has a 2 liter active laser medium volume - d = 5 cm, L = 1 m; it houses the reaction tube, flashlamps, cable ends and other equipment needed to establish, initiate, contain, and exhaust the laser gas chemical charge. The chemical reaction in the gases initially stored in each reaction tube is ignited by an intense (2 to 4 μs) UV photon flux from 4 flash tubes located in the head. The high energy power supply and storage capacitor system with its fail-safe crow-bar switch (safety gap) and the low inductance system that delivers energy to the flashlamps - 4 cables/lamp - for one laser head are shown in Fig. 15. Initiation of the lasing reaction in the two laser heads can be triggered simultaneously (50 ns max jitter) or one trigger can be delayed with respect to the other by an arbitrary amount (50 ns accuracy). The flow control system which delivers pre-mixed, precisely metered laser gas charges to the laser heads at prescribed P levels is comprised of 3 separated gas racks which handle reactants and a flow control console which handles only

diluent and control gases: Fig. 15. The 105 System has high pulse laser energy capabilities: to 80 joules per head in a 1 μsec pulse with multi-line, HF FT lasing. It also can be used to generate high energy laser pulses from other IR chemical and UV excimer mechanisms. In terms of maximum laser pulse energy and power levels and of flexibility (operation on several chemical laser mechanisms and in several optical geometries), the 105 System represents a unique laboratory test capability that was well suited for this program.

A major portion of the first year of our program was spent in the procurement and fabrication of the pulsed laser system and in its installation in our laboratory (Ref. 14). Several of the major components of the laser system installation are shown in Fig. 15. Figure 16 shows how the equipment is positioned in the laboratory; the 105 PCL system interfaces with and uses several of the laboratory subsystems: gas storage racks and barricades, vacuum pump, vacuum dump tank, scrubber, exhaust ducting, reactor/fan exhaust system (on roof). We note with appreciation that several of the laser system components - one laser head, one power and triggering system, the reactant rack system, and the flow control console - have been made available to us on loan as GFE by the Los Alamos National Laboratory.

2.2. Diagnostics and Optical Equipment

Aside from the need for λ discrimination between the OT and FT regions, the resonators components used in our program were relatively simple conceptually. All resonators were stable optical configurations. Beam quality was not an issue; neither were diffraction losses since the simple Fresnel number, N_F, for all resonators used are of the order of 50 or higher. Rather, we were primarily interested in maximizing laser energy and saturation levels in the available gain volumes. Therefore, we used half-symmetric resonator geometries with concave, spherical feedback mirrors (rad.>2 L_{cav}) and planar partially transmitting outcoupling mirrors; the resulting high N_F and large R values give multi-mode operation with good resonator mode volume/gain volume matching.

The primary diagnostics techniques used in the program are shown in Figs. 17 to 19. Figure 17 shows the Scientech calorimeter used to measure the total integrated energy in each laser pulse. It contains a radiation absorbing disc with a flat spectral response from 250 nm to 35 μm and has a 1% maximum radiative energy loss. The sensing elements are a large number of thermo-piles which give the average T level as a function of time at a depth near the front surface of the absorbing body of the sensor; simple analysis relates this T history to the integrated value of the initial energy pulse. Our experience to date indicates that this device can accurately measure total laser energy levels to less than .1 Joule. The integrated spectral content of the laser beam was measured by a Spiricon linear array of pyroelectric detectors attached to the outlet slit of an Acton Research Corp. 275 mm focal length spectrograph; see Fig. 18. Three gratings (blazed at .5, 1.2, and 2.5 μm) are installed in the spectrograph and any one is easily accessed. Thus, this instrument combination can be used over a large spectral range (.3 to almost 4 μm) with a wide wavelength spread at a given central position on the array (e.g., ±.256 μm at 3.0 μm). Figure 19 shows a two-laser-head experimental set-up with the calorimeter and spectroscopic instruments in position.

3. Experimental Results

3.1. Fundamental Transition HF Lasing

Figure 20 shows the layout of the single laser head and instrumentation components used for the facility and instrumentation check-out tests and for the initial study of FT HF lasing. Figure 21 shows the integrated spectral response from a typical run. Lasing is observed on 15 P branch transitions from P_{10} to P_{65}. Approximately 30% of the total laser energy appears in the higher chain-pumped vibrational level transitions: P_{43}, P_{54}, and P_{65}. The effect of initial total pressure level on the spectral content intensity for FT HF lasing is shown in Fig. 22. The relative intensity of the different lasing transitions in each spectra is approximately the same from P_i = 55 to 300 torr. This is consistent with the fact that all important laser pumping and

deactivating kinetic mechanisms are two-body chemical processes and, therefore, scalable in terms of a P x time variable. The molar mixture used for these tests - see Fig. 21 - is typical of high performance operation conditions for this type of laser; Ref. 12. In our system the $F_2/He/O_2$ components are stored in premixed bottles (as delivered from the supplier) in a 30/63/7 ratio. The resulting 4% O_2 content in the test mix (after adding H_2 and SF_6) suppresses the pre-test ("dark") reaction of the F_2 and H_2 after they are mixed in the laser tube and before the flash tubes are energized (15 to 20 seconds). As seen in Fig. 23, the FT HF laser energy data are in good agreement with the results from Ref. 12 where they are comparable.

FT laser pulse intensities and durations were measured using an IR sensor observing the diffuse reflection from interactions of the laser beam with a blackened surface: see Fig. 20. Figure 24.a shows typical intensity results for brief test sequence over a range of initial mix pressure level. The behavior is as expected; that is, with increased P_i, pulse duration decreases (approximately with P_i^{-1}) and pulse intensity increases (approximately with P_i^2) which is consistent with the approximate linear increase of total pulse energy E with P_i seen in Fig. 23. The timing of the laser pulses with respect to the lamp current discharges from the capacitors (sensed by an induction coil installed on one of the cables between the capacitor and the laser head: Figs. 15 and 19) is shown in Fig. 24.b for a range of initial capacitor voltages. Also shown is the lamp current trace for a larger capacitor (6.0 μF compared to 2.8 μF) which was installed late in our program to allow the study of increasing flashlamp duration in the generation of OT lasing pulses. Note that for the same level of initially stored capacitor energy (the 2 upper traces in Fig. 24.b), the discharge current is approximately doubled for the C = 6.0 μF experiment: from 2.6 μs to 5.8 μs. Total calorimeter data are shown in Fig. 25 for several FT lasing runs (Fig. 21 mix) for which the primary variables initial pressure, capacitor charge voltage, and resonator outcoupling fractions were varied over limited ranges. The effect of capacitor voltage can be seen in the two right-hand traces; the output energy is approximately

proportional to $V^{1.5}$. Comparison of the 4 center traces in Fig. 25 shows that the beam energy into the calorimeter is approximately 10% higher for the tests with the 40% outcoupled mirror compared to those with the 20% outcoupled mirror. With the aid of Fig. 3, it can be shown that this result corresponds to about a 10% round-trip cavity loss in addition to the desired window transmission "loss." This additional loss most likely is caused by the four passes per round trip through the two CaF_2 windows in the cavity which separate the externally mounted resonator mirrors from the laser medium in the initial test configuration (Fig. 20).

Blackened paper samples were used to interact with the main laser beam. The primary purpose here is to indicate when the cavity mirrors and the medium are sufficiently well aligned to give maximum laser energy output in a uniform energy intensity beam. The burn paper technique was very satisfactory for our purposes; no more than three alignment tests were required when cavity components were changed to produce a uniform and repeatable output beam. It also provides interesting qualitative diagnostic results from taking open shutter photographs of the blow-off phenomena caused by the laser beam interactions with the target surfaces. Typical burn paper results are described in Ref. 13.

The results of the initial FT laser test series were satisfactory; they can be summarized as follows: (1) high reliability of the test operations (less than 5% of the test attempts either failed to fire or demonstrated appreciable pre-reaction effects), (2) ease of operation (when necessary, a down-time of less than 2 minutes between tests could be achieved), (3) good repeatability of test results, (4) good quality of the data produced by the diagnostic techniques, and (5) demonstration of expected performance levels (specifically in terms of energy level/pulse, spectral content, and pulse durations as functions of key input test parameters).

3.2. Overtone Transition HF Lasing

3.2.1. Overtone Lasing Test Equipment and Variables

The initial test configuration used for the study of HF overtone, OT, lasing is shown in Fig. 26. It comprised a 2-mirror resonator with its feedback mirror and outcoupling mirror/window easily accessible on an optical table and external to the gain medium; that is, the gain medium (which is produced by a very fast exothermic reaction and is, in effect, a controlled explosion) was confined in the laser head by AR coated CaF_2 windows in the same manner as it was confined for the FT lasing experiments: Fig. 20.

The mirrors and outcoupling mirror/windows used in the OT laser experiments are described in Fig. 27 along with the other optical components procured for the study. The nominal reflectivity levels in FT and OT wavelength regions are given in the COATINGS column. Six outcoupling elements at four outcoupling levels (1-R) - .01, .02, .05, .10 - were available for the 1st OT region: RO-2, RO-7, RO-6, RO-5. The R/λ properties of the .02 (nominal) outcoupler, RO-7, as provided to us by the manufacturer, are shown in Fig. 28. As discussed earlier, the multi-layered reflective coatings of the resonator components (designed by the manufacturer to our specifications: maximum and minimum R in the 1st OT and FT wavelength regions, respectively) were intended to promote OT lasing and suppress FT lasing: see Figs. 2 and 3. Fig. 29 shows the R/λ properties for a resonator feedback mirror in the 2nd OT region; note that the reflectivity has been minimized in both the 1st OT and the FT regions (λ = 1.35 μm and λ = 2.7-3.0 μm).

With a few exceptions, the optical element coatings were of good quality when procured and retained their integrity over the duration of the study; a few resonator components (for FT and OT lasing) were used in several hundred test operations and displayed no degradation (visible inspection and lasing performance, when available). One exception was the steady removal over a relatively few tests of the anti-reflection, AR, coatings on the sides of the CaF_2 laser head windows (LF-1, LO-1 in Fig. 27) exposed to the laser medium; presumably, this coating "erosion" was caused by

exposure to the corrosive laser product HF. This had a significant influence on our OT studies; that is, a cavity round-trip loss of .08 to .10 (.02 to .025 per pass through a reflective window surface), in addition to the other cavity losses and outcoupling fraction, would drastically reduce (and possibly prevent) OT lasing from our 1 m gain length medium: see Fig. 3. Thus, as will be discussed, it was necessary to modify our facility to eliminate the inner resonator windows. Evidence that the resonator windows inner AR coatings had degraded and introduced significant cavity losses was seen in the FT laser results for different outcoupling fractions as discussed earlier with respect to Fig. 25. The other two optical element problems involved only FT wavelength coatings. First, the copper feedback mirrors with high reflectivity coatings, RF-1, (Fig. 27) were received from the manufacturer with partially separated coatings; they had to be returned for grinding and recoating which caused a delay in the program. Second, the coating on FT outcoupler, RF-5, exhibited serious "flaking" - Fig. 30 - after exposure to the laser medium for several tests when we installed the windowless cavity; see Figs. 31 and 32. Again, we attribute this to the laser reaction product HF. Fortunately, we were able to improve our test operation procedures - higher He pressure in the mirror enclosure, better slide valve timing - which reduced (eliminated?) the exposure time of the coated surface to the laser medium and essentially eliminated coating degradation during the rest of the study.

It will be seen in the following discussions that it was difficult to produce a significant level of HF OT lasing using the laser hardware that has performed so well as an HF FT laser. Therefore, several equipment modifications were made in attempts to promote OT lasing and suppress FT lasing; see Fig. 31. The upper sketch shows the initial 2-external-mirror resonator system described in Fig. 26. The first modification was the use of a 3-mirror resonator which adds an additional 2 mirror reflections per cavity round trip; the primary purpose here is to suppress FT lasing as shown in Fig. 2. The second modification, the windowless resonator, was necessitated by the AR coating degradation on the inner

surfaces of the laser heads which added a cavity loss that may have been large enough to suppress OT lasing in the resonators with windows. Photos of the windowless cavity hardware are shown in Fig. 32. Key features of the design are: (1) the feedback mirror and the outcoupling mirror/window support the pressure difference between the laser medium and laboratory ambient conditions; their coated inner surfaces define the resonator properties. The laser head is evacuated between tests and pressurized (usually to P > 1 atm) during the reaction process in a test operation. The mirror holders are designed to seal the laser head against these P extremes and to allow the fine, 2-axis, positioning adjustments necessary to align the cavity; they must have the structural integrity and rigidity to maintain their relative position after alignment during the slow (laser head charging) and fast (reaction) P changes that occur in a test operation. The windowless resonator must also protect the mirror coatings from the corrosive effects of the laser medium gases. This is done by using helium-filled chambers at each end of the resonator (Figs. 31 and 32). These chambers are isolated from the gain region by gate valves that block the resonator cross-section at the two .75" diam. area constrictions. In a test operation, which starts with the laser head and mirror chambers at vacuum, the chambers are filled with He (through a separate charging line) to the Pi level for that experiment, the head is filled to Pi with laser reactants (using the charging procedures previously described; see Fig. 13); the gate valves are opened by a remote command from the central console to the solenoid actuator on each valve, which establishes the windowless geometry between the resonator mirrors, and the flashlamps are fired, which triggers the reaction process in the head. The gate valves are opened less than a second before reaction initiation so that there is a negligible amount of mixing between the reactants and the chamber He before the reaction starts. The P rise during the reaction (the order of a factor of 5 for the different mixes studied) will start a positive flow of reactants into the window chambers (and transmit a weak compression wave through the He charge); however, the reactants are prevented from reaching the mirror surfaces in significant concentrations by the exhaust system which opens less than a second after the reaction and quickly evacuates the laser

head and mirror chambers. These considerations (and the need for fast operation of the gate valves) established the cross-sectional area of the constriction sections in the window isolation system design. The constrictions act as apertures in the resonator and significantly reduce the effective gain region volume available in the laser head (by a geometric factor of 7.11); however, the gain length and cavity length are not affected so that the main objectives of the program are not compromised. After solving some development problems (e.g., mirror holder "stiffness" during alignment adjustments, gate valve sealing, event timing to minimize mixing) the windowless mirror isolation system was found to be reliable over the operating ranges of our experiments. We consider that its addition to our program in response to evolving results - its design, development and reliable operation - was a worthwhile accomplishment in that it significantly expanded the capabilities of the 105 pulsed laser test facility.

Two other equipment modifications that we determined to be necessary as the program progressed are shown in the two lower sketches in Fig. 31. First, as discussed in the last paragraph, the windowless cavity modifications reduced the geometric resonator active mode volume of the laser head reaction tube from 2" id to .75" id. Therefore, during lasing a large volume of gain medium exists that is not driven by the primary cavity flux and could support parasitic lasing modes (if appropriate mode geometries exist in the medium enclosing surfaces) and amplified stimulated emission, ASE, (or superradiance) passing through the gain medium at odd angles). Because of the low power gain differences between the HF FT and OT mechanisms, these effects probably are of concern only for FT lasing. The worry is that if parasitic modes and ASE exist they will "steal" energy quanta from the inverted HF(v) population that would otherwise contribute to the OT and FT laser mechanisms in the primary resonator mode volume. We attempted to prevent this by placing apertures at several locations along the gain medium as shown in Fig. 31; photos of two aperture assemblies are shown in Fig. 33. The constrictions in the window isolation chambers acted as two additional apertures. Simple ray tracing analysis suggested that

the only likely parasitic modes (e.g., those with glancing or low angle incidence off the inner surface of the reaction tube) would be intercepted by the apertures. They also would eliminate most of the long length paths starting in the outer gain volumes along which significant ASE fluxes could be generated.

The final major equipment modifications incorporated during the program involved the shortening of the gain length from the nominal 1 m value in the basic 105 PCL system. The intent here is to reduce/eliminate ASE within the primary resonator mode volume. The shortening was done by inserting a ceramic tube (same id as the constriction in the mirror isolation chambers) into the gain region as shown in the bottom sketch of Fig. 31. Two insert lengths were used giving L_g = 26 cm and 50 cm test configurations in addition to the nominal L_g = 1 m configuration. During a test operation, the reactant mixture is present in the inserted tube; however, since the tube wall is opaque, F atoms are not produced and the lasing reaction is not generated inside the tube when the flashlamps are fired. Undoubtedly, the tube gases will react at some later time due to mixing with the products of the irradiated mix. However, a significant mix length inside the tube will not react for at least 10 μs and, by then, the main lasing pulse will have occurred. The shortened gain medium experiments were conducted with apertures distributed along the active region as shown in Fig. 31.

A wide range of laser mixture ratios was investigated in the program. Figure 34 shows how the mixtures were varied with respect to mix 1.1, which generated the high-performance HF FT laser data shown in Figs. 21 to 24. As configured for this study, the 105 PCL system allows the introduction of 3 separately stored gases into the mixing tank in the flow control (laser head charging) system. Gas #1 is the F_2 source; it is received from the supplier in bottles which have been charged (to our specifications) with a 30/7/63 F_2/O_2/He mix; this mix is constant over the total mix range studied. As shown in Fig. 34, 3 variable ranges were studied with several permutations: (1) the H_2 concentration range was increased and decreased with respect to that in mix 1.1; (2) the diluent level (in addition to the He

already in gas #1) was varied over a factor of 3 range at each H_2 level, and (3) the additional diluent specie was changed from SF_6 to He. Our initial intuition was that optimum OT laser performance was most likely to be found with the reactant mix that produced optimum FT lasing: mix 1.1. However, if this was not true, exploratory studies over the mix ranges defined in Fig. 34 should identify the optimum mixture ratio range. Note that mix 2.4 corresponds closely to the mixture ratio used in Ref. 15 in which 1st OT lasing on several HF vibrational levels (up to V = 5) was reported. Presumably the lasing reaction in the Ref. 15 study was initiated by a pulsed electron beam discharge but neither their experimental techniques nor the test data were described in sufficient detail to allow evaluation of the results as presented.

3.2.2 Overtone Lasing Results and Analysis

Examples of data from the upper two test configurations in Fig. 31 are shown in Fig. 35. The left hand spectrograph trace shows the existence of weak, but finite, FT lasing in a 2 mirror resonator, a result which implied either that the λ discriminating mirrors were not completely suppressing FT lasing or that ASE was producing a significant superradiant laser flux in one pass through the gain medium. This first led us to try the 3 mirror test configuration which produced results typified by the center traces in Fig. 35. It is seen that the FT lasing intensity is only reduced a small amount when compared to the 2 mirror result. Then, data typified by the right hand trace in Fig. 35 were taken with an open cavity (one mirror removed). These results - spectra and energy pulse - showed that a significant level of ASE lasing was produced by the lasing medium in its initial configuration. Also, the near-equivalence of the lasing energy in the open and closed cavities implied that FT resonant lasing is well suppressed by the low reflectivity mirrors (for the 3-mirror resonator and probably for the 2-mirror resonator). Note that the ASE flux will be essentially the same from both the open cavity and the resonators because of the high transmissivity of the coatings and the mirror substrate (silicon) at FT wavelengths. At any rate, the measured FT lasing with OT optics in the resonator was at an

energy level of only about 10% of the full FT lasing level available for that medium, which suggested that the OT mechanism might have sufficient gain in which to operate (a caution here is off-axis ASE that isn't captured by the total calorimeter); however, when the spectrograph/detector array system was switched to the OT wavelength region (lower trace) no evidence of OT lasing was found.

On the assumption that the residual FT lasing (optical in the laser system with and without resonator optics) was preventing the establishment of OT lasing, we decided to investigate the addition of gases to the lasing mix that could absorb radiation at FT λs but not at OT λs. The transmission spectra of two candidate additives - CO_2 and NF_3 - which have strong absorption bands in the 2.6 to 3.1 μm wavelength region are shown in Fig. 36. Initial tests in this series were conducted with CO_2 added to mix 1.1 (Fig. 34) according to the relationship shown in Fig. 37 which also presents spectral and pulse energy data with OT mirrors for a series of runs with CO_2 concentrations ranging from a = 0 to a = .154 (.154/1.154 = .133). At a $\approx$ .10, Fig. 38 shows that CO_2 addition also largely eliminates FT lasing when FT resonator optics are installed. However, OT lasing was not observed as FT lasing was suppressed as can be seen in the lower traces in Fig. 37. Therefore, the study of absorbing gas additions to promote OT lasing was stopped.

As discussed earlier, we had observed the deterioration of the AR coating on the inner surfaces (exposed to the lasing reaction products) of the CaF_2 laser head windows after a relatively small number of test operations. Because the round-trip cavity loss introduced by the removal of the AR coating could be large enough to suppress OT lasing, we modified the laser head to have a windowless resonator geometry: Figs. 31 and 32. Typical OT data taken with the windowless configuration are shown in Fig. 39. The left hand trace shows the residual FT lasing spectra generated with OT resonator optics. Note that both the FT lasing energy levels with FT optics and with OT optics are much smaller than they were in the initial OT test series: Fig. 35. This is a result of the smaller resonator mode volume in the windowless

configuration which is defined by the .75" dia. constriction sections in the window enclosures. The FT laser pulse energy levels are larger than they would be if they were reduced directly in proportion to the mode volume reduction; this is to be expected since the inner-cavity window losses have been removed, but it also may be partially a result of parasitic mode lasing and ASE that are fed by the gain regions in the head outside of the geometric mode volume.

The right hand trace in Fig. 39 shows the OT laser spectral region observed for the listed test conditions. Apparently, a weak level of 1st OT lasing was generated in this experiment. This conclusion was reached by comparing the λ values of 8 laser-like pips in the signal trace (determined from interpolation between the end point λs set by the grating/detector array combination used) with the λs for the P-band OT transitions available in the test spectral region. This comparison is shown in the lower part of Fig. 39 where it is seen that the agreement between the measured points and certain allowed transitions is quite good and well within the uncertainty range of the measurements. It is interesting to see that OT lasing was observed between 3 pairs of HF vibrational levels: 2-0, 4-2, 5-3. That is, P_{31}, lasing apparently did not occur (although there is a possibility that the lasing transition identified at $P_{20}(8)$ is really $P_{31}(2)$ because of the closeness of the λs for those two transitions). Note the similarity here with HF FT lasing results; that is, Fig. 21 shows that FT lasing from the V = 3 level is almost negligible. Similarly, the FT lasing from the V = 4 and V = 5 levels includes 6 lines of reasonable intensity; OT lasing was also observed from these levels. An interesting feature of the OT lasing spectra is that 2 cascade processes were observed for 2 pairs of the lasing transitions.

The diagnostic arrangement used in the test series that produced the results shown in Fig. 39 did not allow the separation of FT and OT laser pulse energy levels; that is, the E measurements shown for each run is the total laser pulse energy or the sum of the two lasing mechanisms for that experiment. However, the

relative strength of the FT and OT lasing lines in the spectral traces suggests that no more than 1/3 of the measured total laser pulse energy could be attributed to the OT mechanism. If so, the OT laser energy level is less than 1/10 of the nominal FT lasing energy for the same medium properties (3.9 J as listed in Fig. 39). Thus, while it was interesting that OT lasing had been demonstrated - including lasing transitions, P_{42} and P_{53}, produced by the chain reaction - we concluded that it was necessary to search for experimental conditions that produced OT lasing at a significant fraction (> .25) of the HF FT laser (with FT optics) optimum pulse energy level.

Four directions were followed in attempts to increase the efficiency of OT lasing from the apparently low level seen in Fig. 39. These investigations all used windowless resonator configurations since this approach had been demonstrated to give positive results. First, apertures were distributed through the reaction tube to reduce the possibilities of parasitic mode lasing and ASE driven by the reacted gas gain regions outside of the geometric mode. Second, the gain region was shortened to 50 cm and to 26 cm for the same reasons that the apertures were added. Both of these changes are sketched in Fig. 31 and their designs were described earlier. Third, the 2.8 μF capacitor which provides the discharge energy for the flashlamp in the laser head was replaced by a 6.0 μF capacitor. The objective here was to increase the laser pulse length in case the time required to develop the OT lasing resonator flux was longer than (or competitive with) the duration of inverted conditions in the chemical reaction. Figure 24.b compares capacitor discharge pulses at the two capacitance levels and the same stored energy level. Fourth, concentrations of the laser mix reactants and diluents were varied over the ranges described in the matrix shown in Fig. 34; the general purpose here was to determine whether the optimum chemical mechanism for OT lasing was different than the optimum mechanism for FT lasing; the latter had previously been associated with mix 1.1 in Ref. 12 and in this program. The study of a range of mixes was partially motivated by Ref. 15 where it was reported that optimum OT lasing was achieved with a highly diluted (with He) initial laser charge;

mix 2.4 in Fig. 34 essentially duplicates the optimum lasing mix of Ref. 15.

Several hundred test operations were conducted to study the fixes described in the last paragraph, both by themselves and in combination. Unfortunately, no significant improvement in OT laser performance was demonstrated although several runs demonstrated weak OT lasing spectra of the type shown in Fig. 39. Samples of these results for the short gain region and high capacitance experiments is shown in Fig. 40. Several points can be made. (1) ASE has been largely suppressed at the short L_g = 26 cm for mix 1.1. (2) A very small level of FT lasing was still observed for mix. 1.1 with OT optics in the resonator. It is not clear whether this is caused by ASE or non-suppressed resonant lasing in the 2-mirror cavity, however, because of its low energy level we did not attempt to resolve this issue. (3) No significant OT lasing was observed for mix 1.1. (4) Mix 2.4 give a significantly smaller FT laser energy pulse (FT optics) than mix 1.1. (5) No FT lasing was measured for mix 2.4 with OT resonator optics which is consistent with the lower FT lasing/FT optics result. (6) As with mix 1.1, no significant OT lasing was observed for mix 2.4.

At this point it was not clear why an appreciable level of OT lasing could not be generated in the 105 PCL facility. Several program modifications designed to improve the OT lasing mechanism had been tried - some that required relatively major test equipment changes - and with the exception of the windowless cavity change, none produced positive results. One phenomenon that was still suspect involved the time required to establish a significant OT laser cavity flux after the initiation of the chemical reaction by the flashlamp discharge. The change in capacitor from 2.8 μF to 6.0 μF was an attempt to alleviate this problem; although this change did essentially double the capacitor discharge time and, implicitly, the laser pulse length, it probably also reduced the medium gain level. Thus, the gain reduction may have negated the extended pulse time effect in the generation of OT laser cavity flux. Figure 41 shows a simple analysis that attempts to quantify the OT lasing build-up issue.

It leads to two interesting conjectures: (1) Because of the difference in zero power g_o between the OT and FT mechanisms - assumed to be .001 cm^{-1} and .03 cm^{-1}, respectively - the OT mechanism build-up time (from an initial spontaneous emission flux to a lasing cavity flux is 30-50 times longer than the build-up time for the FT mechanism. (2) For the assumptions that the $g_o(OT)$ = .001 cm^{-1} and that it takes an intensity increase of 10^4 to 10^5 to establish a gain-steady cavity mode, a mode build-up time of about .5 to μs is required. Thus, the analysis is somewhat ambivalent in that it first shows that the OT cavity flux build-up time is much larger than the FT flux build-up time, which suggests that this could be a problem for the OT laser study; however, it also suggests that the absolute time required for OT flux build-up is within the reaction pulse time range available in the experiments (typically several μs). We concluded that these results did not justify additional efforts to increase the pulse times available in the experiments.

4. Discussion of Results

At the completion of the studies (described in the last section) of our modified approaches to the achievement of efficient OT lasing, we had essentially completed our contractual performance period (which included a 3 month, no cost extension) and exhausted our contract and originally-planned, company-funded support. We believe our work produced several positive results that justified its conduction as an SBIR program. These results were in the areas of (1) pulsed chemical laser facility development (reliability, ease and frequency of operation, wide ranges of test variables, repeatability, safety, integrity and durability of components, fast response to component modifications), (2) diagnostics systems development (simple and accurate test operation control; simultaneous measurements of pertinent laser beam properties, sensitivity and dynamic ranges of instrumentation techniques, laser beam interactions with materials, interactive test variable specifications based on most recent measurements), and (3) FT HF laser device performance (high peak pulse energy and instantaneous power performance, wide ranges of laser performance

levels, flashlamp discharge energy and duration). We are exploring new technology areas in which our demonstrated pulsed laser capabilities can be exploited.

Although the results just summarized are significant, we are disappointed that our chain-pumped OT laser results were not carried far enough to contribute to the development of OT lasers for SDIO directed energy applications. Therefore, as a final part of our pulsed HF OT laser program, we decided to conduct a brief study - under company support and using experimental capabilities available in our laboratory - that would add in a meaningful way to the base of knowledge of OT HF laser systems; this work is described in the next section.

5. CW Overtone Transition Lasing in a Steady State Lasing Flow

The Advanced Nozzle Program, ANP, is being conducted under SDIO/DTD support in the PAR combustion-driven, blowdown test facility, BDF, which has been shown to be a flexible, low-cost, high data-rate device capable of operating over wide ranges of flow and geometric (test hardware) variables[16,17,18,19]. Fig. 16 shows the layout of the BDF in our laboratory. The key design concept exploited in the BDF is a short duration test flow (~100 ms). Figure 42 shows combustor pressure and laser intensity histories for a typical test operation; the establishment and duration of steady-state test time is clearly demonstrated by such data. The BDF has two test configurations: 3.3" and 25" wide (gain length). The 3.3" test flow (modified to accommodate up to 6" long nozzle components) has been used in all ANP studies to date.

During the first contract period of the ANP (performance period ending on 15 Oct. 92), investigations were conducted to determine the σ and δ (laser power/total flow rate, laser power/nozzle exit+base area) performance improvements in FT HF lasing resulting from the use of advanced nozzle/injector designs and advanced combustor concepts, individually and in combination. Studies of OT laser performance were not planned (or conducted) in this phase of the ANP. The nozzle concepts studied have been a dual shear

layer lasing flow and the most promising configuration from the HYLTE class of nozzles (multiple jet penetration/mixing), HYLTE-7, developed several years ago at TRW under the SDIO-sponsored Advanced Gain Generator Technology, AGGT, Program[7]. Figure 43 is a sketch of the HYLTE-7 design; also seen in the figure is the bypass combustor concept developed for use in the ANP. Photos of the BDF with the HYLTE-7 nozzle installed are shown in Fig. 44.

Results obtained in the first contract period of the ANP include the demonstration of significant improvements in FT HF lasing performance stemming from the use of an $N_2/F_4/D_2$ combustor instead of an NF_3/D_2 combustor to drive the laser[19].

The second contract performance period of the ANP was not initiated until 1 Feb. 93. Therefore, we decided to conduct a company funded study of CW HF overtone laser performance in the BDF during its unsupported time period (16 Oct. 92 to 30 Jan. 93) using OT resonator equipment (optical components - mirrors, outcouplers - and the windowless resonator system) described earlier as a final contribution to this program. This work was done at test conditions that produced peak σ performance levels for the fundamental transition, FT, HF HYLTE-7 laser with an $N_2/F_4/D_2$ bypass combustor. Two flat, variable reflectivity cavity mirror/window outcouplers (RO-2 and RO-7 with outcoupling fractions of .01 and .02; Fig. 27) and a spherical feedback mirror (RO-1 with a measured reflectivity of .995 - listed at its nominal .99 value in Fig. 27) were used in the OT laser experiments. Figure 45 shows lasing spectra (using the .01 outcoupler) for the A = 1.45 peak HYLTE-7 σ test condition and for a somewhat lower performance A = 1.24 test condition; no fundamental lasing was observed during this test series which indicates that the mirrors were successful in simultaneously supporting OT lasing and suppressing FT lasing and that FT ASE was not generated at significant flux levels.

Laser power data produced by experiments in a relatively small scale facility (such as the BDF is in the HYLTE-7 test configuration) can be strongly influenced by cavity losses;

is, some laser power that could be extracted in a large laser device (with small cavity losses) is not included in the outcoupled (measured) laser power. Also, the short gain media in small-scale facilities generally are not saturated. Therefore, small-scale data must be corrected to infer laser beam power levels for fully-saturated, low cavity loss laser devices. Data from experiments with each outcoupler were combined to construct an OT laser saturation plot for the A = 1.45 test condition: see Fig. 46. The derivation of the correction factor used for cavity losses is given in Fig. 47. The procedure used to scale the corrected points to fully saturated conditions is based on the simple analysis summarized in Fig. 48. The corrected points in Fig. 46 for $L_1 + L_2 = .005$ account only for the loss from the non-transmitting cavity feedback mirror as reported by the supplier; therefore, we believe that their use for construction of a saturation plot is conservative (that is, if there are other losses, higher saturation beam powers will be inferred). As seen in Fig. 46, the average go level of the OT mechanism - approximately .001 cm-1 - is fairly accurately determined by the procedure used. However, because of the low go level, the extrapolation of the measured laser power to its saturated level can have a significant uncertainty range because of the leverage of relatively small errors in the $R_1.R_2$ product. At any rate, the inferred I_{sat} level shown, when combined with the total cavity mass flow rate for these tests, indicates that an approximate $\sigma_{sat} \approx 266$ w/gm/sec has been demonstrated for the HYLTE-7 nozzle when operating as an OT laser at the test conditions giving peak FT HT laser performance. This value is 54% of the $\sigma_{sat} \approx 495$ for the HYLTE-7 nozzle operating as a FT HF laser at the same test conditions[19].

The σ performance levels for both the FT and OT HF lasers are significantly higher than any previously reported for CW HF laser devices. We believe that these results, and the observation that even the present performance level is still of the order of 1/2 the maximum theoretical level for the HF laser chemical process, justify continued study of methods to improve HF laser system flexibility (e.g., FT and OT operation, HF and DF operation) and the system efficiency for laser beam power level. Relative to the

present work, the potential value of CW OT lasing with chain reaction chemical pumping remains an open issue which should be addressed in the near future.

6. References

1. Suchard, S.N. and Pimentel, G.C.; DF Vibrational Overtone Chemical Laser; APL 18, 12 (530); 15 June 71.
2. Hon, J.F. and Novak, J.R.; Chemically Pumped HF Overtone Laser; IEEE JQE QE-11 (698); Aug 75.
3. Bashkin, V.I., et al; An Investigation of a Chemical Laser Emitting Due to an Overtone of the HF Molecule; Sov. JQE 7 (626); May 77.
4. Holleman, G.W. and Injeyan, H.; Multiwavelength 2-5 Micrometer Laser - CW Overtone Laser Demonstration; AFWAL-TR-80-1047 (14); June 80.
5. Jeffers, W.Q.; Scalable Overtone HF Chemical Laser; Patent Applic. 700,123; 11 Feb. 85.
6. Jeffers, W.Q.; Short Wavelength Chemical Laser Technology Development; Final Report - 21 Mar. 86 to 30 Sept. 88; Doc. No. DAAH01-86-C-0440.
7. Duncan, W., Patterson, S., Graves, B., Sollee, J., Yonehara, G., and Deering, J.; Advanced Nozzle Characteristics for Hydrogen Fluoride Overtone Chemical Lasers; Paper No. AIAA-92-2977; AIAA 23rd Plasmadynamics & Laser Conference; Nashville, TN; 6-8 July 1992.
8. Warren, W.R.; The Parallel Internal-Master-Oscillator Power-Amplifier for Phase Matching the Output Beams of Multiline Lasers; TR-0078(9990)-1; The Aerospace Corp.; 16 Feb. 78.
9. Suchard, S.N.; Lasing from the Upper Vibrational Levels of a Flash-Initiated H2-F2 Laser; TR-0074(4531)-1; The Aerospace Corp.; Sept. 74.
10. Hofland, R.; The Aerospace Corp.; Private Communication.
11. Herbelin, J.M. and Emanuel, G.; Einstein Coefficients for Diatomic Molecules; TR-0074(4530)-5; The Aerospace Corp.; 30 Jan. 74.
12. Polanyi, J.C.; Proposal for an Infrared Maser Dependent on Vibrational Excitation; J. Chem. Phys., 34(1), 347-348, 1961.

13. Amimoto, S.T., et al; Polyatomic-Buffered Pulsed DF/HF Laser Compatible with Solid-Reagent Generator and Chemical Pump; TR-0084(4930-01)-3; The Aerospace Corp.; 31 Jan 84.
14. Warren, W.R. and Schneider, L.E.; Pulsed Hydrogen Fluoride Overtone Chemical Laser Studies; Annual Report, 11/1/89-10/31/90; Cont. No. F49620-90-C-0008; PAR-TM-90-109; 1 Nov. 1990.
15. Ashidate, S.; Pulsed HF Overtone Laser; CLEO Conf. on Lasers and Electro-Optics; TR-7871.3-I591; Baltimore, MD; May, 1991.
16. Warren, W.R. and Schneider, L.E.; "New Fluid Dynamic Techniques in Chemical Laser Research;" SPIE Tech. Symp. on High Power Gas Lasers; Los Angeles, CA; 17 Jan. 1990; Published in Proceedings ISBN 0-8194-0266-4, Vol. No. 1225; June 1990.
17. Warren, W.R., Schneider, L.E., and Rodriguez, J.N.; "Combustion-Driven Blowdown Facilities for Chemical Laser Research;" Paper No. AIAA-91-1455; AIAA 22nd Fluid Dynamics, Plasmadynamics & Lasers Conf.; Honolulu, HI; 24-27 June, 1991.
18. Warren, W.R., Schneider, L.E., Howell, J., Warren, D., Herbelin, J.M., and Patterson, S.; "CW Lasing on the BiF[A-X] Mechanism in a Combustion-Driven Blowdown Test Facility;" Paper No. AIAA 93-3210; AIAA 24th Plasmadynamics and Lasers Conf.; Orlando, FL; 6-9 July, 1993.
19. Warren, W.R., Schneider, L.E., and Warren, D.; N_2F_4/D_2 Combustion Drivers for CW HF Lasers; Paper No. AIAA 93-3232; AIAA 24th Plasmadynamics and Lasers Conf.; Orlando, FL; 6-9 July 1993.

POTENTIAL WAVELENGTH DOMAINS FOR HF CHAIN LASER TRANSITIONS

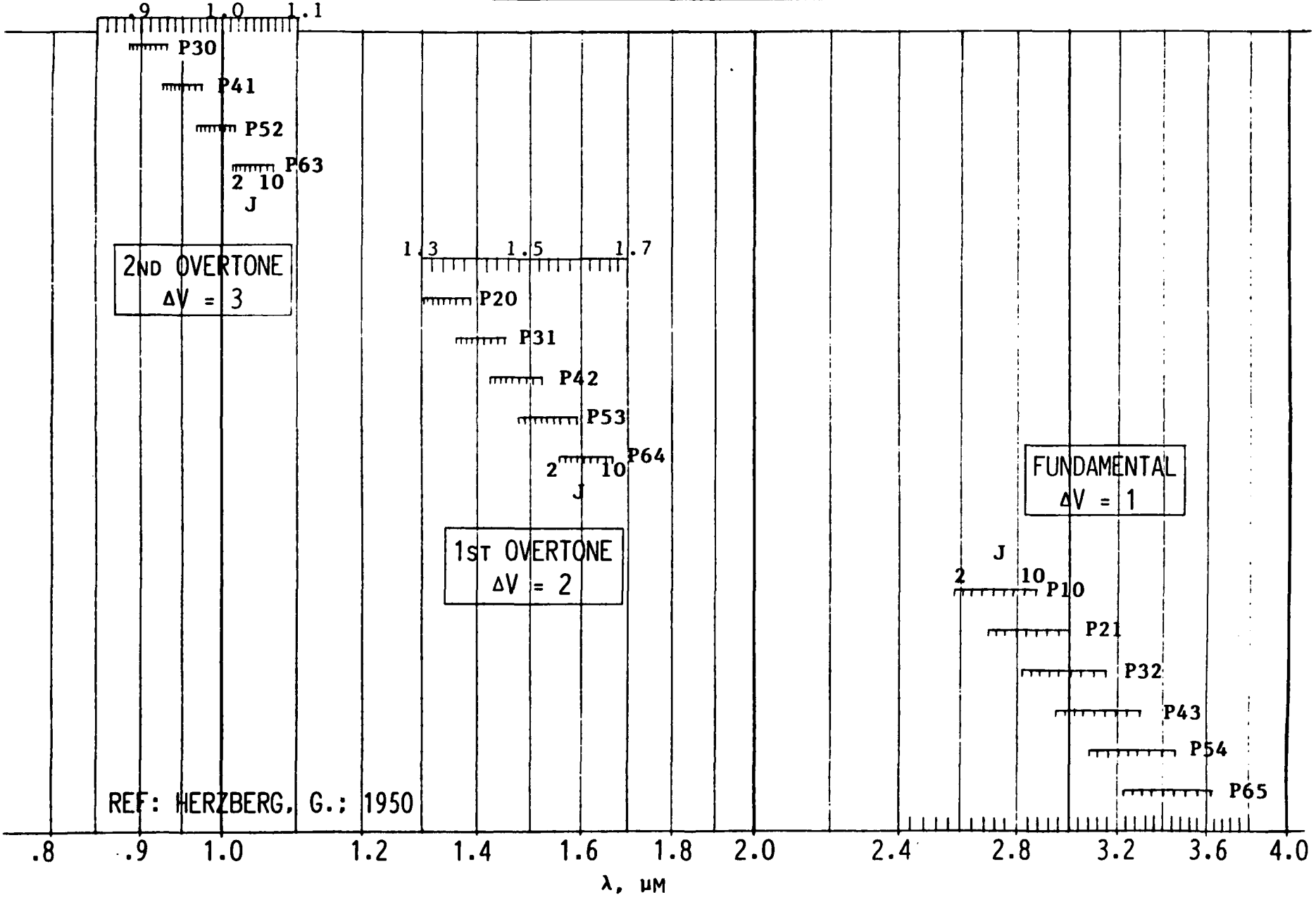

Fig. 1.a

PACIFIC APPLIED RESEARCH

ω_e =	4138.52			HF TRANSITIONS AND CORRESPONDING WAVELENGTH, λ (nm)										
$\omega_e x_e$ =	90.069													
$\omega_e y_e$ =	0.98													
B_e =	20.939													
α_e =	0.77													
γ_e =	0.9171													
Ref: G.Herzberg							J							
Nostrand,1950		v'	v"	1	2	3	4	5	6	7	8	9	10	
	2nd OT	7	4	1056.83	1061.27	1066.27	1071.85	1078.02	1084.81	1092.23	1100.32	1109.10	1118.59	
	1st OT	7	5	1625.43	1635.13	1645.77	1657.41	1670.06	1683.79	1698.63	1714.64	1731.88	1750.41	
	FT	7	6	3344.49	3382.28	3422.74	3466.03	3512.32	3561.82	3614.75	3671.35	3731.89	3796.68	
	3rd OT	6	2	739.24	741.66	744.44	747.59	751.11	755.01	759.31	764.02	769.15	774.72	
	2nd OT	6	3	1009.68	1013.89	1018.61	1023.86	1029.66	1036.01	1042.95	1050.49	1058.66	1067.48	
	1st OT	6	4	1552.70	1561.92	1572.01	1583.01	1594.94	1607.86	1621.79	1636.79	1652.91	1670.21	
	FT	6	5	3194.51	3230.58	3269.11	3310.27	3354.20	3401.10	3451.15	3504.60	3561.68	3622.67	
	3rd OT	5	1	706.60	708.89	711.51	714.46	717.75	721.39	725.40	729.77	734.54	739.70	
	2nd OT	5	2	964.91	968.90	973.36	978.30	983.74	989.69	996.17	1003.20	1010.81	1019.01	
	1st OT	5	3	1483.60	1492.37	1501.92	1512.31	1523.56	1535.70	1548.77	1562.82	1577.90	1594.05	
	FT	5	4	3051.92	3086.29	3122.94	3162.01	3203.65	3248.03	3295.33	3345.74	3399.51	3456.86	
	3rd OT	4	0	675.64	677.81	680.27	683.04	686.12	689.52	693.25	697.32	701.75	706.53	
	2nd OT	4	1	922.45	926.22	930.43	935.08	940.18	945.75	951.81	958.37	965.45	973.07	
	1st OT	4	2	1418.03	1426.34	1435.39	1445.20	1455.79	1467.20	1479.47	1492.63	1506.72	1521.80	
	FT	4	3	2916.50	2949.21	2984.03	3021.09	3060.53	3102.48	3147.13	3194.65	3245.26	3299.16	
	2nd OT	3	0	882.18	885.76	889.72	894.10	898.89	904.10	909.76	915.88	922.48	929.57	
	1st OT	3	1	1355.84	1363.73	1372.29	1381.54	1391.51	1402.24	1413.75	1426.07	1439.25	1453.32	
	FT	3	2	2788.01	2819.11	2852.17	2887.29	2924.60	2964.24	3006.37	3051.14	3098.74	3149.38	
	1st OT	2	0	1296.90	1304.37	1312.46	1321.20	1330.59	1340.67	1351.46	1363.01	1375.33	1388.48	
	FT	2	1	2666.18	2695.73	2727.08	2760.34	2795.63	2833.07	2872.79	2914.95	2959.72	3007.28	
	FT	1	0	2550.72	2578.77	2608.50	2639.99	2673.35	2708.69	2746.14	2785.84	2827.93	2872.58	

Fig. 1.b FUNDAMENTAL AND OT P-BRANCH TRANSITIONS IN GROUND STATE HF

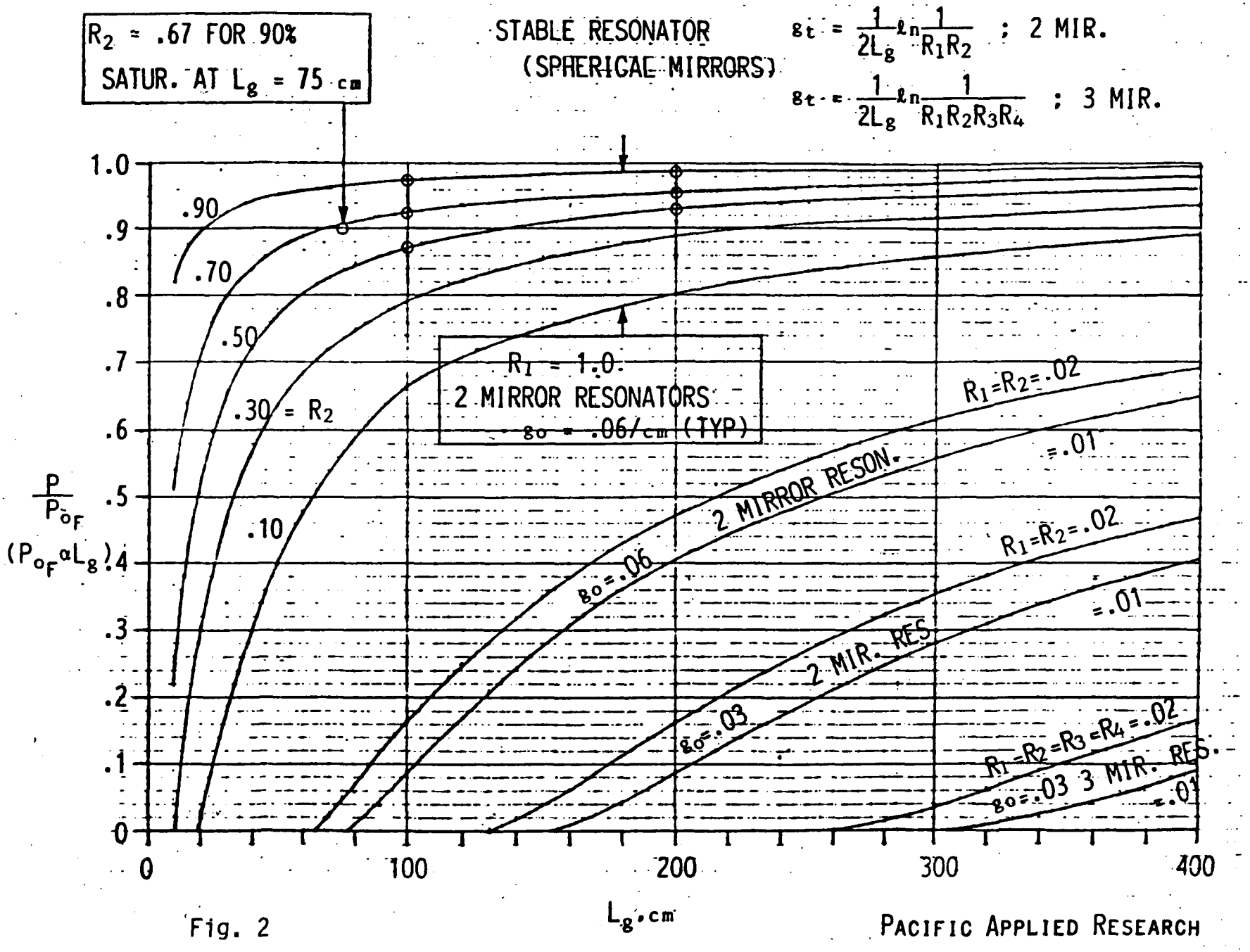

Fig. 2

PACIFIC APPLIED RESEARCH

HF CHEMICAL LASER/OVERTONE TRANSITIONS, $\Delta v = 2$

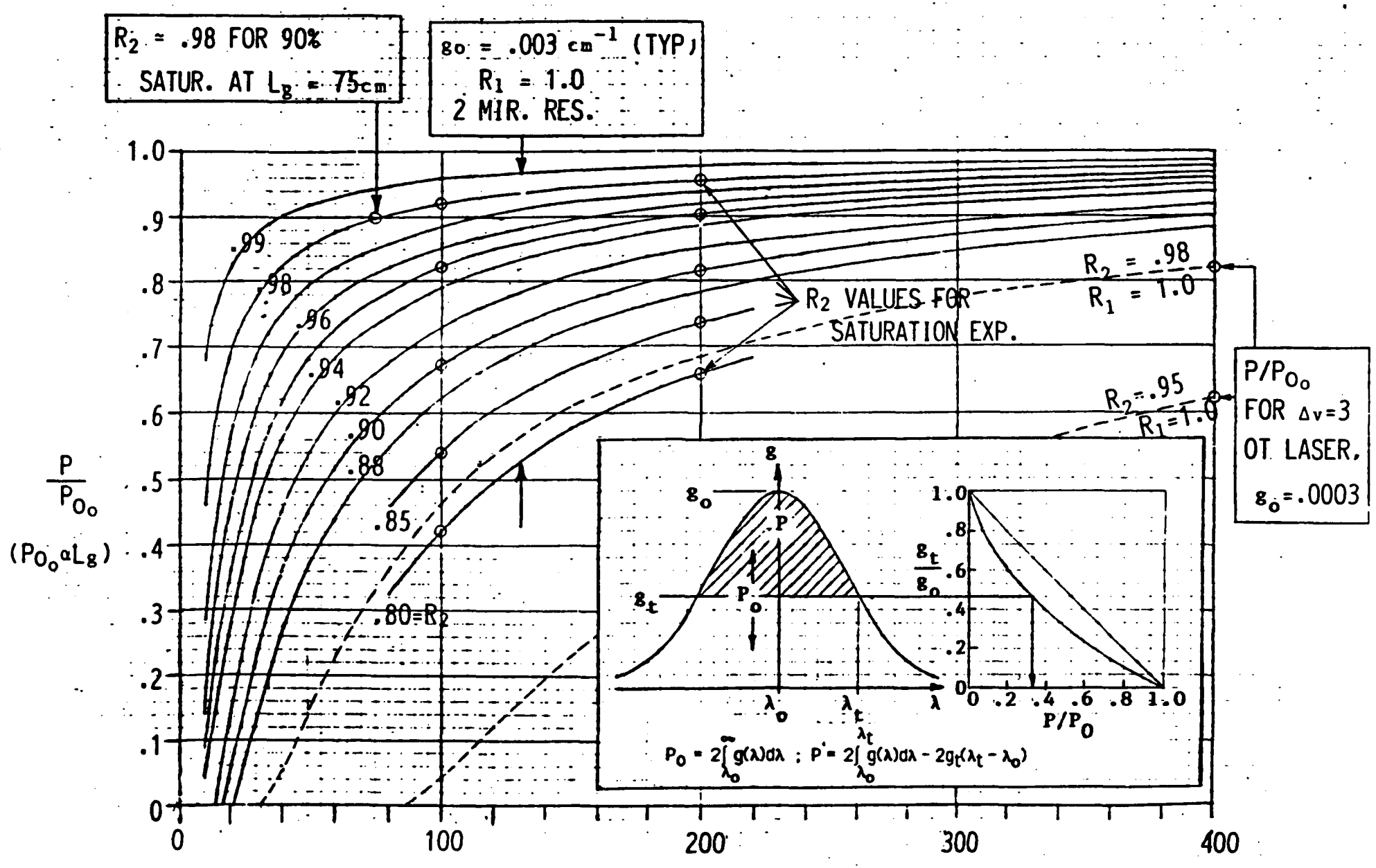

Fig. 3

PACIFIC APPLIED RESEARCH

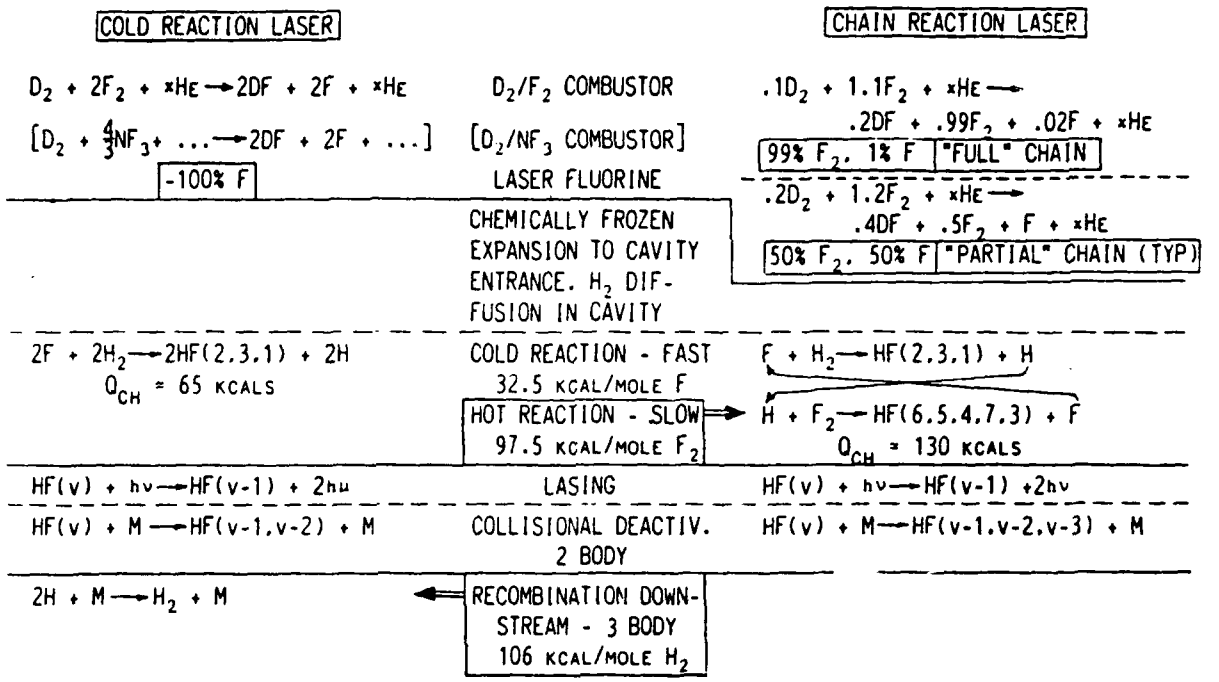

FIG. 4 COMPARISON OF COLD AND CHAIN REACTION MECHANISMS FOR FUNDAMENTAL, $\Delta v = 1$, HF CHEMICAL LASERS (SIMPLIFIED)

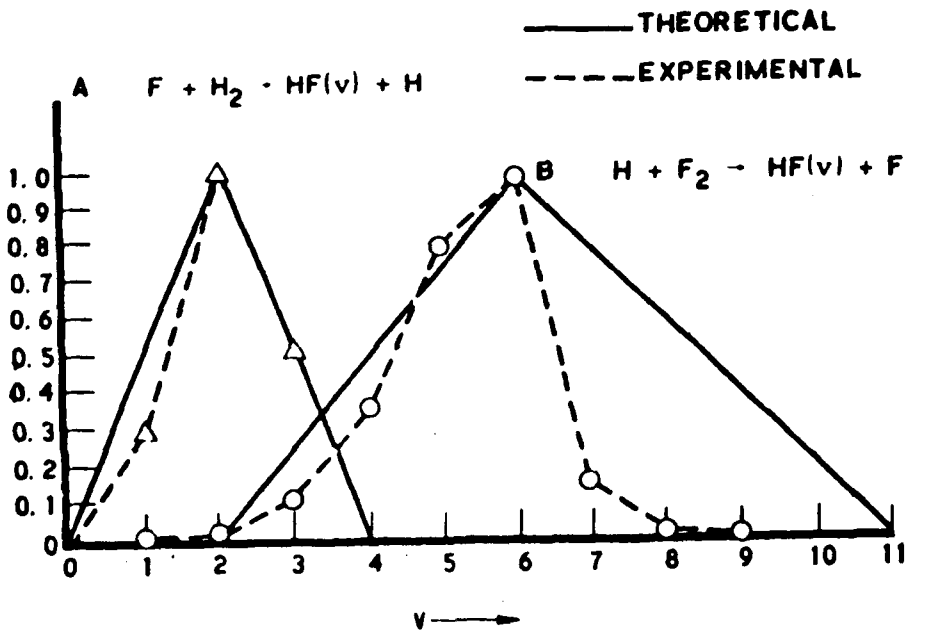

FIG. 5 Comparison of Experimental and Predicted Initial Vibrational Population Distributions for $F_2 + H_2$ Reactions (Source: Herbelin, J.M. and Cohen, N.; TR-0075(5641)-2, The Aerospace Corp., 15 Sept. 1974)

FIG. 6

PRINCIPAL KINETIC RATES FOR THE COLD REACTION LASER

$F + H_2 \longrightarrow HF + H$

ROTATIONAL EQUILIBRIUM

SOURCE:
N. COHEN
1978

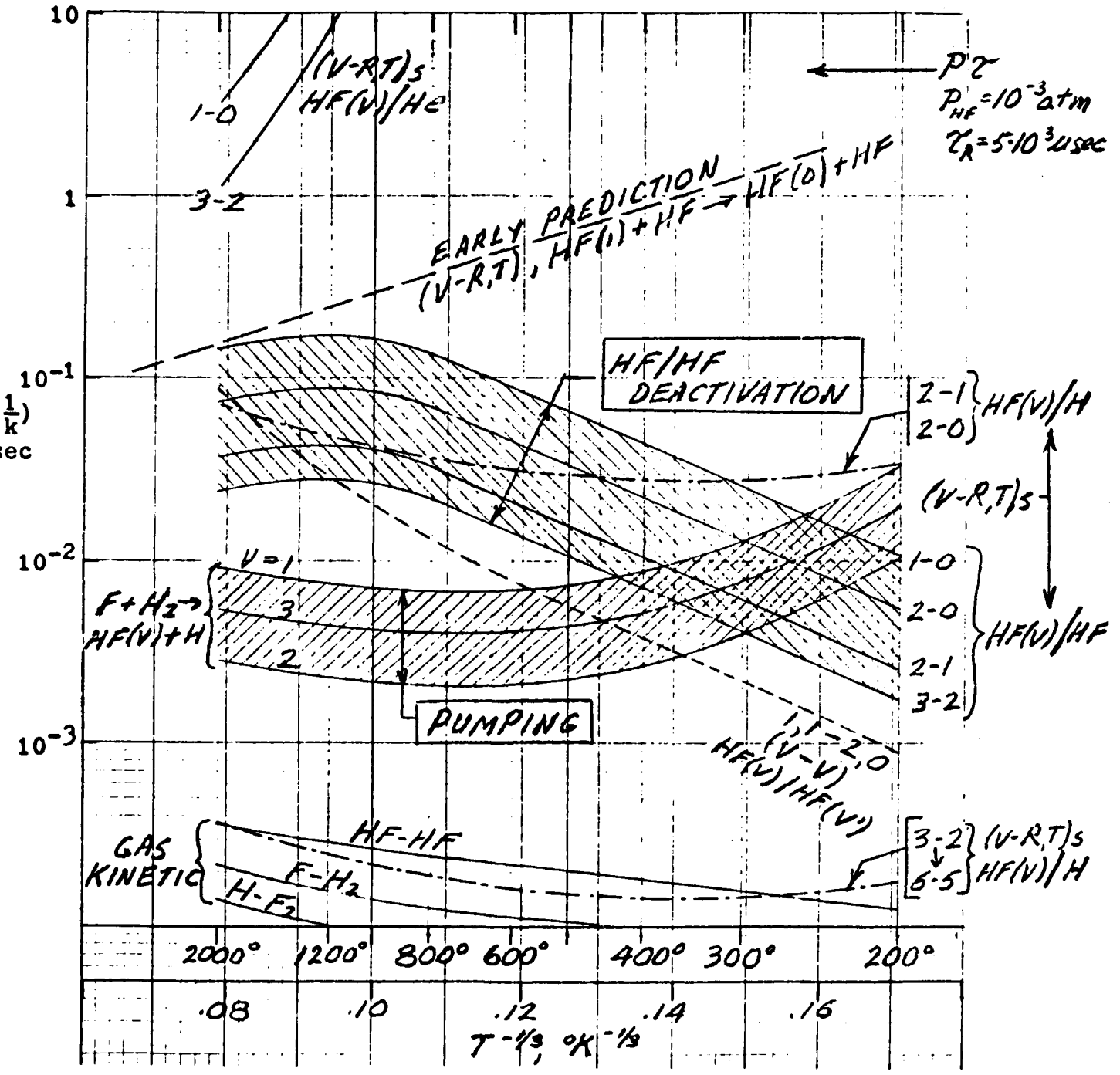

PACIFIC APPLIED RESEARCH

FIG. 7

PRINCIPAL KINETIC RATES FOR THE CHAIN REACTION SYSTEM

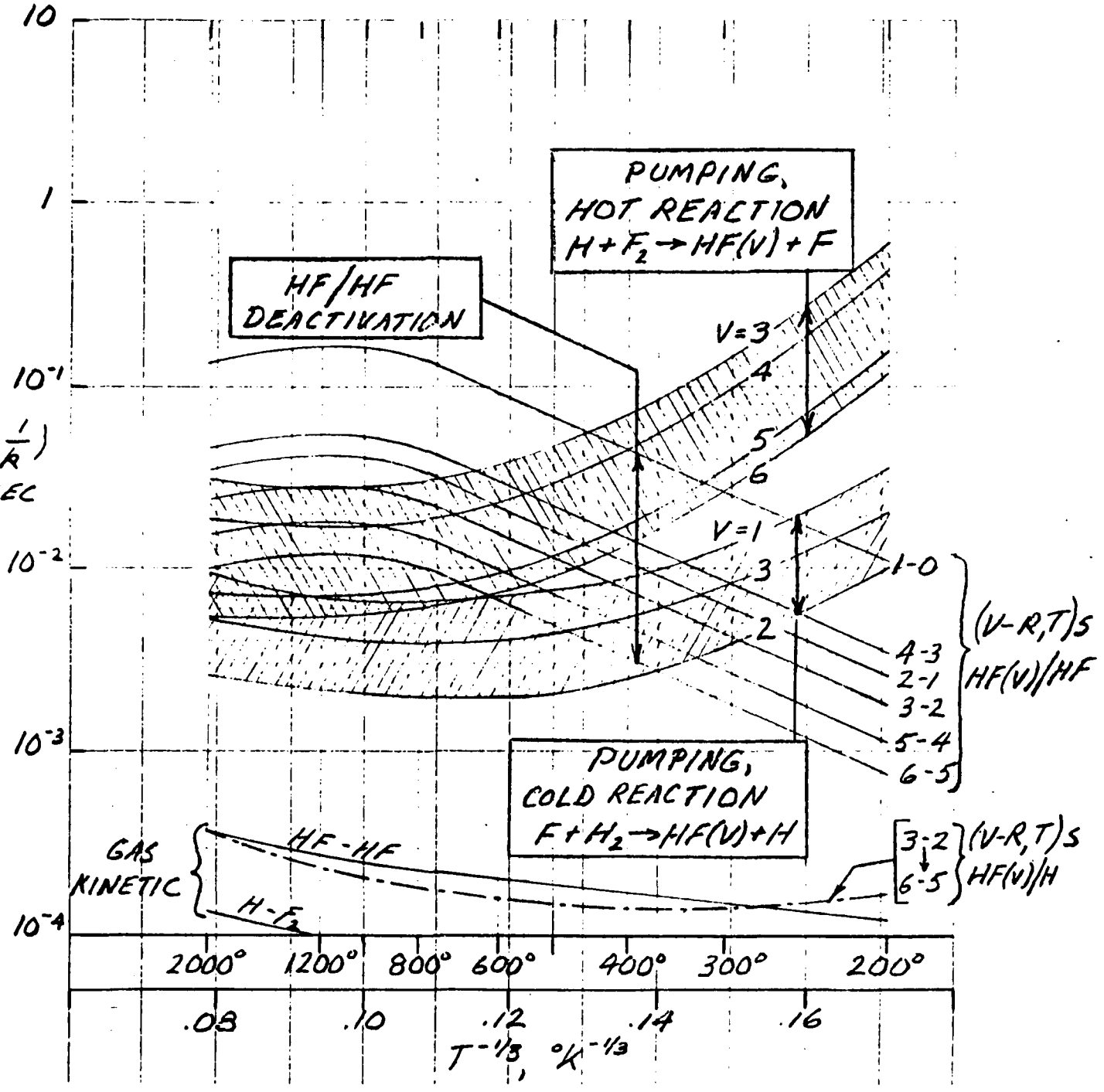

$F + H_2 \rightarrow HF + H$

$H + F_2 \rightarrow HF + F$

ROT. EQUIL.

SOURCE: N. COHEN 1978

PACIFIC APPLIED RESEARCH

FIG. 8

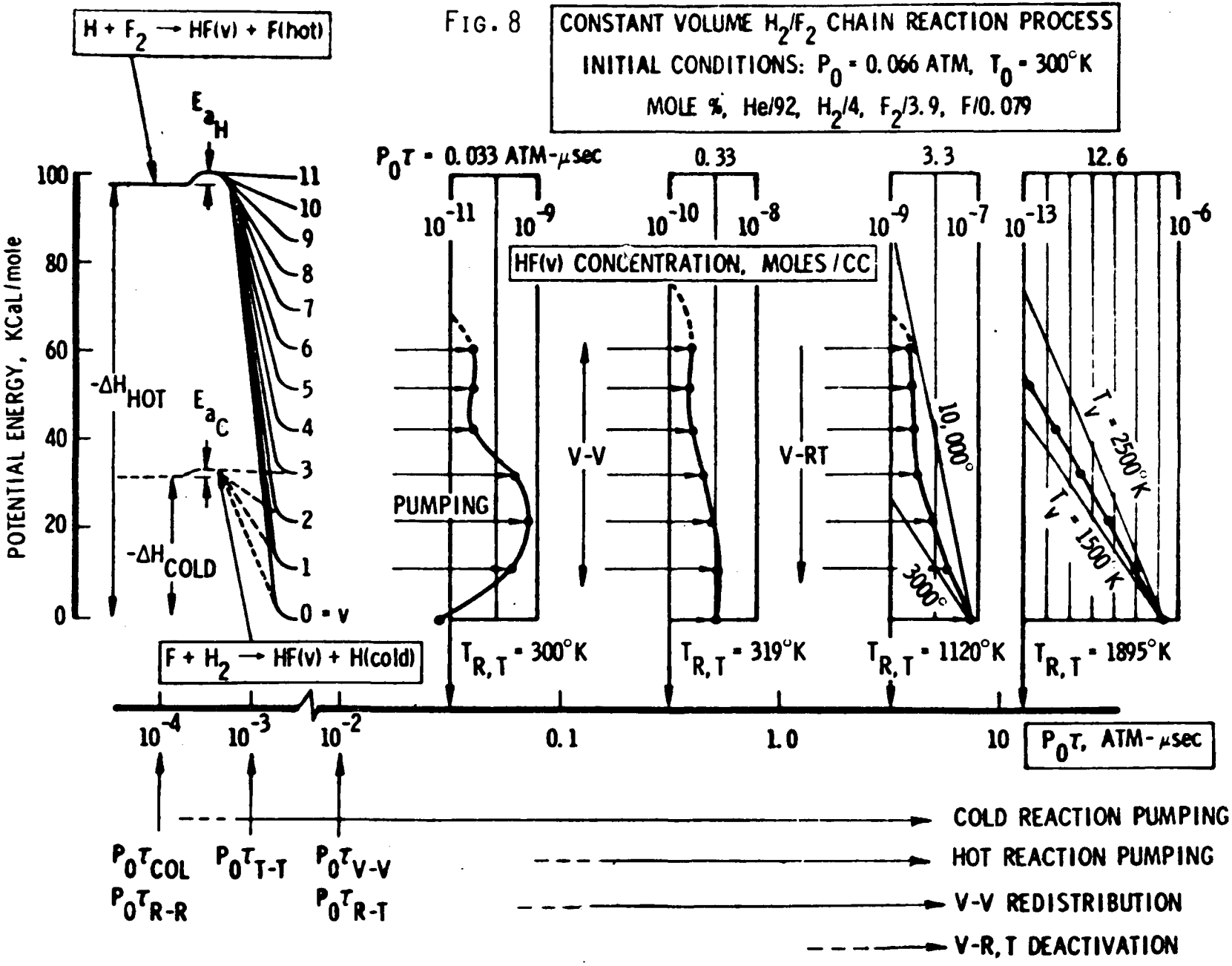

PACIFIC APPLIED RESEARCH

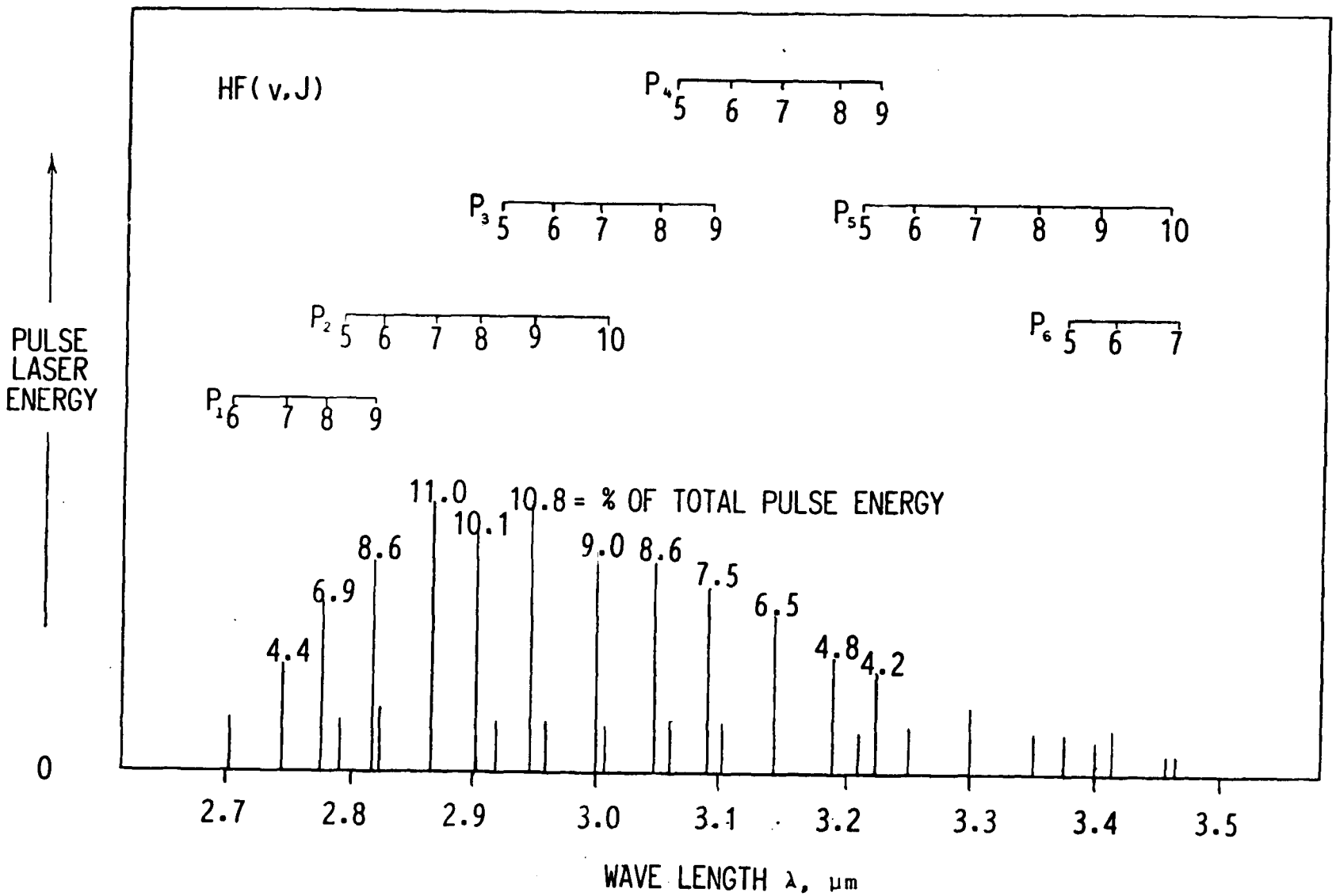

HF TRANSITIONS PRODUCED BY PULSED CHAIN REACTION F_2 -H_2 LASER

FIG. 9

PACIFIC APPLIED RESEARCH

FIG. 10 HF LASER ENERGY FROM DIFFERENT VIBRATIONAL LEVELS
FUNDAMENTAL, $\Delta V = 1$, TRANSITIONS

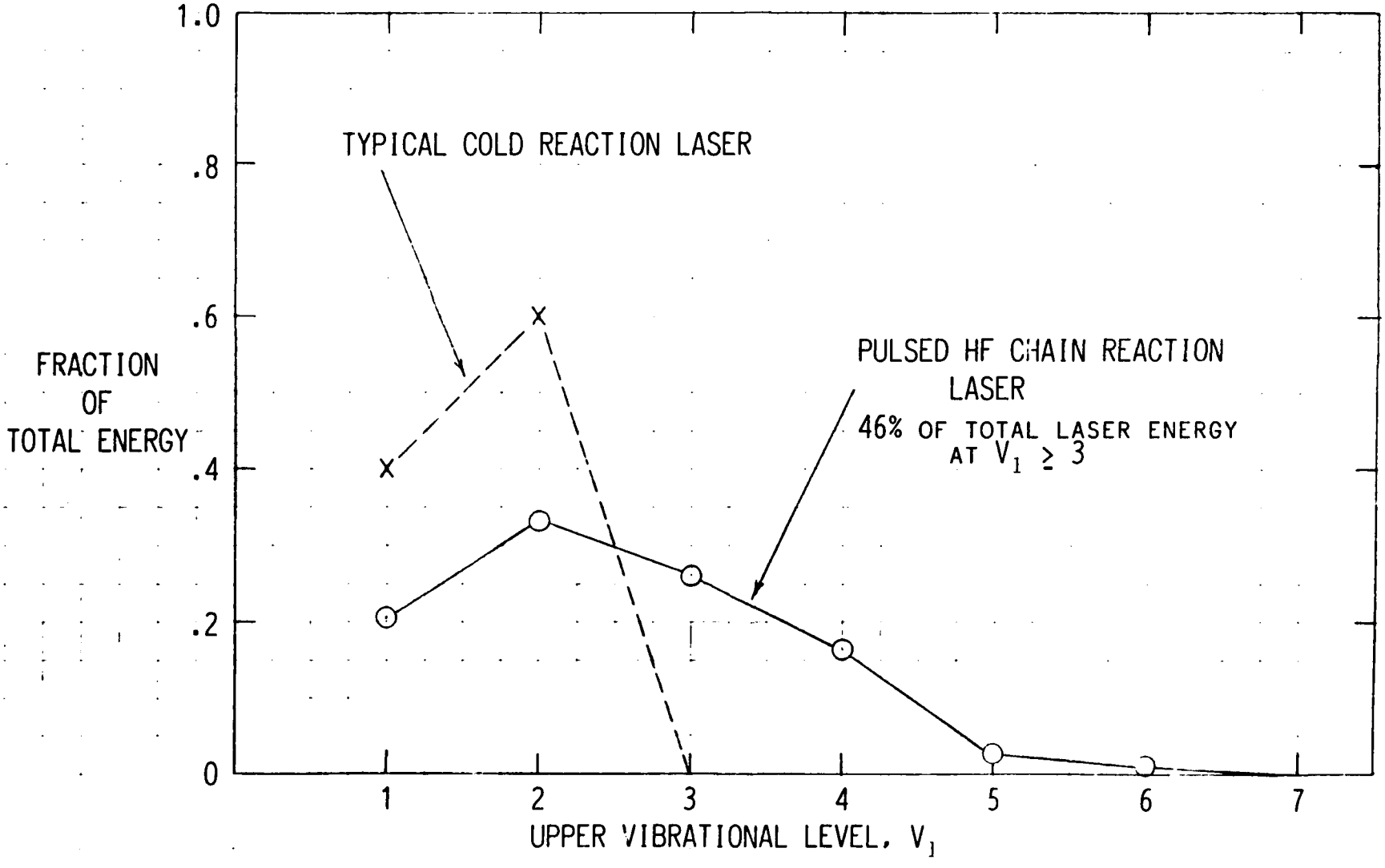

PACIFIC APPLIED RESEARCH

FIG. 11 EINSTEIN A COEFFICIENTS FOR HF

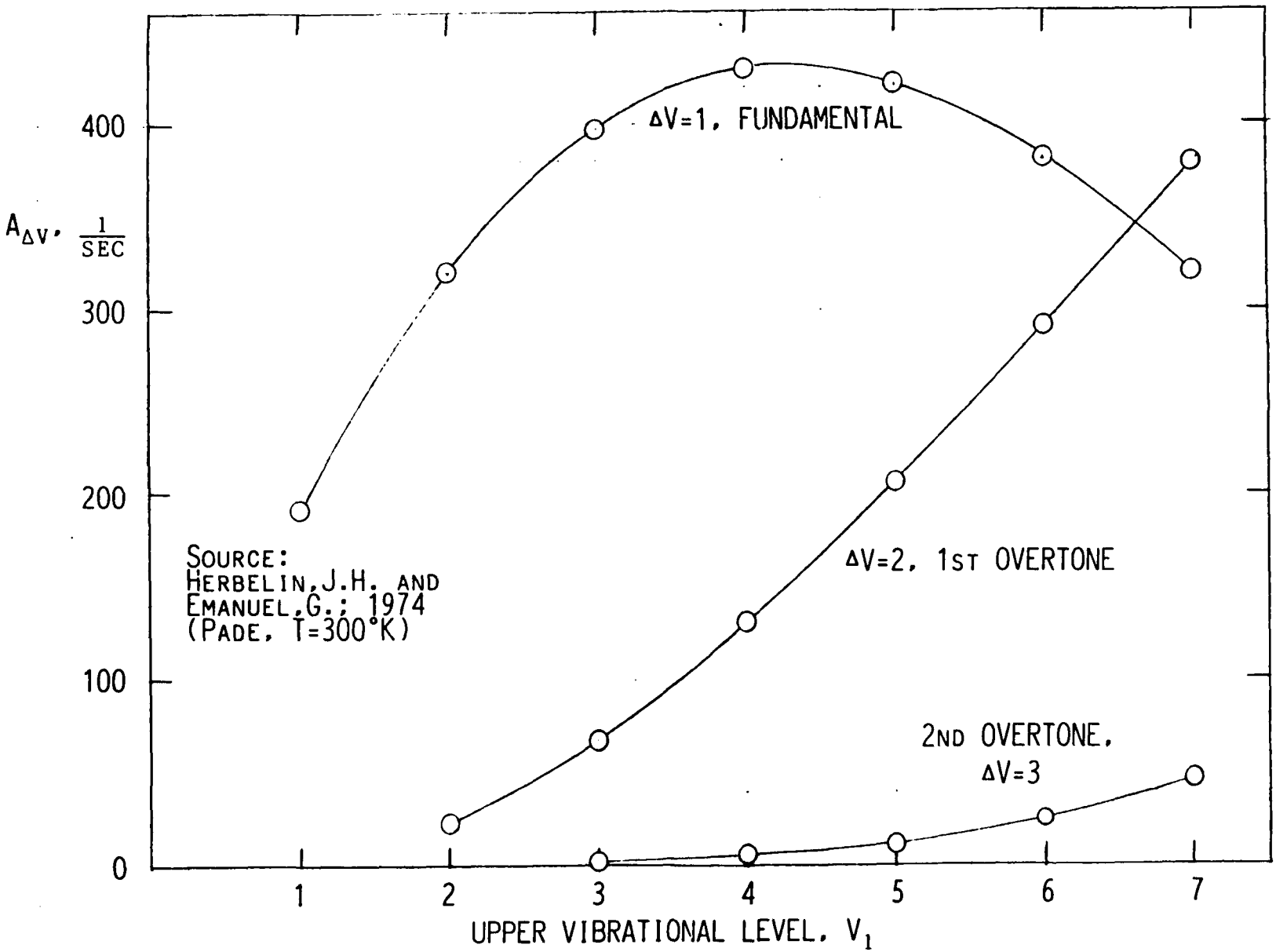

PACIFIC APPLIED RESEARCH

FIG. 12

RELATIVE GAIN / CROSS-SECTION BEHAVIOR FOR TYPICAL HIGH V LEVEL TRANSITIONS IN HF OTs

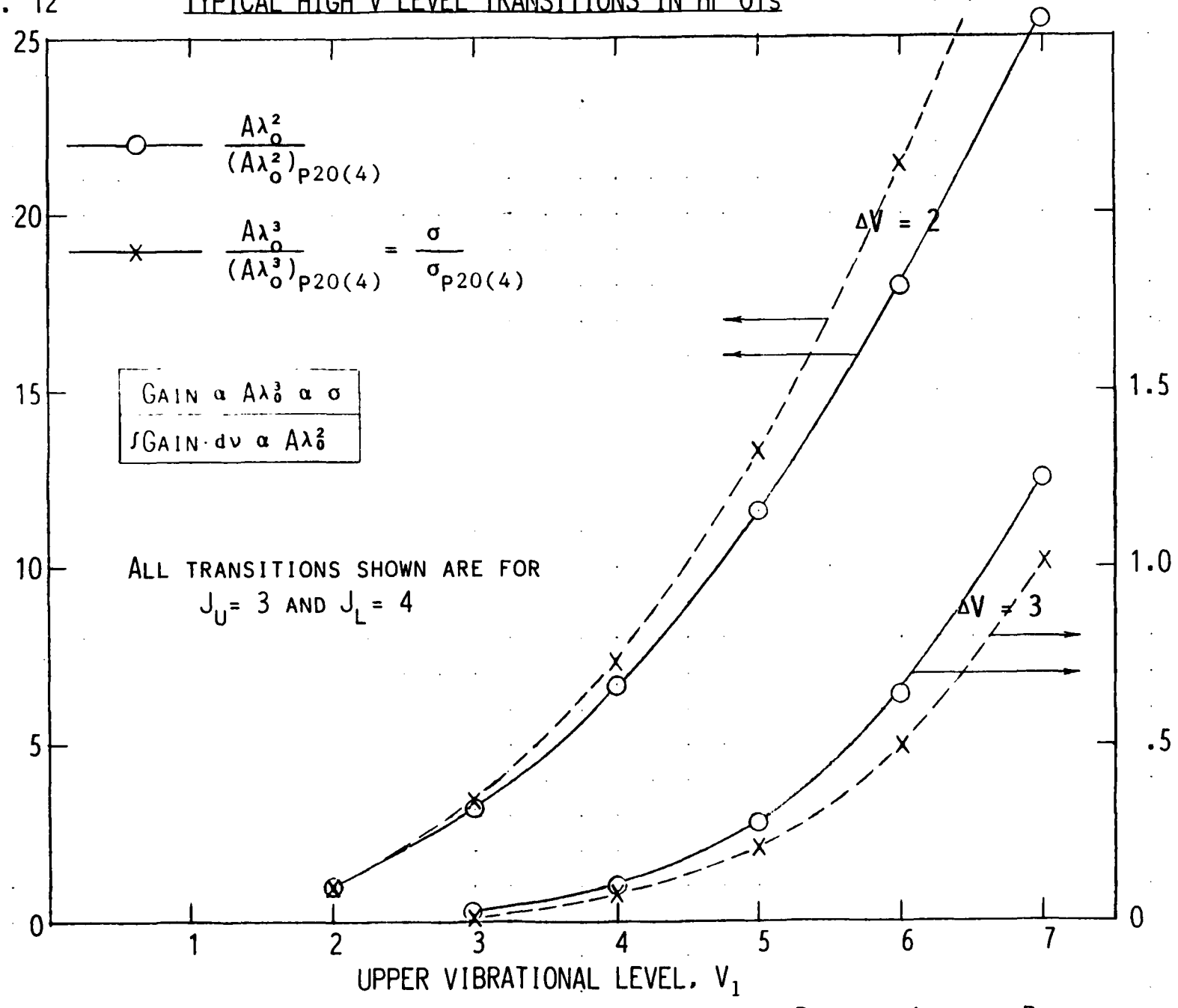

PACIFIC APPLIED RESEARCH

PAR MODEL 105 PULSED CHEMICAL LASER SYSTEM

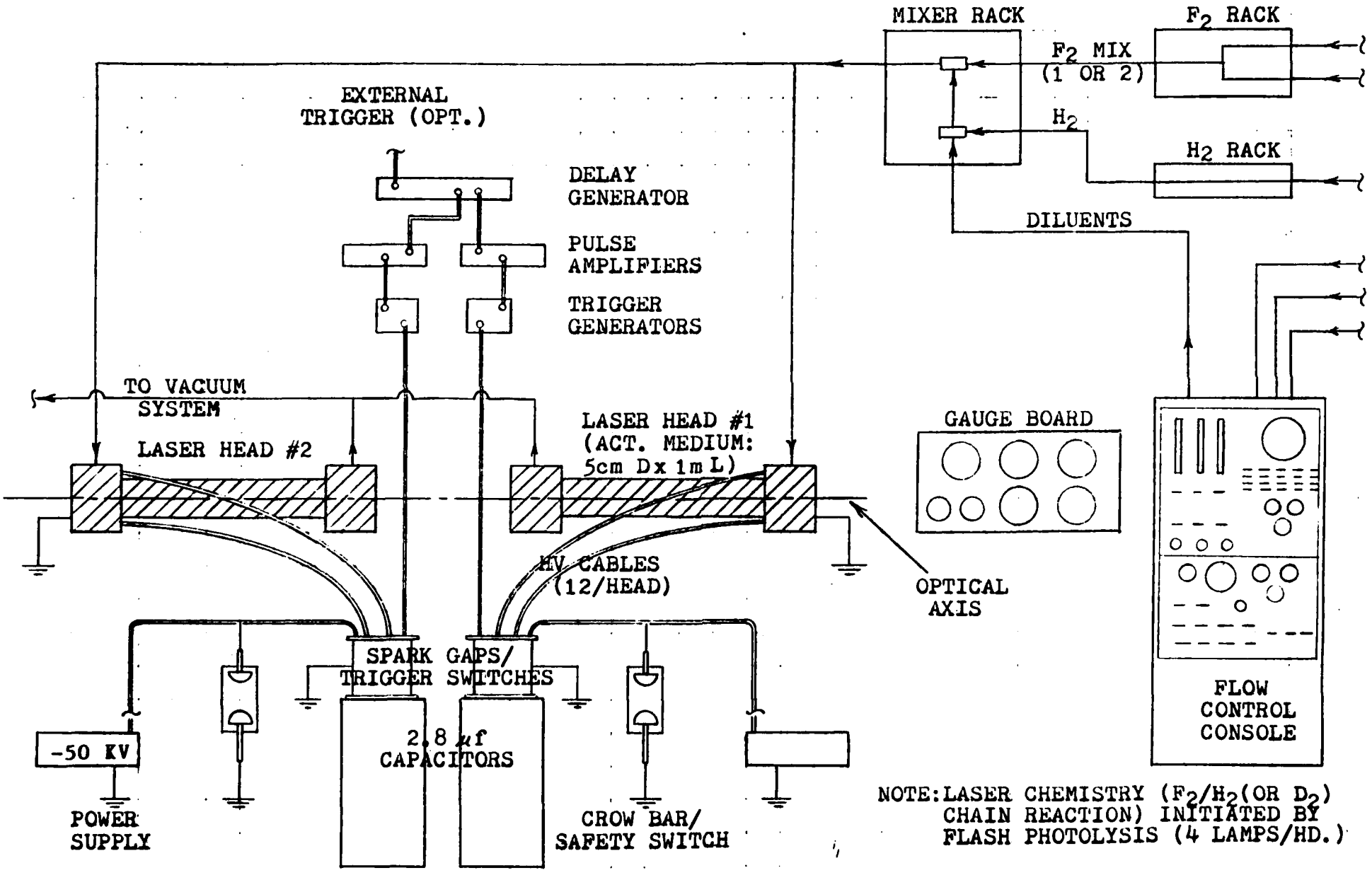

NOTE: LASER CHEMISTRY (F_2/H_2(OR D_2) CHAIN REACTION) INITIATED BY FLASH PHOTOLYSIS (4 LAMPS/HD.)

Fig. 13

PACIFIC APPLIED RESEARCH

MODEL 105 PULSED CHEMICAL LASER SYSTEM

LASER HEAD

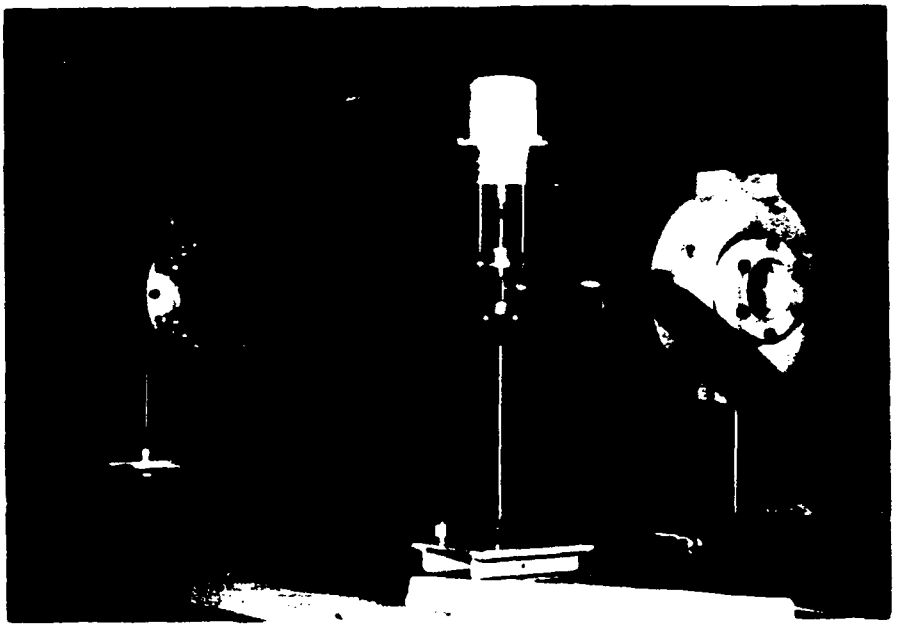

FLOW CONTROL CONSOLE

Fig. 14

PACIFIC APPLIED RESEARCH

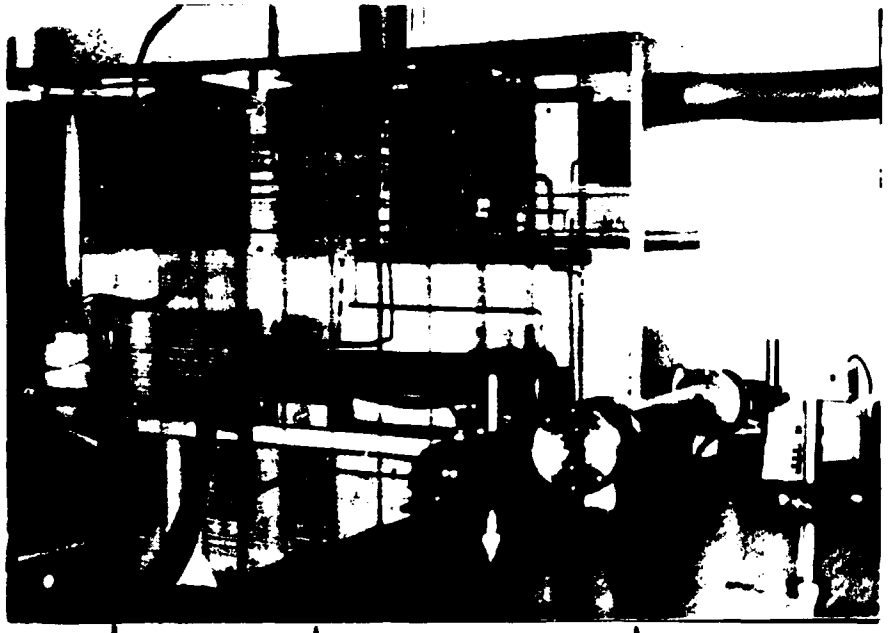

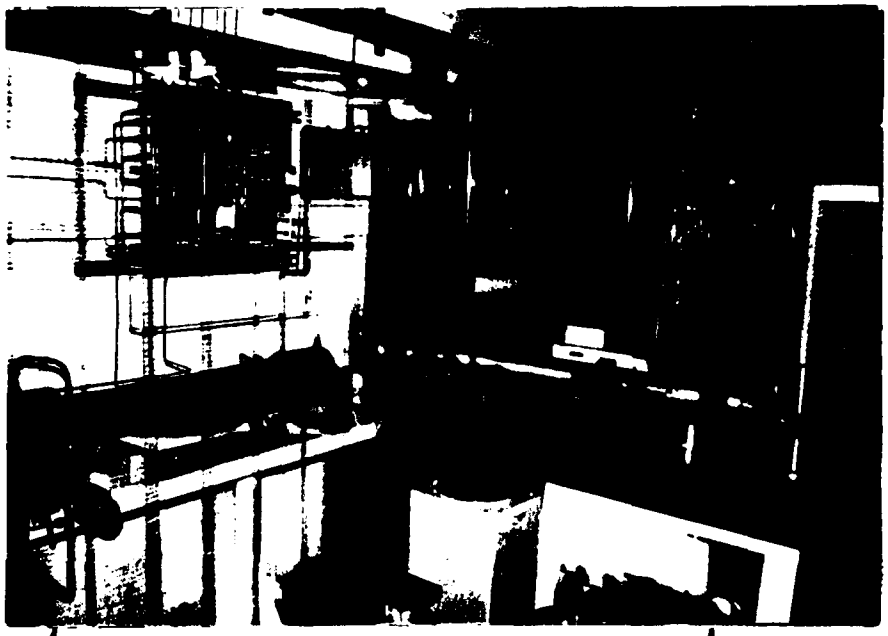

POWER SYSTEM FIRST HEAD (CAPACITOR, SWITCH, TRIGGER, CROWBAR)

FIRST LASER HEAD

SECOND LASER HEAD

MIXER RACK (FLOW CONTROL SYSTEM)

FLOW CONTROL CONSOLE

PULSED HYDROGEN FLUORIDE OVERTONE CHEMICAL LASER STUDIES

EXPERIMENTAL EQUIPMENT

Fig. 15

PACIFIC APPLIED RESEARCH

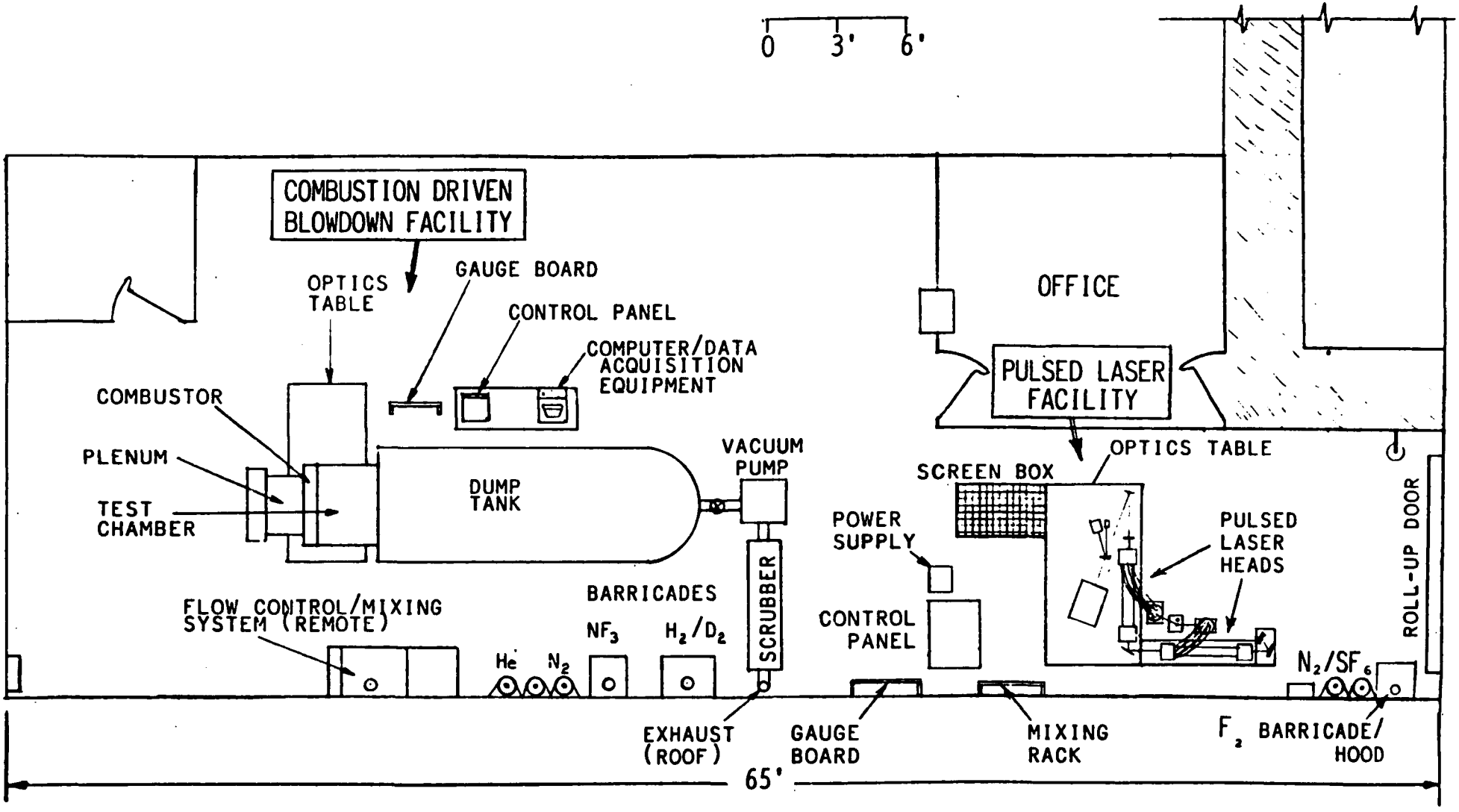

Fig. 16 LAYOUT OF TEST FACILITIES AND SUPPORT SYSTEMS IN THE LABORATORY

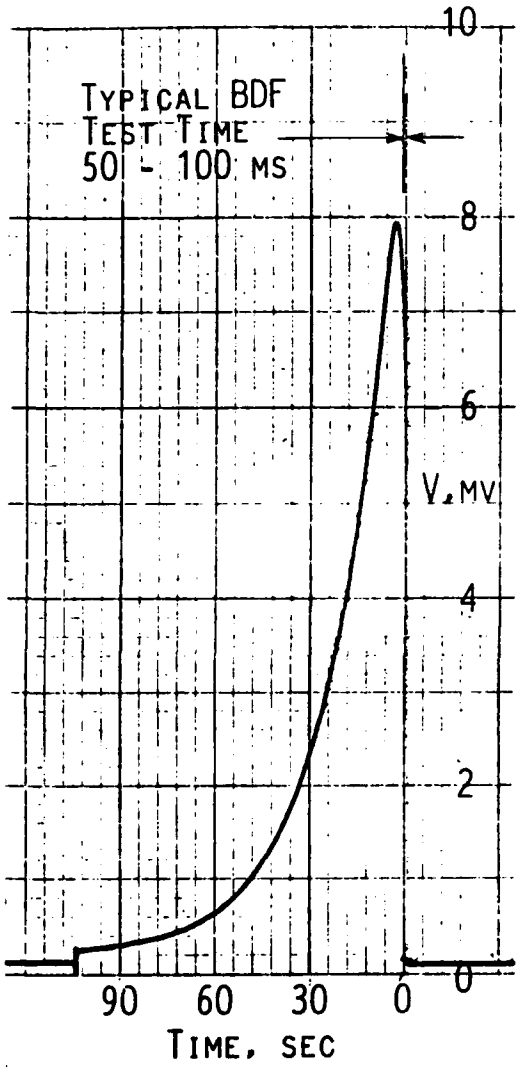

CHART RECORDER SIGNAL

CALORIMETER GIVES THE INTEGRAL OF LASER ENERGY DELIVERED DURING THE SHORT TEST TIME

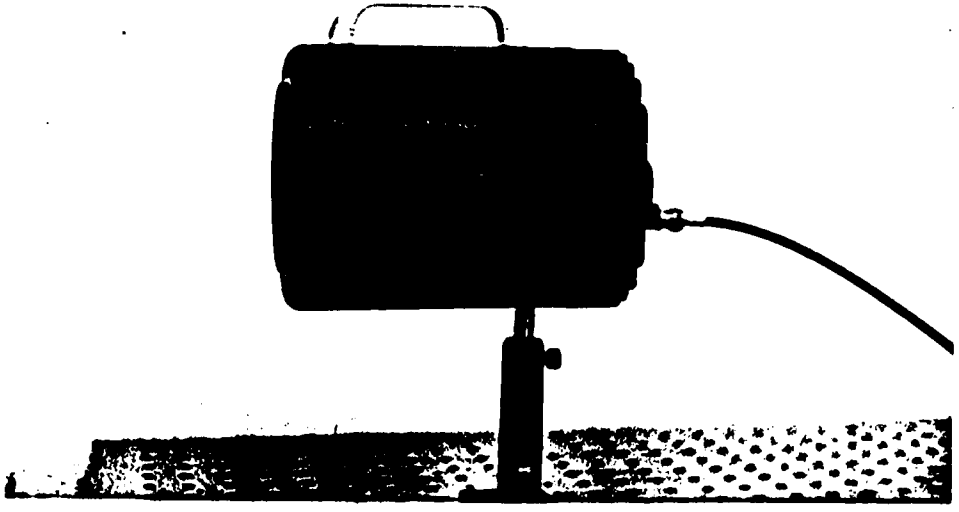

SCIENTECH DISC CALORIMETER

SURFACE ABSORBING - SERIES 36
(4 " DIAMETER APERTURE)

FIG. 17 LASER TOTAL ENERGY CALORIMETER

PACIFIC APPLIED RESEARCH

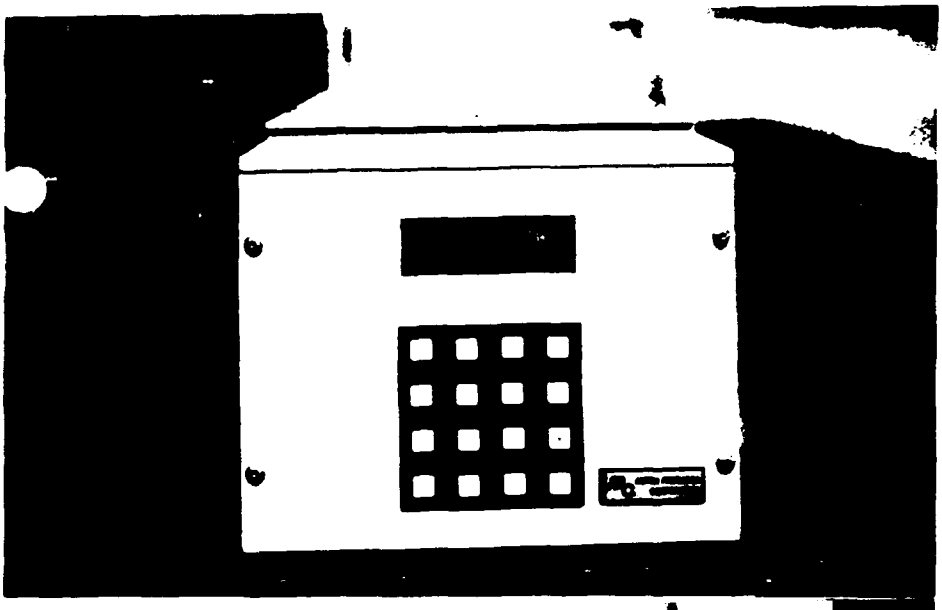

ACTON RESEARCH CORP.

SPECTRAPRO-275 MM FOCAL LENGTH
DIGITAL SCANNING MONOCHROMATOR
AND SPECTROGRAPH
(GRATINGS BLAZED AT 2.5.1.2..5 µM)

SPIRICON, INC.

LASER PROBE LINEAR DETECTOR ARRAY
(PYROELECTRIC) WITH CONTROLLER
MODEL NO. LP-256-11
(256 ELEMENTS IN 25.6 MM
LONG ARRAY)

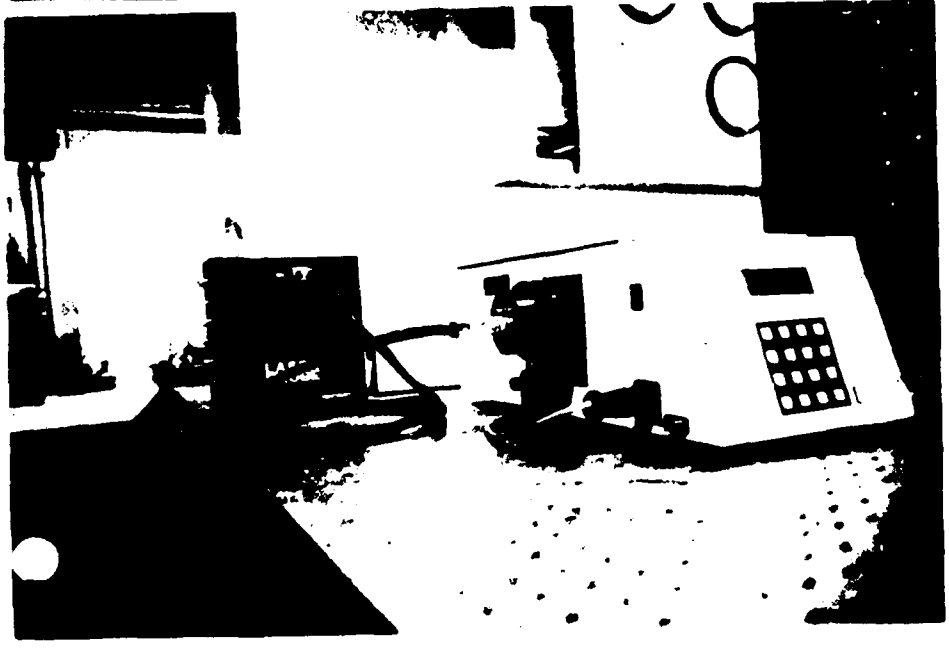

SPECTROGRAPH AND
ARRAY/CONTROLLER
ASSEMBLY

Fig. 18 SPECTROSCOPIC DIAGNOSTICS

PACIFIC APPLIED RESEARCH

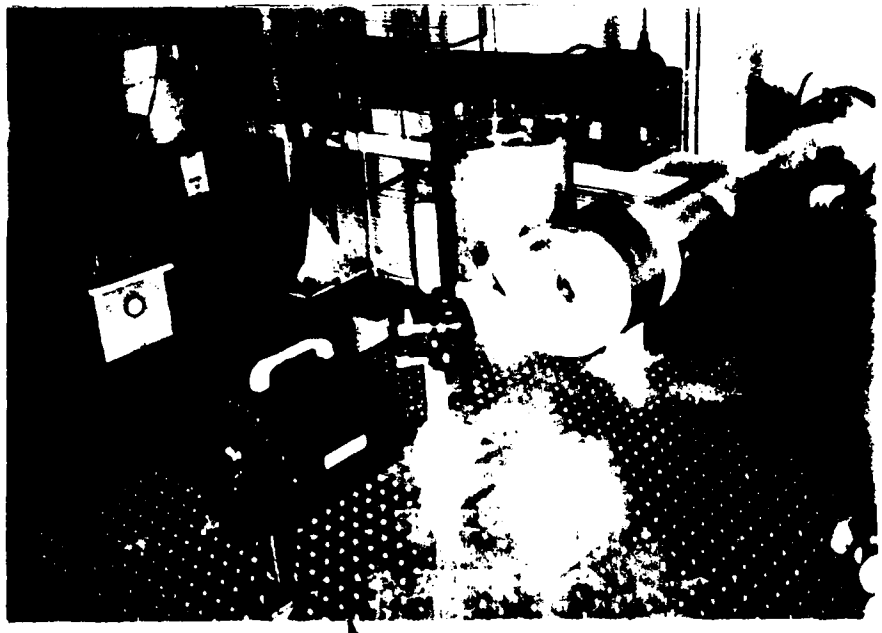

LASER PROBE LINEAR DETECTOR ARRAY (PYROELECTRIC) WITH CONTROLLER (SPIRICON, INC.)

DIGITAL SCANNING MONOCHROMATOR AND SPECTROGRAPH; FL=275MM (GRATINGS BLAZED AT 2.5, 1.2, .5 μM) (ACTON RESEARCH CORP.)

SURFACE ABSORBING DISC CALORIMETER (4" DIA. APERTURE) (SCIENTECH, INC.)

PULSED HYDROGEN FLUORIDE OVERTONE CHEMICAL LASER STUDIES

EXPERIMENTAL EQUIPMENT

Fig. 19

PACIFIC APPLIED RESEARCH

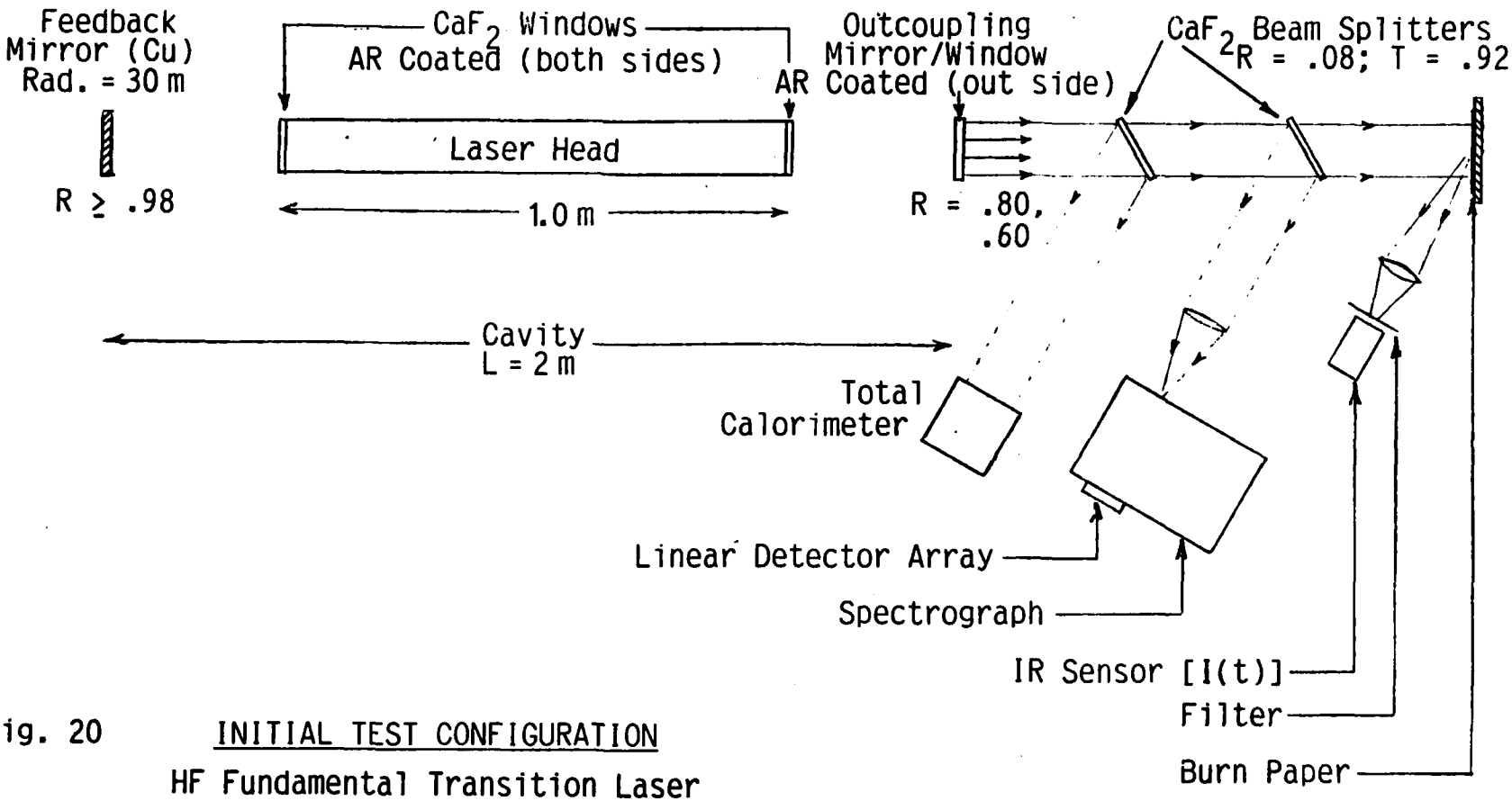

Fig. 20 INITIAL TEST CONFIGURATION

HF Fundamental Transition Laser

Pacific Applied Research

$.20F_2 + .04O_2 + .41He + .09H_2 + .26SF_6$

$P_i = 200\,t$; $V = 40\,KV$; $22.6\,J = E_{TOT}$

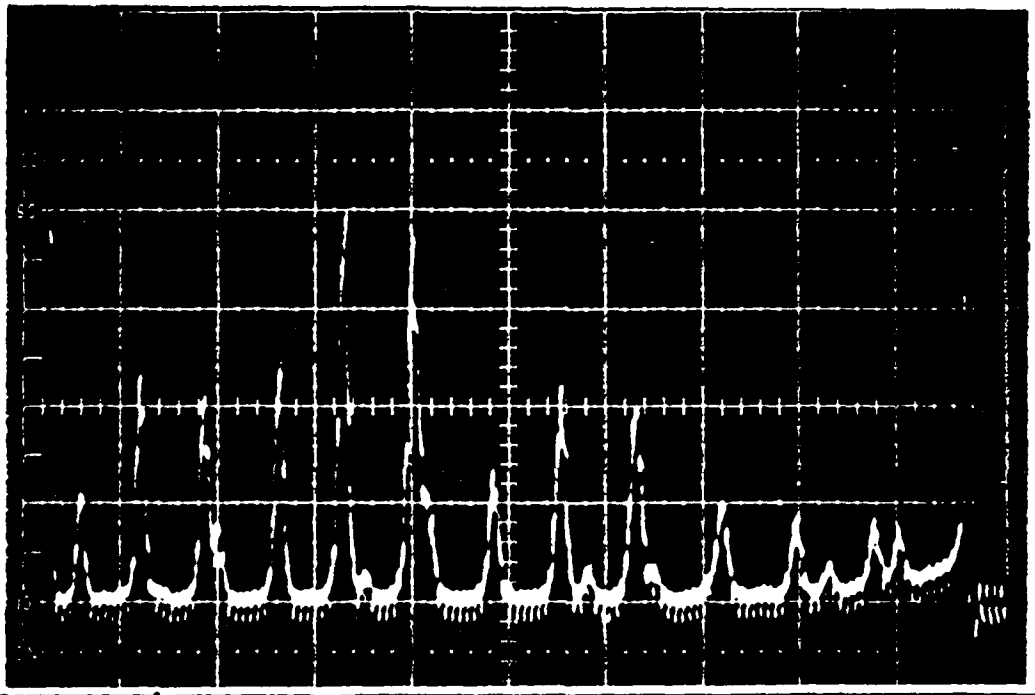

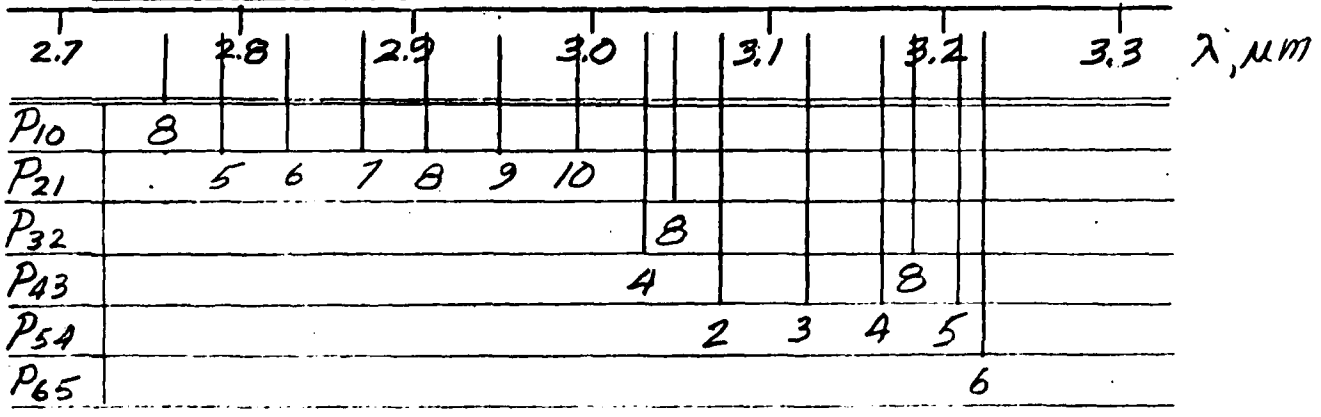

Fig. 21 SPECTRAL CONTENT OF FUNDAMENTAL TRANSITION LASER PULSE

SPECTRAL CONTENT OF FUNDAMENTAL TRANSITION LASER PULSES

INITIAL PRESSURE EFFECT, V = 40KV

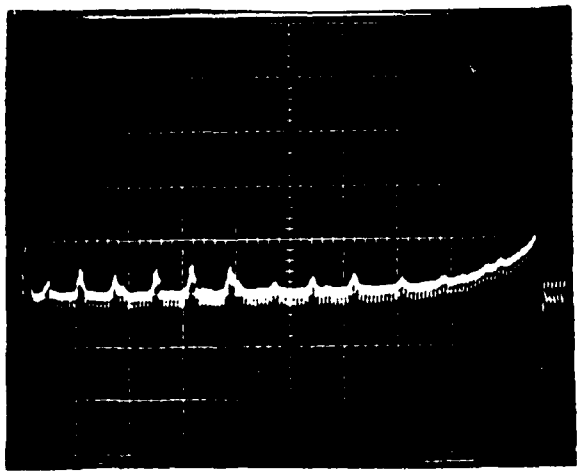

P = 55 TORR; E_C = .26 J
E = 1.6 J/L

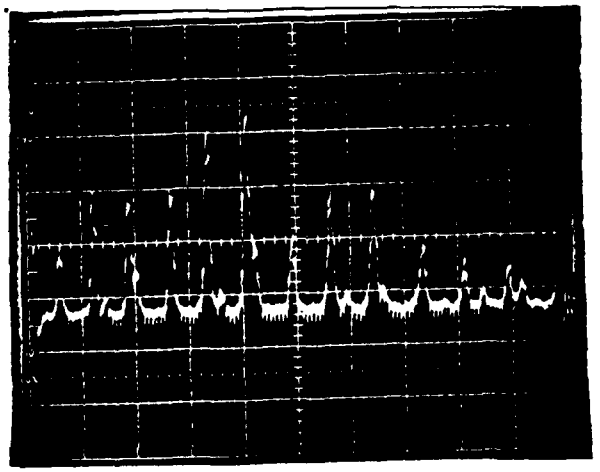

P = 200 TORR; E_C = 1.9 J
E = 11.9 J/L

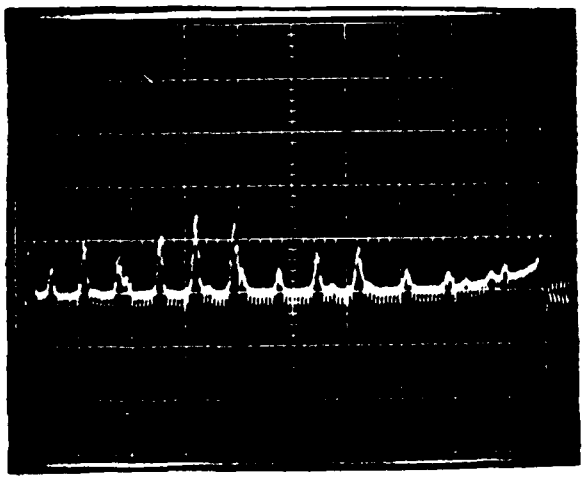

P = 100 TORR; E_C = .71 J
E = 4.4 J/L

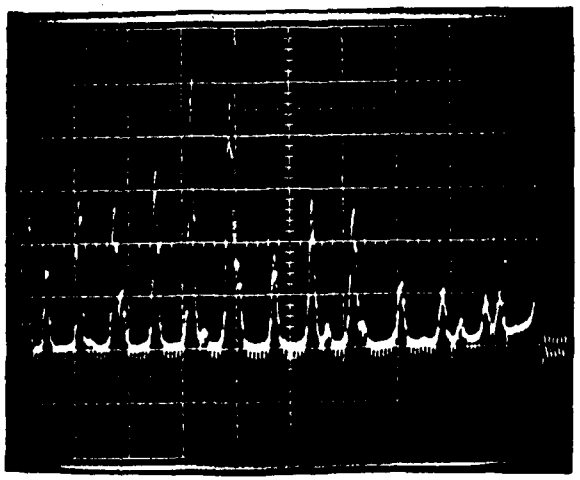

P = 300 TORR; E_C = 3.1 J
E = 19.4 J/L

Fig. 22

PACIFIC APPLIED RESEARCH

● Data from Ref. 12
20 F_2: 8-10 H_2: 25 SF_6: 1.6-6.6 O_2: Balance He
V = 45 kV; C = 2.8 μF

× Data from Figs. 21 and 22
20 F_2: 9 H_2: 26 SF_6: 4 O_2: 41 He
V = 40 kV; C = 2.8 μF

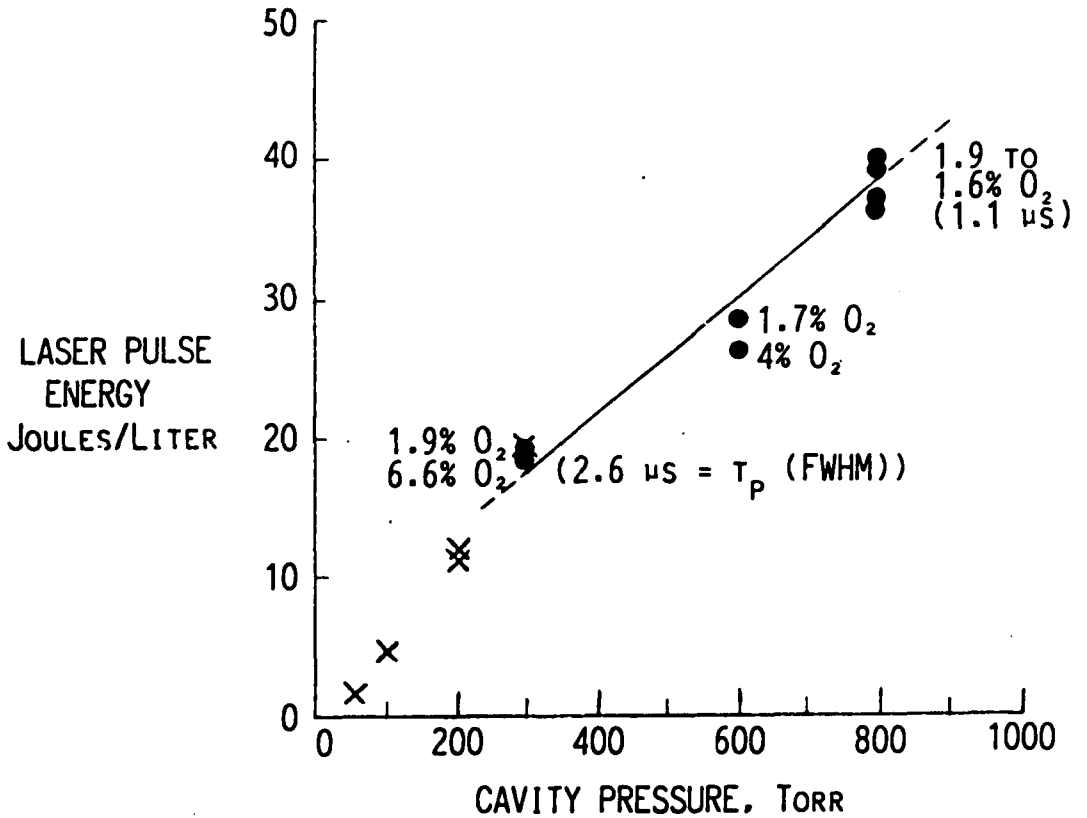

Fig. 23 THE EFFECT OF INITIAL CHARGE PRESSURE ON PULSE HF CHAIN LASER OUTPUT.

EFFECT OF INITIAL PRESSURE LEVEL ON FT LASER PULSE INTENSITY HISTORY

C = 2.8 μF
V = 47 kV
Mix 1.1

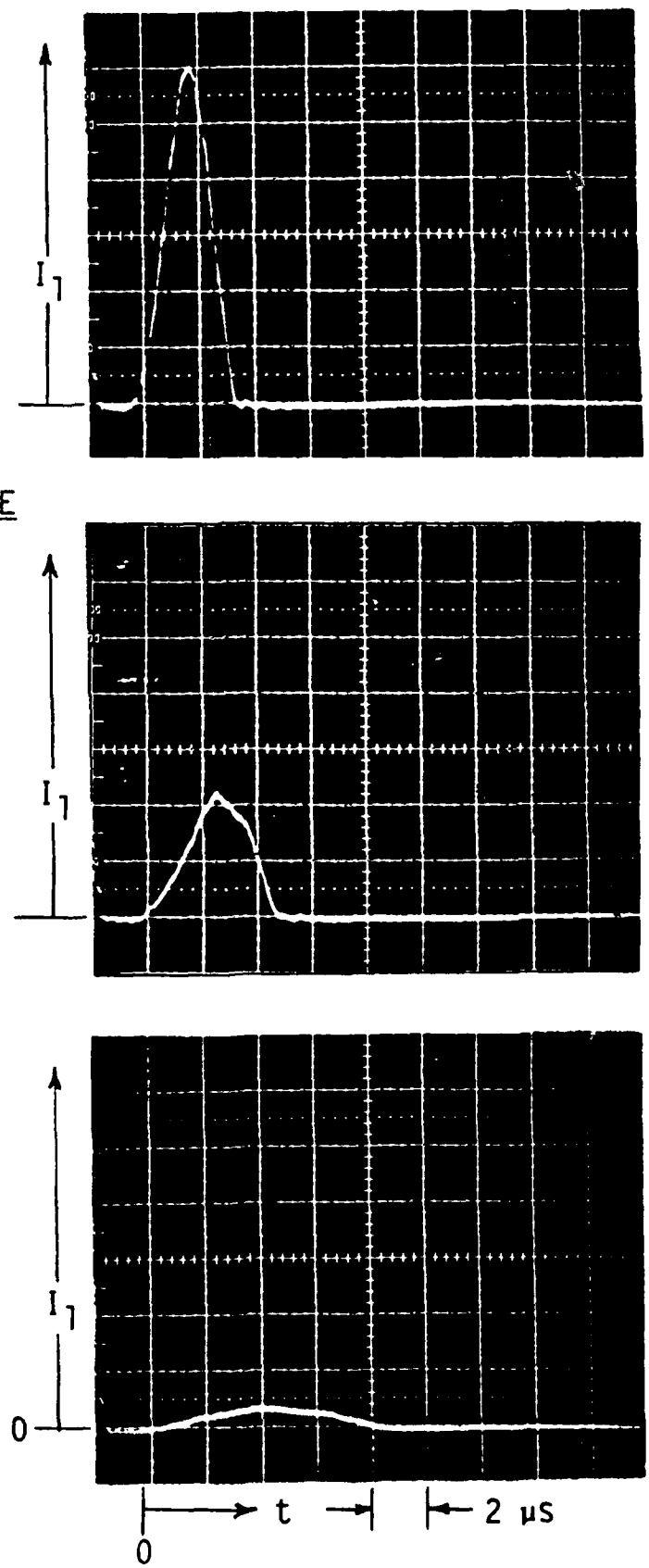

Fig. 24.a

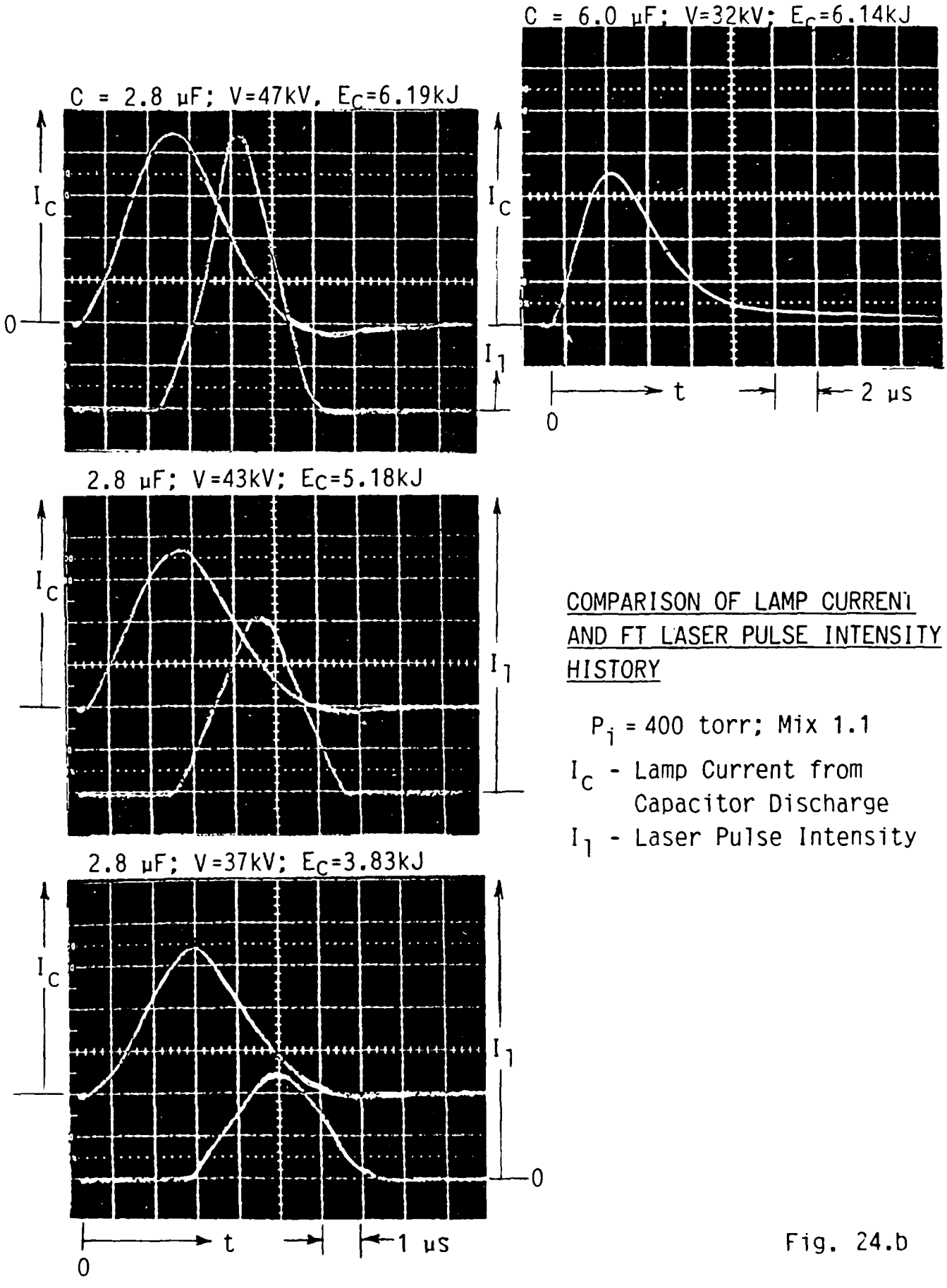

COMPARISON OF LAMP CURRENT AND FT LASER PULSE INTENSITY HISTORY

P_i = 400 torr; Mix 1.1

I_C - Lamp Current from Capacitor Discharge

I_1 - Laser Pulse Intensity

Fig. 24.b

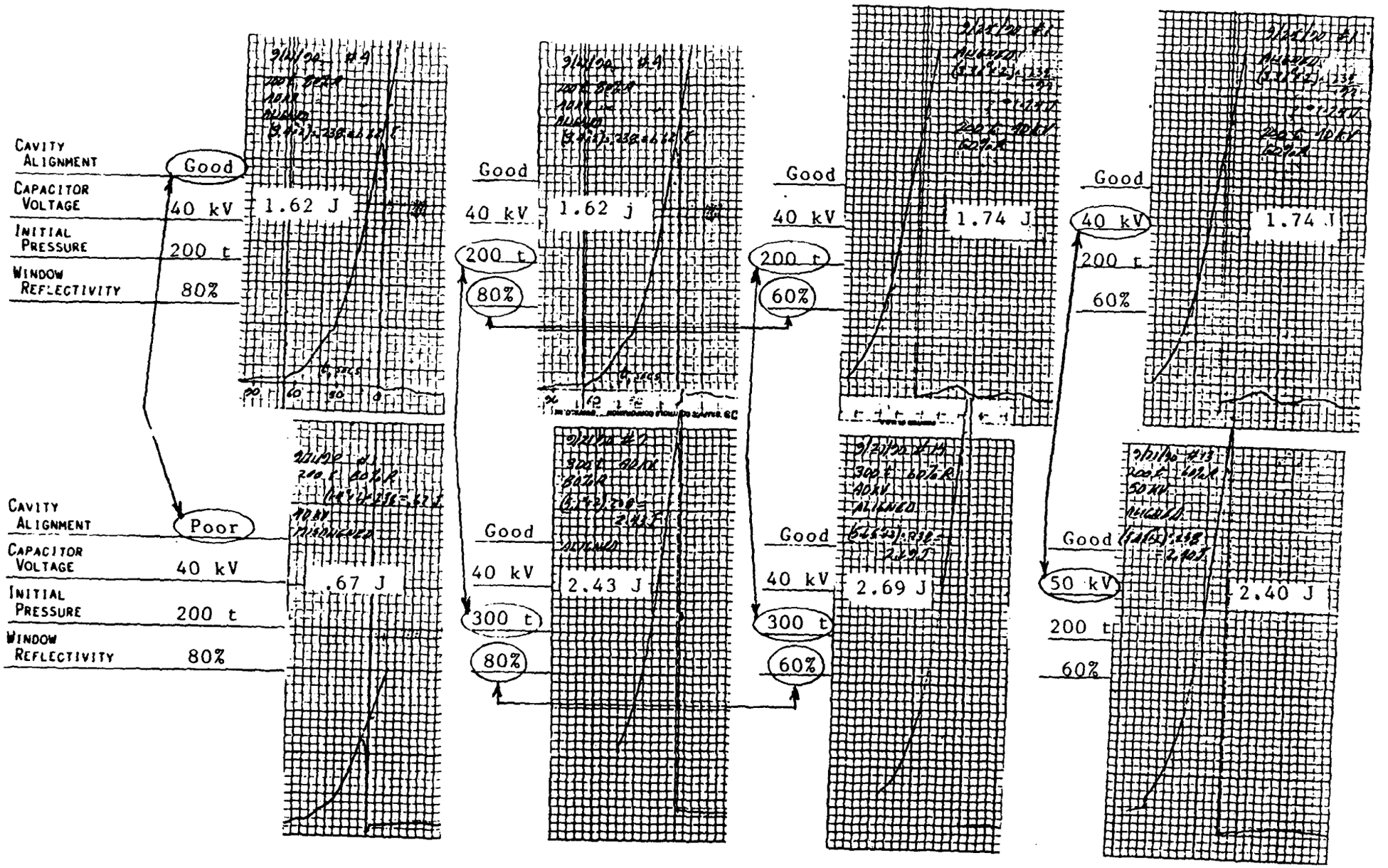

Fig. 25

SAMPLE TOTAL CALORIMETER DATA

PACIFIC APPLIED RESEARCH

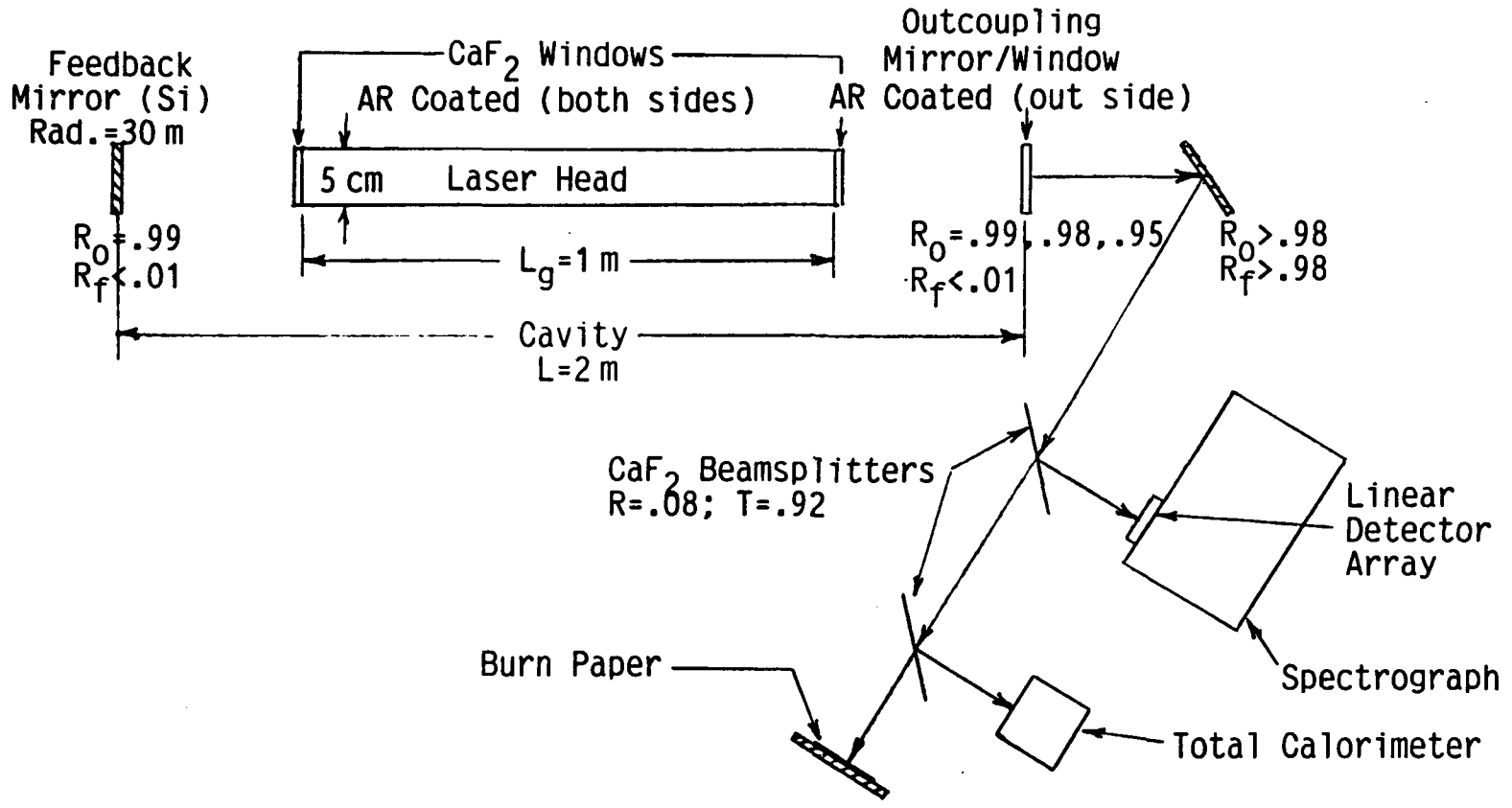

Fig. 26

INITIAL TEST CONFIGURATION

HF Overtone Transition Laser

OPTICAL COMPONENTS

	DIA.	THK.	COATINGS FRONT SIDE / BACK SIDE	QTY.
LASER WINDOWS				
LF-1, CaF2, flat	3"	1cm	FT:AR&MgF2 / FT:AR&MgF2 OT1: - /OT1: -	4
LO-1, CaF2, flat	3"	1cm	FT: - / FT: - OT1:AR&MgF2 /OT1:AR&MgF2	4
RESONATORS				
*RF-1, Copper, CC	3"	1cm	FT: 98.0+ / FT: - OT1: - /OT1: -	2
RF-4, CaF2, flat	3"	8mm	FT: 60.0 / FT: AR OT1: - /OT1: -	1
RF-5, CaF2, flat	3"	8mm	FT: 80.0 / FT: AR OT1: - /OT1: -	1
*RO-1, Silicon, CC	3"	6mm	FT:<1.0 / FT: AR OT1: 99.0 /OT1: -	2
RO-2, Silicon, flat	3"	6mm	FT:<1.0 / FT: AR OT1: 99.0 /OT1: -	2
RO-5, Silicon, flat	3"	6mm	FT:<1.0 / FT: AR OT1: 90.0 /OT1: -	1
RO-6, Silicon, flat	3"	6mm	FT:<1.0 / FT: AR OT1: 95.0 /OT1: -	2
RO-7, Silicon, flat	3"	6mm	FT:<1.0 / FT: AR OT1: 98.0 /OT1: -	1
RO-8, Copper, flat 2" x 2.5"		1cm	FT: 98.0+ / FT: - OT1: 99.0 /OT1: -	3
RO-9, Silicon, flat 2" x 2.5"		6mm	FT:<1.0 / FT: AR OT1: 99.0 /OT1: -	3
FLUX REDUCER				
**FO-4, Copper, CC	3"	1cm	FT: 98.0+ / FT: - OT1: 98.0+ /OT1: -	1
**FO-5, Copper, CV	1.5"	1cm	FT: 98.0+ / FT: - OT1: 98.0+ /OT1: -	1
ISOLATORS				
IF-1, Silicon, flat	3"	6mm	FT: 98.0+ / FT: - OT1: 1.0 /OT1: AR	2

	DIA.	THK.	COATINGS FRONT SIDE / BACK SIDE	QTY.
DIAGNOSTIC REFLECTORS				
D-1, Copper, flat	3"	1cm	FT: 98.0+ / FT: - OT1: 98.0+ /OT1: -	2
D-3, CaF2, 10° wedge	3"		FT: 50.0 / FT: - OT1: - /OT1: -	1
D-3, CaF2, 10° wedge	3"		FT: - / FT: - OT1: 50.0 /OT1: -	2
D-4, CaF2, 50cm FL	3"		FT: AR / FT: AR OT1: AR /OT1: AR	2
2nd OT (OT2)				
LO2-1, CaF2, flat	3"	1cm	FT(OT1): - /FT(OT1): - OT2: AR&MgF2/OT2: AR&MgF2	3
*RO2-1, CaF2, CC	3"	8mm	FT(OT1): 1.0/FT(OT1): AR OT2: 99.0+ /OT2: -	2
RO2-4, CaF2, flat	3"	8mm	FT(OT1): 1.0/FT(OT1): AR OT2: 95.0 /OT2: -	2

FT = 2.70um
OT1 = 1.35um
OT2 = 0.9um

* The concave (CC) mirror r=30m

** The concave (CC) mirror r=4m
convex (CV) mirror r=2m

Fig. 27

Rocky Mountain Instrument Co.
1501 South Sunset St.
Longmont, CO 80501

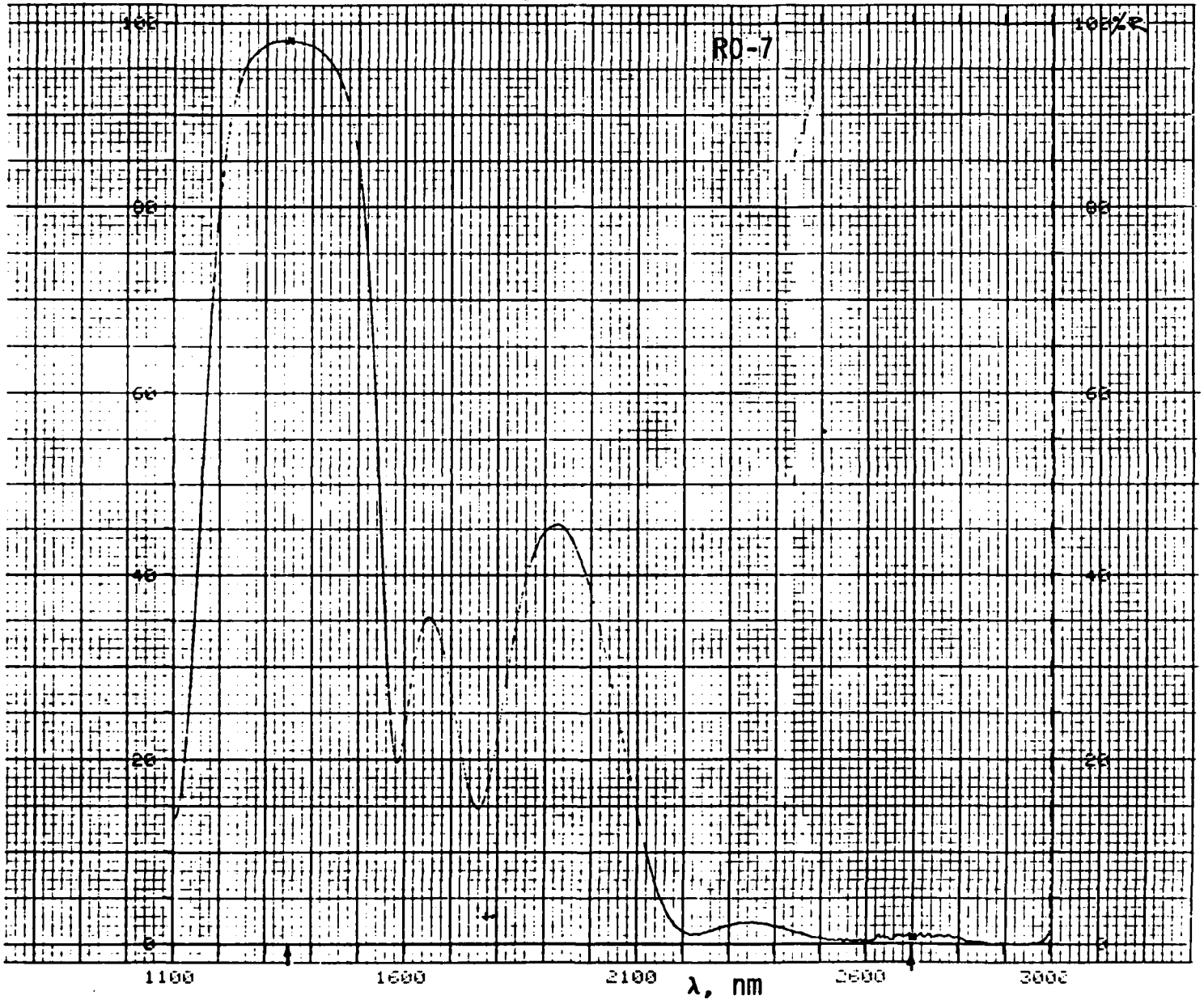

Fig. 28 REFLECTIVITY VS WAVELENGTH

1st Overtone Mirror Outcoupler

Rocky Mountain Instrument Co.
1501 South Sunset St.
Longmont, CO 80501

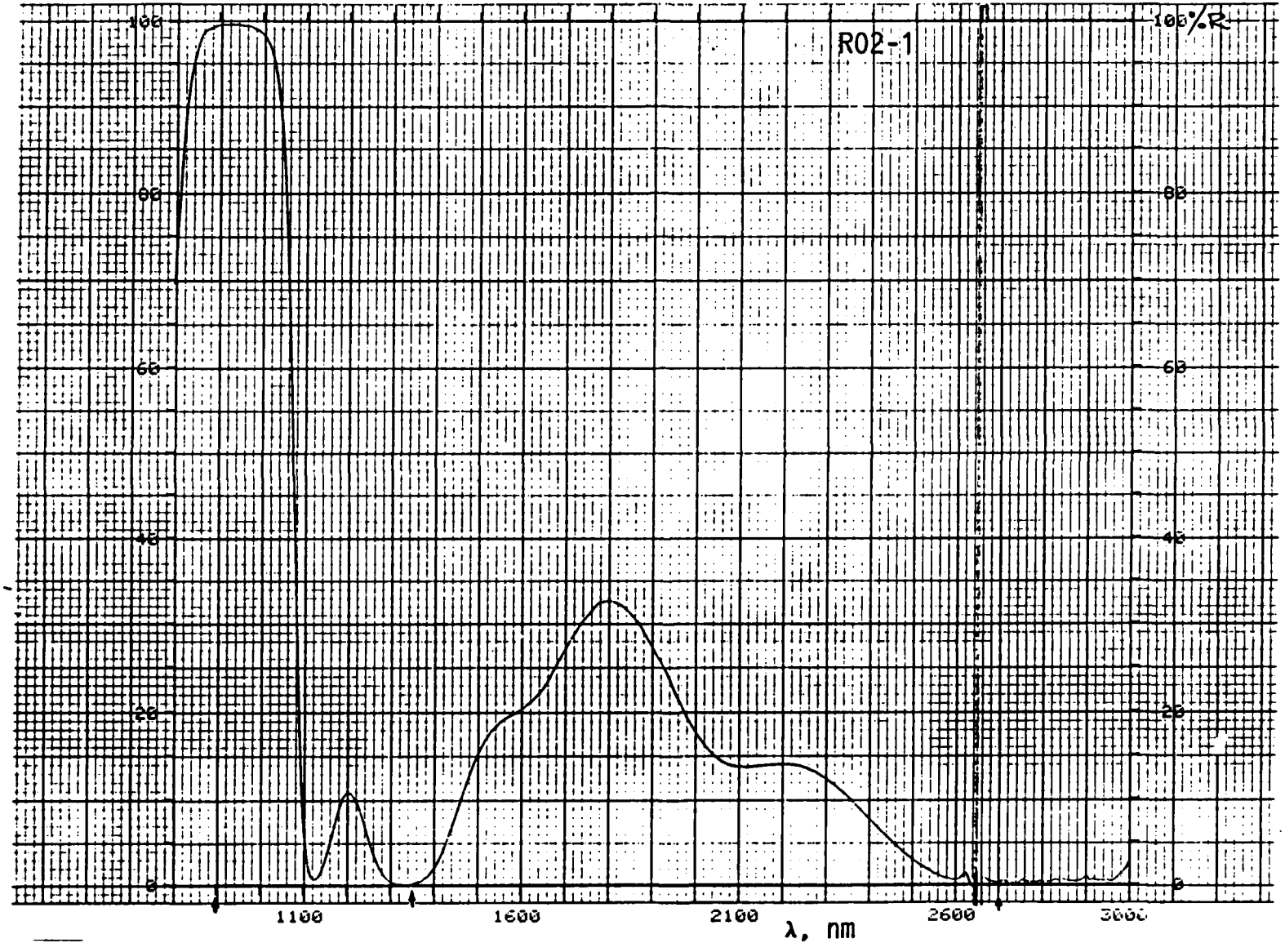

Fig. 29 REFLECTIVITY VS WAVELENGTH
2nd Overtone Feedback Mirror

DEGRADATION OF OPTICAL COATING

FT Mirror/Window; RF-5, Refl. = 80%

Fig. 30

RESONATOR CONFIGURATIONS USED IN THE HF OVERTONE LASER EXPERIMENTS

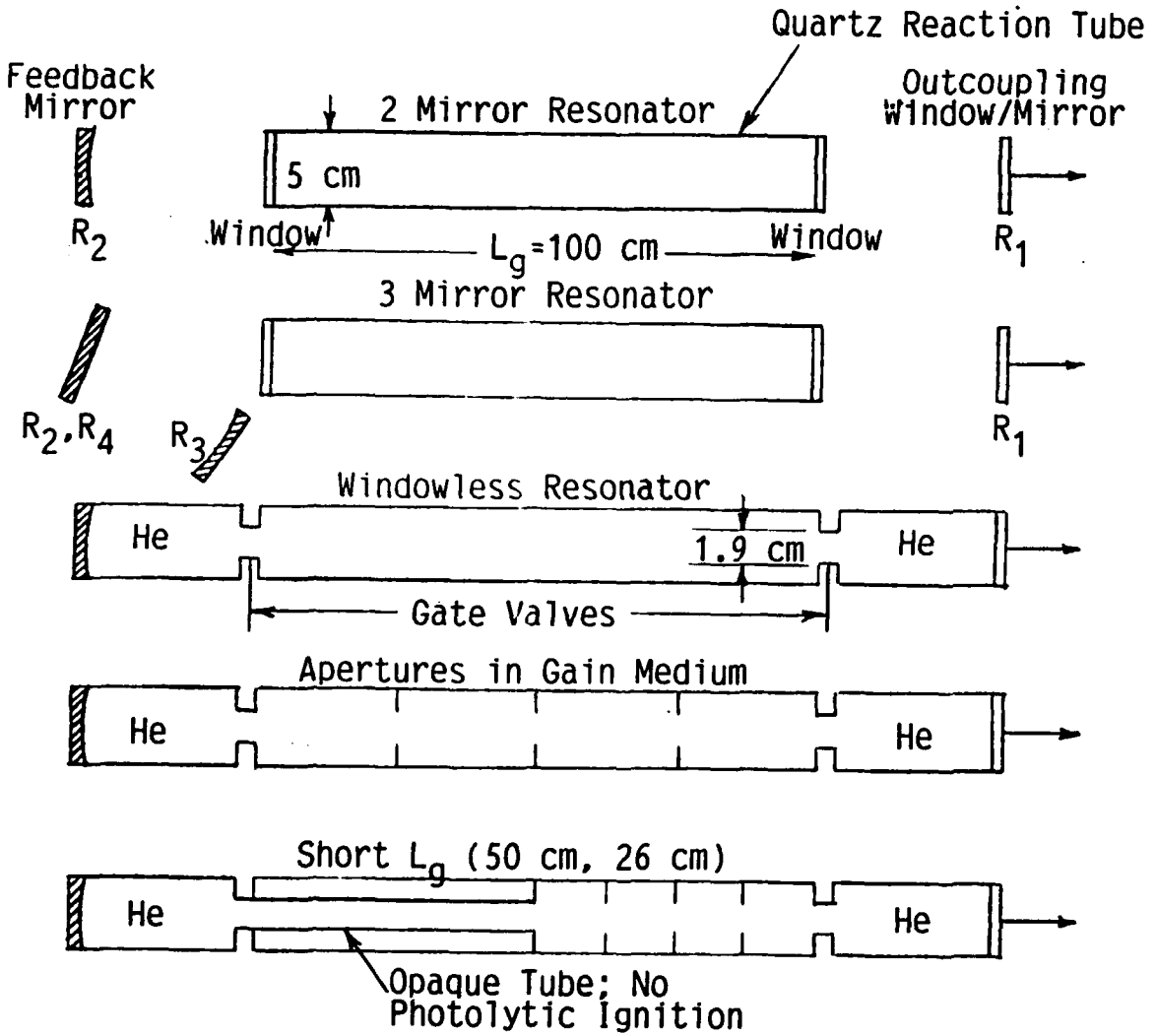

Initial optical configuration. FT lasing not suppressed. No OT lasing.

FT lasing persisted; identified as amplified spont. emission, ASE. No OT lasing.

Cavity window losses removed. FT ASE not eliminated. Weak OT lasing observed.

Reduce probabilities of parasitic Lasing and ASE. FT ASE reduced but not eliminated. No improvement in OT lasing.

FT ASE almost eliminated. No improvement in OT lasing.

Fig. 31

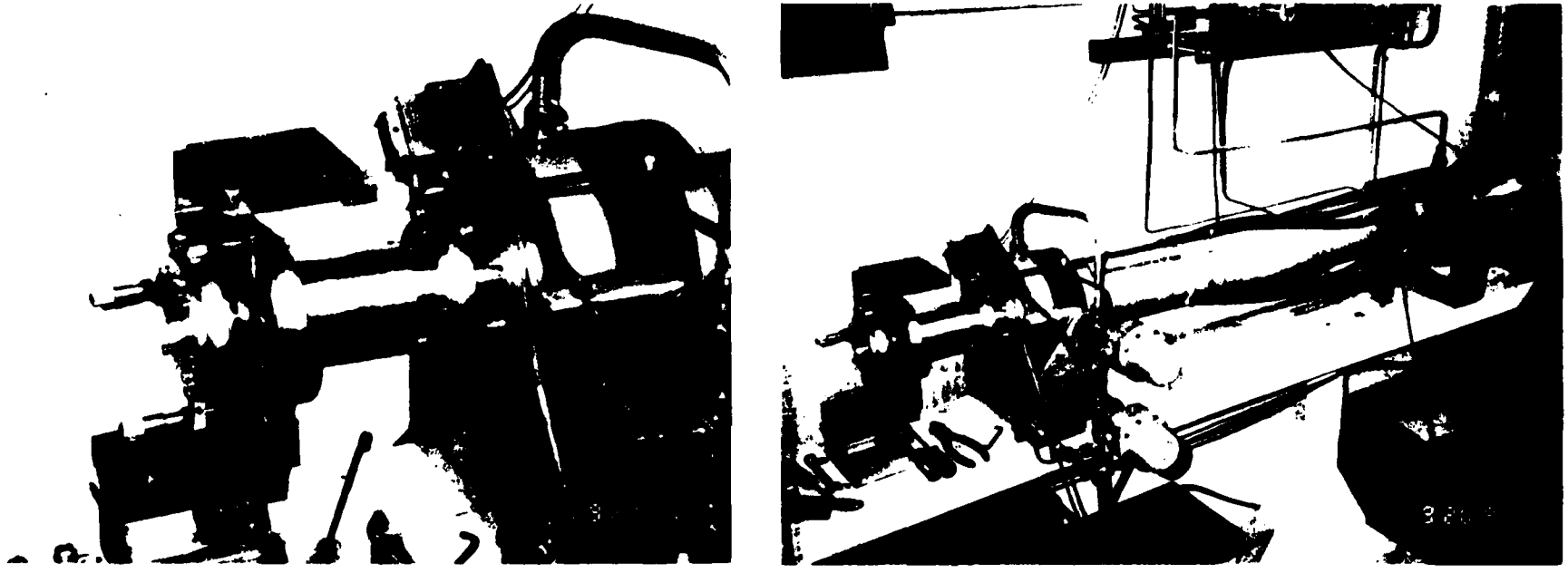

LOW-LOSS CAVITY TEST EQUIPMENT

Vacuum Mirror/Window Mounts Installed on Laser Head

Fig. 32

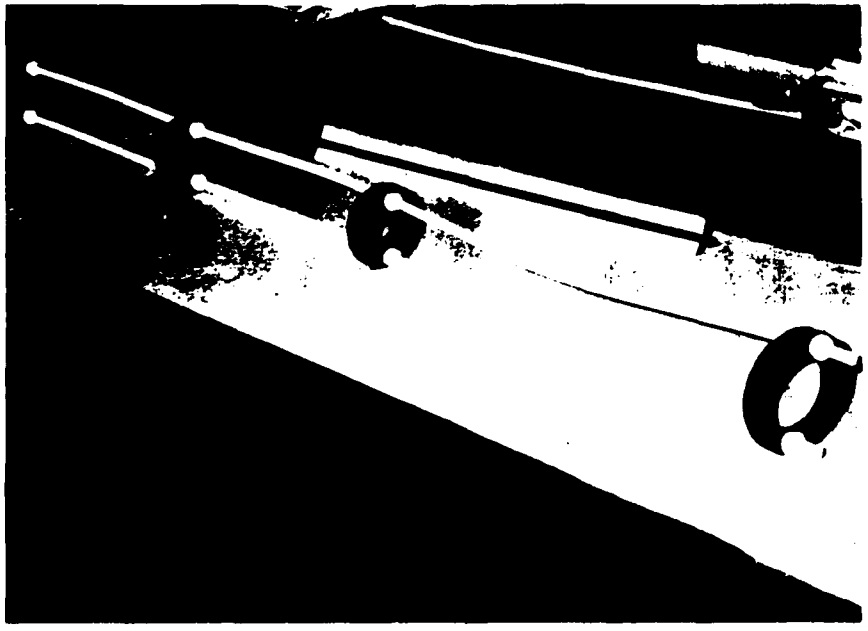

L_g = 100 cm

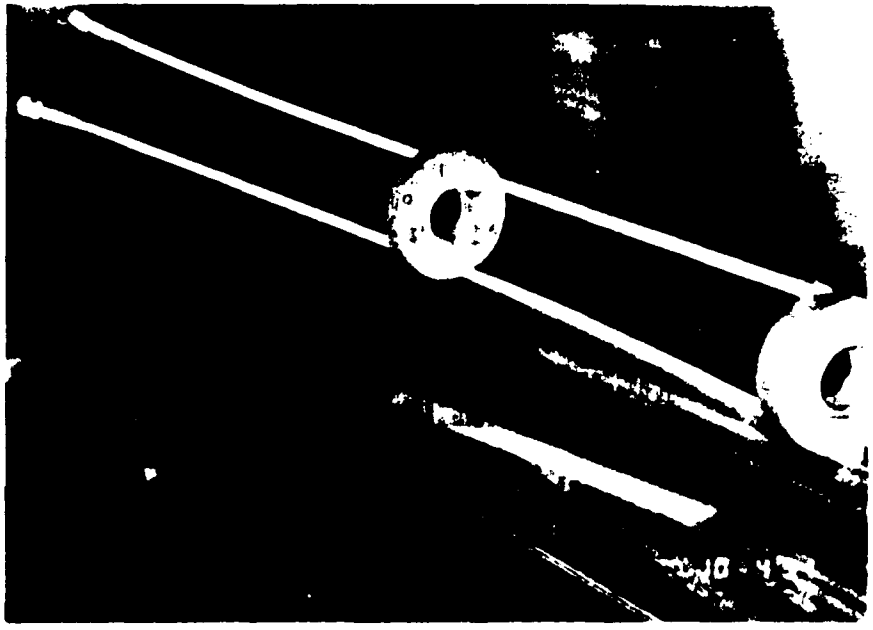

L_g = 50 cm

GAIN REGION APERTURE ASSEMBLIES

5 cm OD; 1.9 cm ID

Fig. 33

HF LASER INITIAL MIX MATRIX

$\Sigma X_i = 200$

Mix No.				
		Nominal H_2		
1.1	39 F_2 + 9 O_2 + 81.8He	+ 17.6H_2	+ 52.6SF_6	
1.2	29.3F_2 + 6.8O_2 + 61.6He	+ 13.2H_2	+ 89.1SF_6	More Dilute
1.3	19.7F_2 + 4.5O_2 + 41.2He	+ 8.9H_2	+ 125.7SF_6	↓
1.4	10.0F_2 + 2.3O_2 + 21.0He	+ 4.5H_2	+ 162.2SF_6	
2.1	39 F_2 + 9 O_2 + 81.8He	+ 17.6H_2	+ 52.6He	
2.2	29.3F_2 + 6.8O_2 + 61.6He	+ 13.2H_2	+ 89.1He	More Dilute
2.3	19.7F_2 + 4.5O_2 + 41.2He	+ 8.9H_2	+ 125.7He	↓
2.4	10.0F_2 + 2.3O_2 + 21.0He	+ 4.5H_2	+ 162.2He	
		+50% H_2 Nom.		
3.1	39 F_2 + 9 O_2 + 81.8He	+ 26.4H_2	+ 43.8SF_6	
3.2	29.3F_2 + 6.8O_2 + 61.6He	+ 19.9H_2	+ 82.5SF_6	More Dilute
3.3	19.7F_2 + 4.5O_2 + 41.2He	+ 13.4H_2	+ 121.2SF_6	↓
3.4	10.0F_2 + 2.3O_2 + 21.0He	+ 6.8H_2	+ 159.8SF_6	
4.1	39 F_2 + 9 O_2 + 81.8He	+ 26.4H_2	+ 43.8He	
4.2	29.3F_2 + 6.8O_2 + 61.6He	+ 19.9H_2	+ 82.5He	More Dilute
4.3	19.7F_2 + 4.5O_2 + 41.2He	+ 13.4H_2	+ 121.2He	↓
4.4	10.0F_2 + 2.3O_2 + 21.0He	+ 6.8H_2	+ 159.8He	
		-33% H_2 Nom.		
5.1	39 F_2 + 9 O_2 + 81.8He	+ 11.7H_2	+ 58.5SF_6	
5.2	29.3F_2 + 6.8O_2 + 61.6He	+ 8.8H_2	+ 93.5SF_6	More Dilute
5.3	19.7F_2 + 4.5O_2 + 41.2He	+ 5.9H_2	+ 128.7SF_6	↓
5.4	10.0F_2 + 2.3O_2 + 21.0He	+ 2.9H_2	+ 163.8SF_6	
6.1	39 F_2 + 9 O_2 + 81.8He	+ 11.7H_2	+ 58.5He	
6.2	29.3F_2 + 6.8O_2 + 61.6He	+ 8.8H_2	+ 93.5He	More Dilute
6.3	19.7F_2 + 4.5O_2 + 41.2He	+ 5.9H_2	+ 128.7He	↓
6.4	10.0F_2 + 2.3O_2 + 21.0He	+ 2.9H_2	+ 163.8He	
	← Gas Supply #1 → Fluorine	← Gas #2 → Hydrogen	← Gas #3 → Diluent	

Fig. 34

Pacific Applied Research

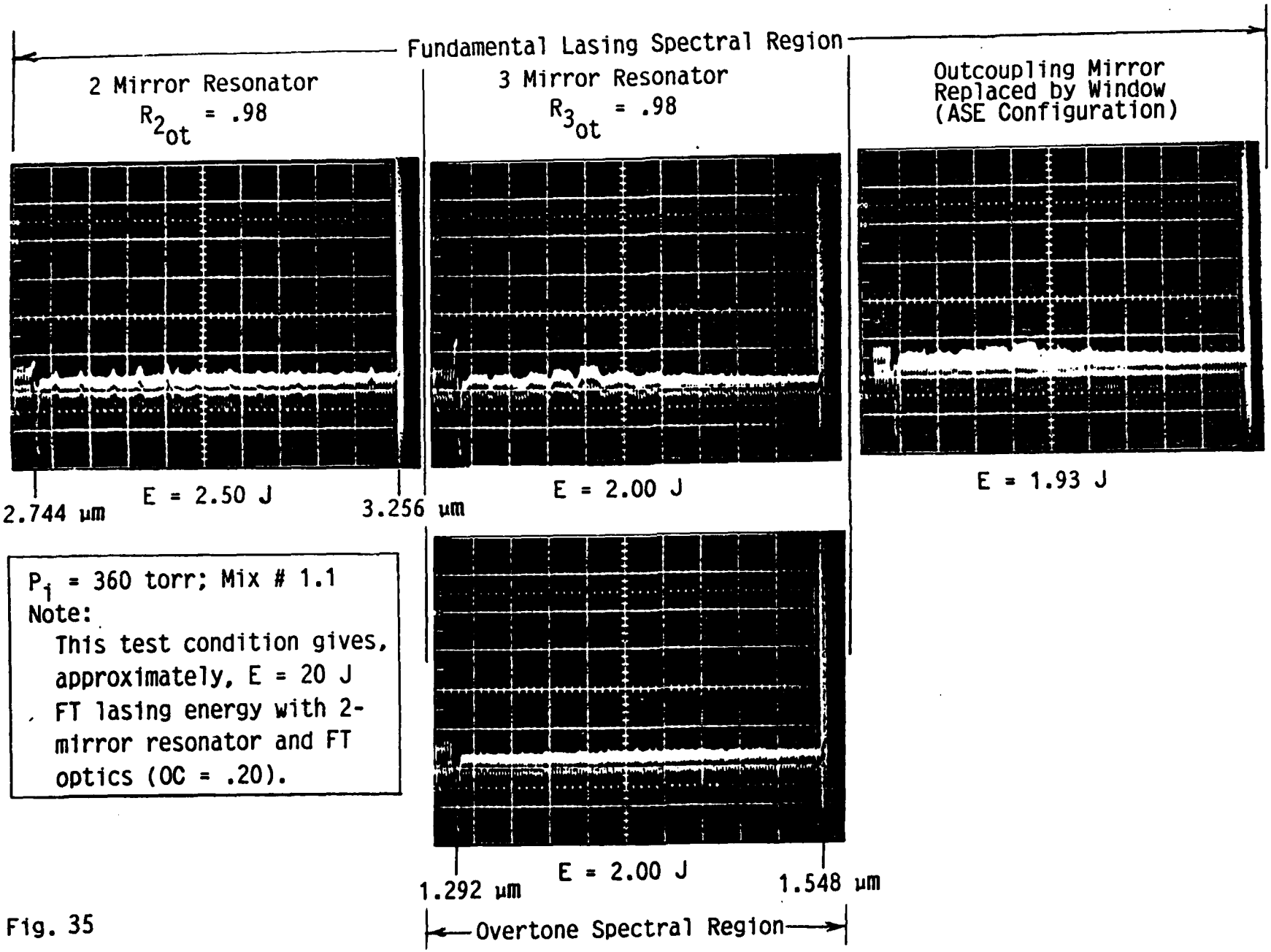

Fig. 35

PERSISTENCE OF FT LASING IN 2-MIRROR AND 3-MIRROR RESONATORS AND IN OPEN CAVITY (ASE) CONFIGURATIONS
All Resonators Have OT Laser Optical Components

Pacific Applied Research

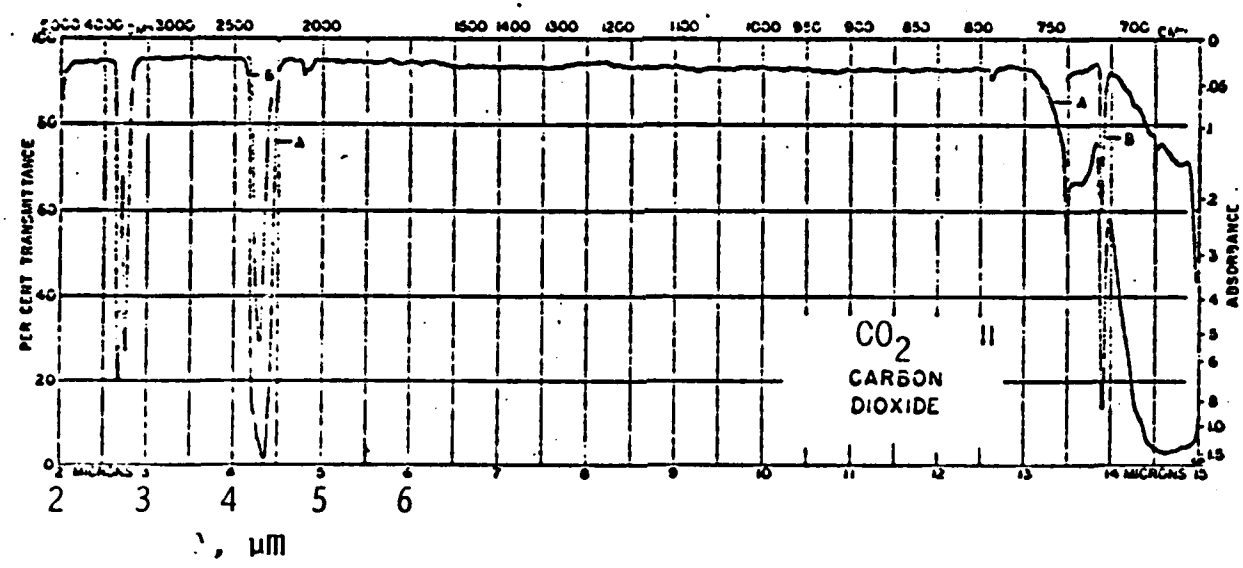

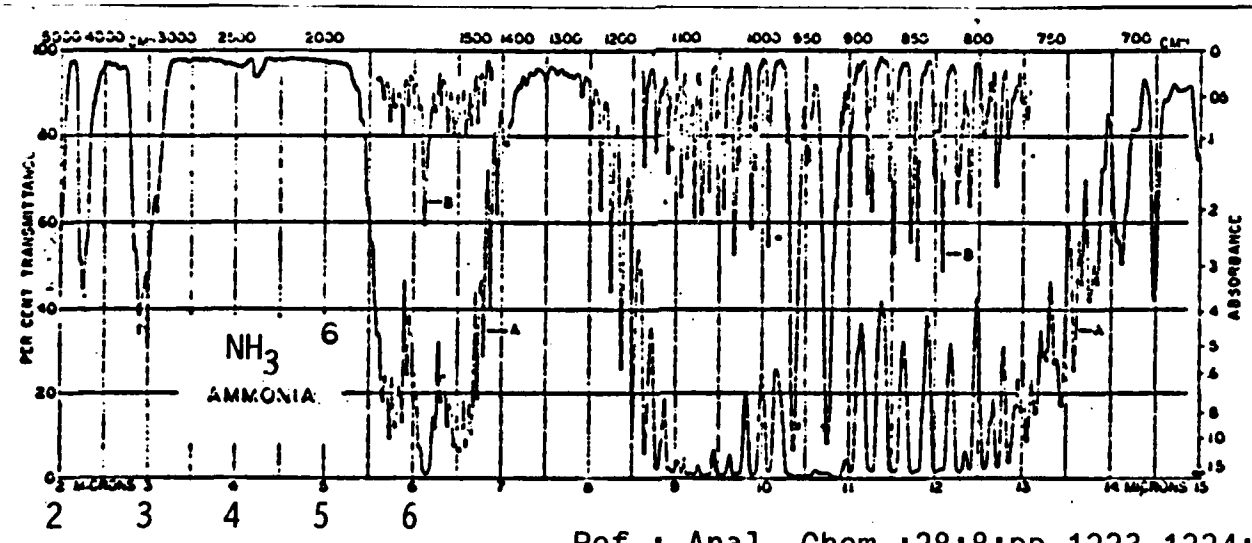

Ref.: Anal. Chem.;28;8;pp 1223,1224; Aug., 56

Fig. 36 CANDIDATE REACTANT MIX GAS ADDITIVES FOR SUPPRESSION OF FT HF LASING

Pacific Applied Research

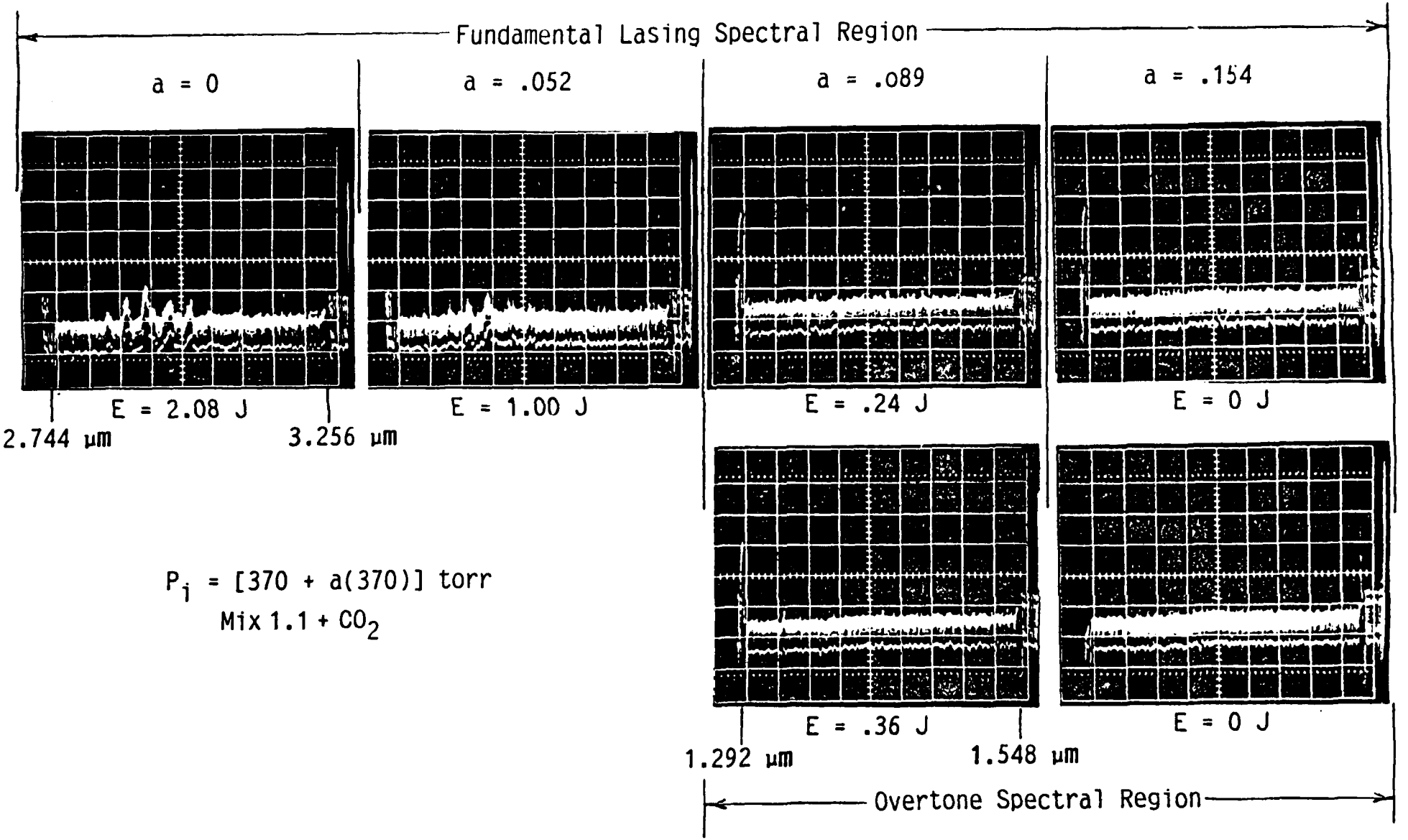

Fig. 37 SUPPRESSION OF FT HF LASING BY ADDING CO_2 TO INITIAL REACTANT MIXTURE
All Tests with 3-Mirror Resonators and Overtone Laser Optical Components; $R_{3_{ot}}$ = .98

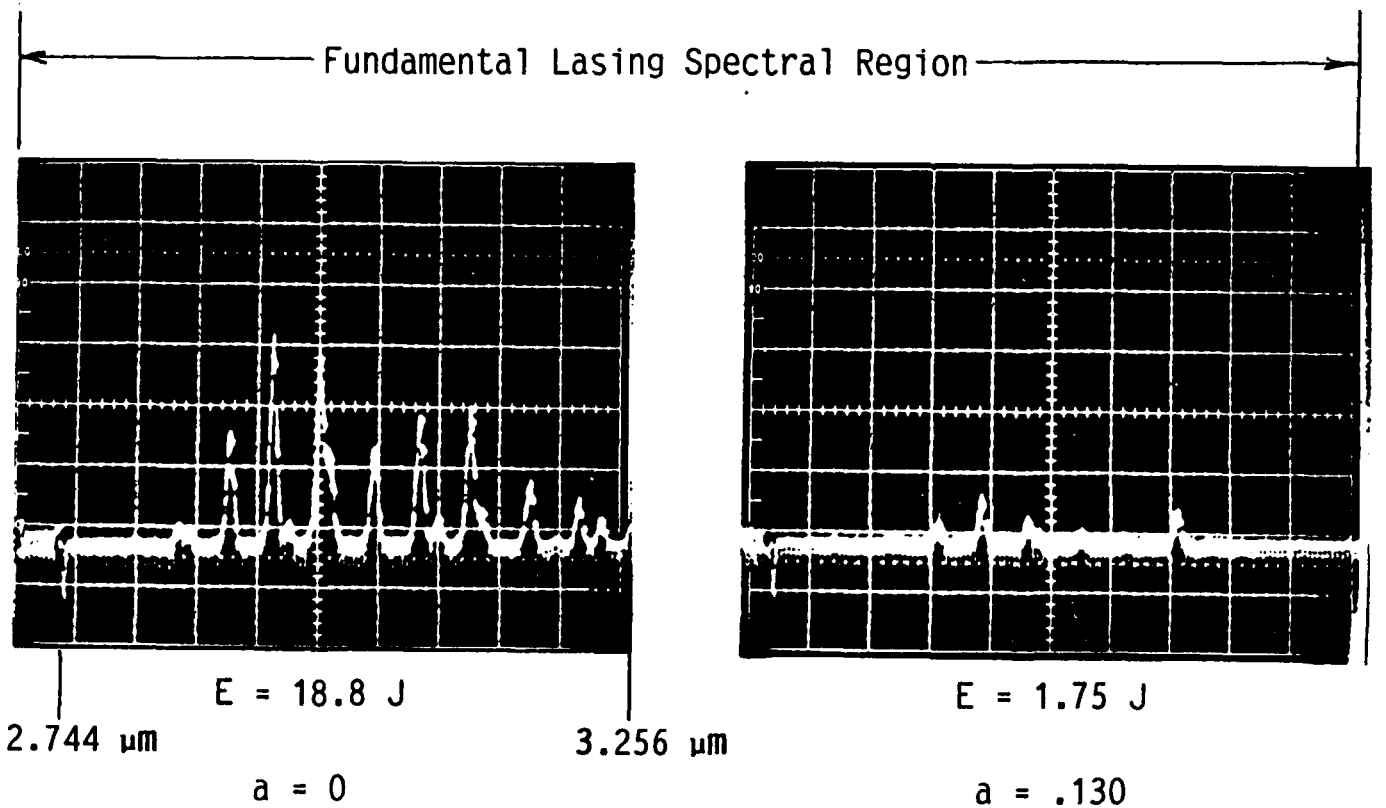

P_i = [366 + a(366)] torr
Mix 1.1 + CO_2

SUPPRESSION OF FT HF LASING BY ADDING CO_2 TO INITIAL REACTANT MIXTURE

All Tests with 2-Mirror Resonators and Fundamental Laser Optical Components; $R_{2_{ft}}$ = .60

Fig. 38

Pacific Applied Research

EVIDENCE OF 1st OVERTONE HF LASING INCLUDING CHAIN REACTION TRANSITIONS

No Internal Resonator Windows; D_g=1.9 cm; L_g=1.0 m; Mix 1.1; C=2.8 μF; V=46 kV; E(FT Opt.)=3.9 J

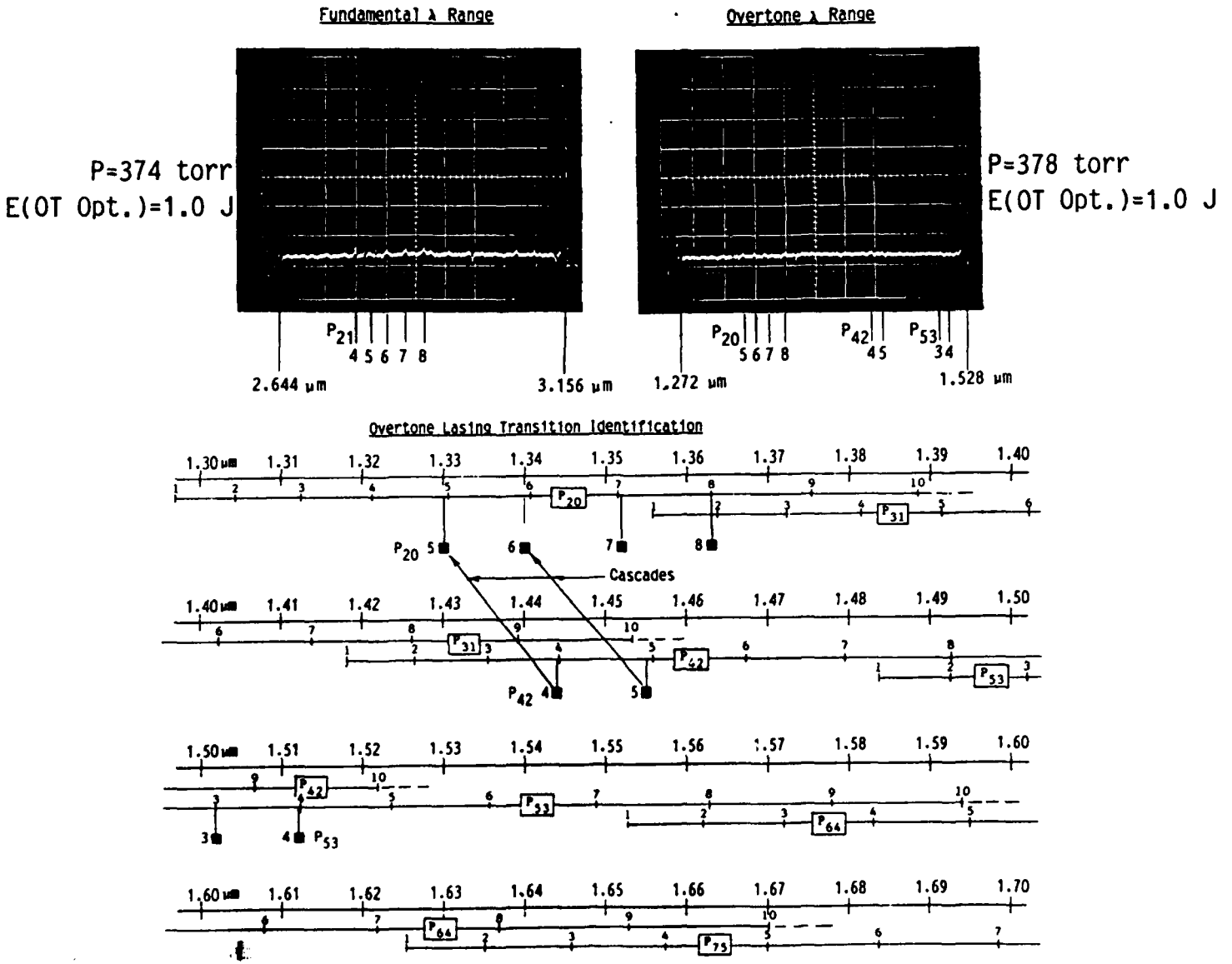

Fig. 39

PACIFIC APPLIED RESEARCH

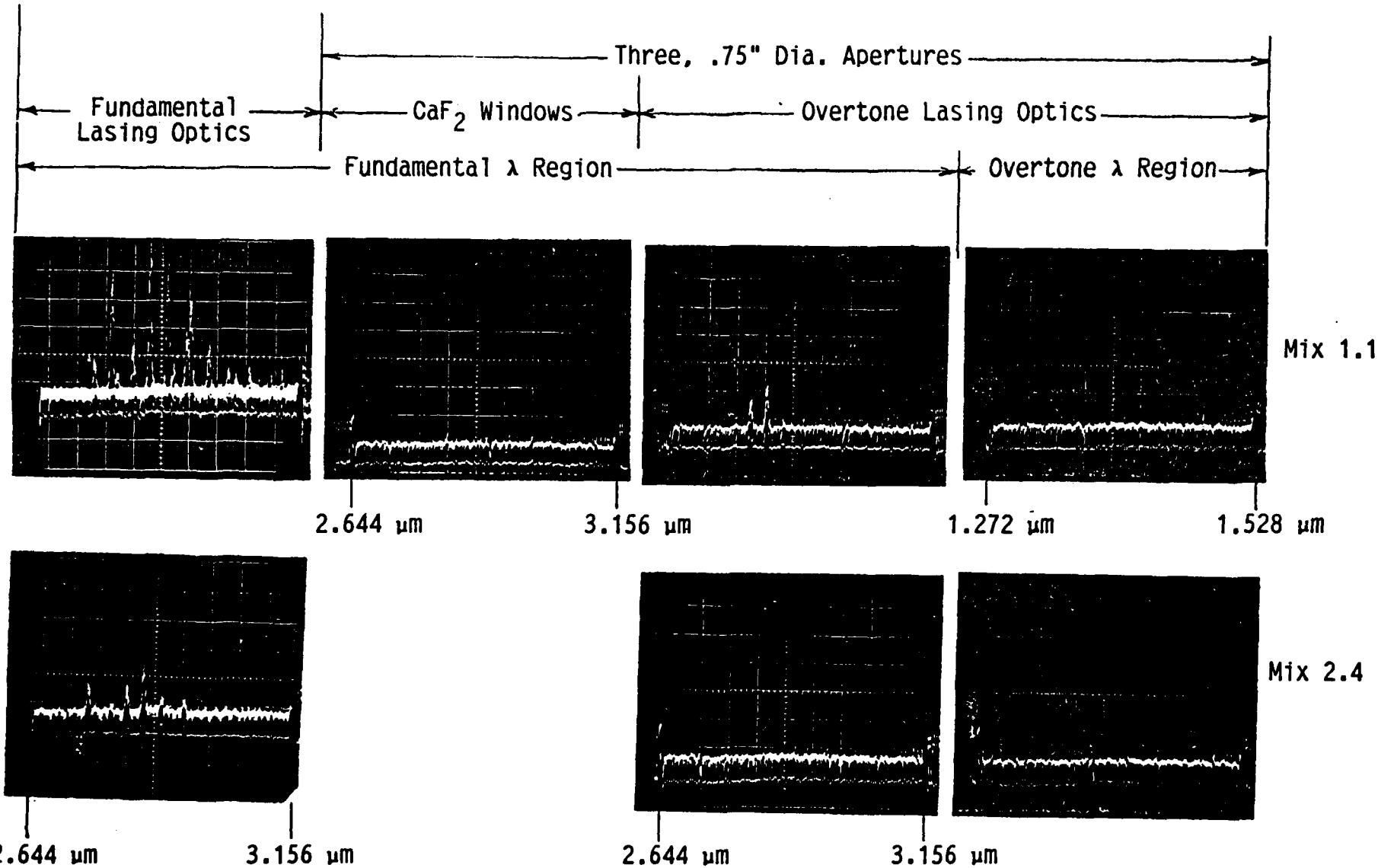

COMPARISON OF FT AND OT LASING PERFORMANCE FOR TWO REACTANT MIXES

L_g = 26 cm; C = 6.0 μF

Fig. 40

Pacific Applied Research

BUILD-UP OF RESONATOR LASING FLUX INTENSITY

ROUND TRIP TIME:
$t_R = 2 \cdot L_c / c \approx 10$ ns
$t_N = 10 \cdot$

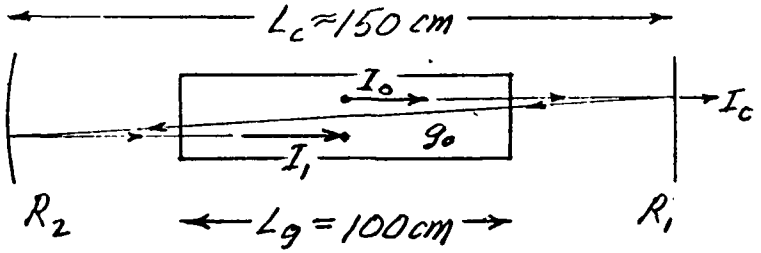

I_o = Initial spont. em. flux in resonator

I_N = Resonator flux for fully developed lasing mechanism

Intensity increase in one round trip $\longrightarrow \quad \frac{I_1}{I_o} = e^{2L_g \cdot g_o (R_1 \cdot R_2)}$

Intensity increase in N round trips $\longrightarrow \quad \frac{I_N}{I_o} = \left(\frac{I_1}{I_o}\right)^N \Longrightarrow \boxed{N = \frac{\ln I_N/I_o}{\ln I_1/I_o}}$

Number of RTs to reach specified intensity increase $\longrightarrow N = \frac{\ln I_N/I_o \; (= \ln 10^4)}{2 \cdot L_g \cdot g_o + \ln(R_1 \cdot R_2)} = \frac{9.210}{200 \cdot g_o + \ln(R_1 \cdot R_2)}$

$N = \frac{6.905}{200 \cdot g_o + \ln(R_1 \cdot R_2)}$ FOR $\frac{I_N}{I_o} = 10^3$

OVERTONE LASING (TYP.)
$g_o = .001\ cm^{-1}$; $R_1 \cdot R_2 = .96$

$\frac{I_N}{I_o} = 10^4 \longrightarrow N = 58$ RTs; $t_N = .58$ μs

$= 10^3 \longrightarrow N = 43$ RTs; $t_N = .43$ μs

FUNDAMENTAL LASING (TYP.)
$g_o = .03\ cm^{-1}$; $R_1 \cdot R_2 = .80$

$\frac{I_N}{I_o} = 10^4 \longrightarrow N = 1.6$ RTs; $t_N = .016$ μs

$= 10^3 \longrightarrow N = 1.1$ RTs; $t_N = .011$ μs

$g_o = .0005\ cm^{-1}$; $R_1 \cdot R_2 = .96$

$\frac{I_N}{I_o} = 10^4 \longrightarrow N = 156$ RTs; $t_N = 1.56$ μs

$10^3 \longrightarrow N = 117$ RTs; $t_N = 1.17$ μs

Fig. 41

Pacific Applied Research

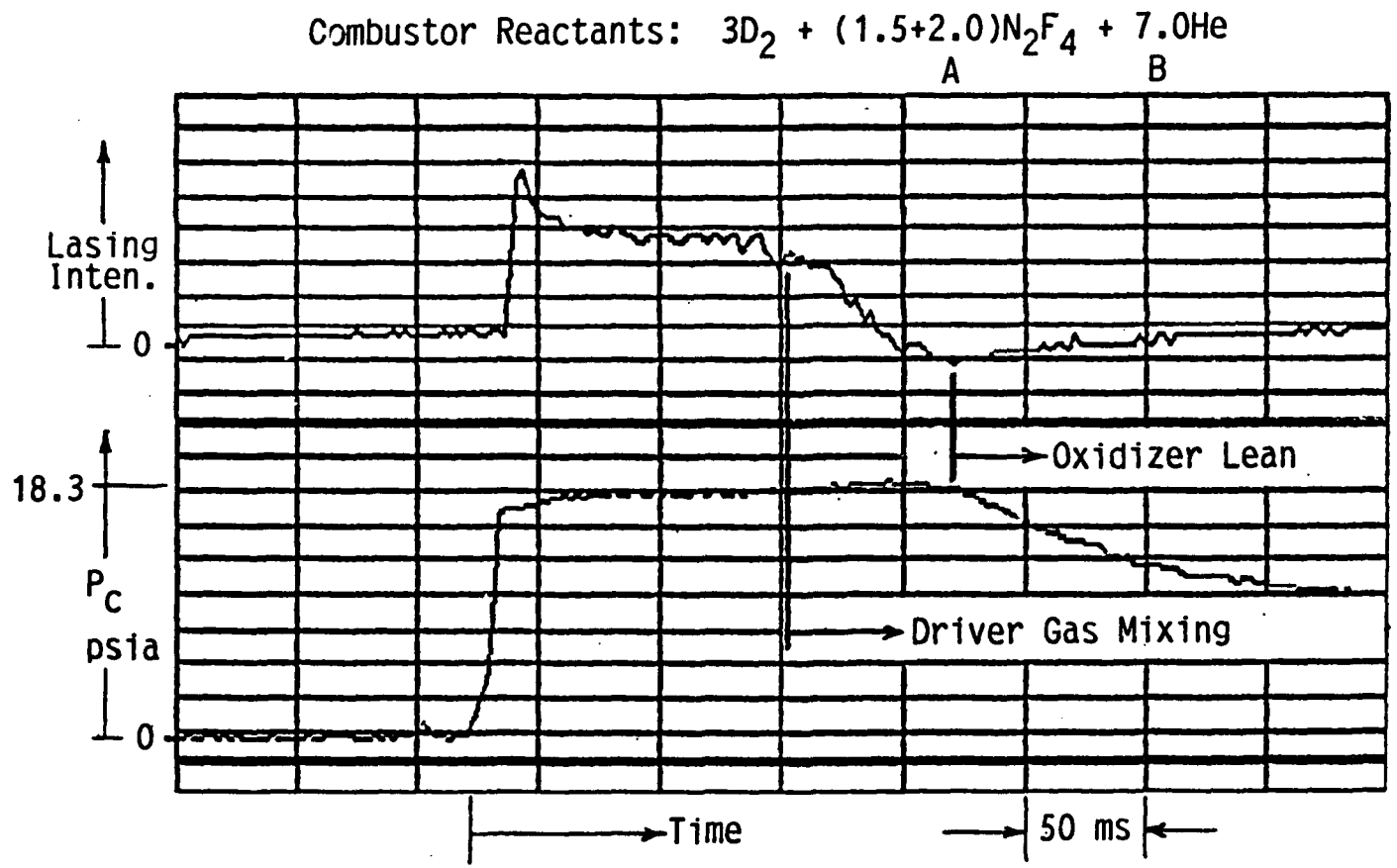

COMBUSTOR PRESSURE AND LASING INTENSITY DURING A BDF TEST OPERATION

Fig. 42

Pacific Applied Research

BYPASS COMBUSTOR / HYLTE -7 NOZZLE TEST CONFIGURATION

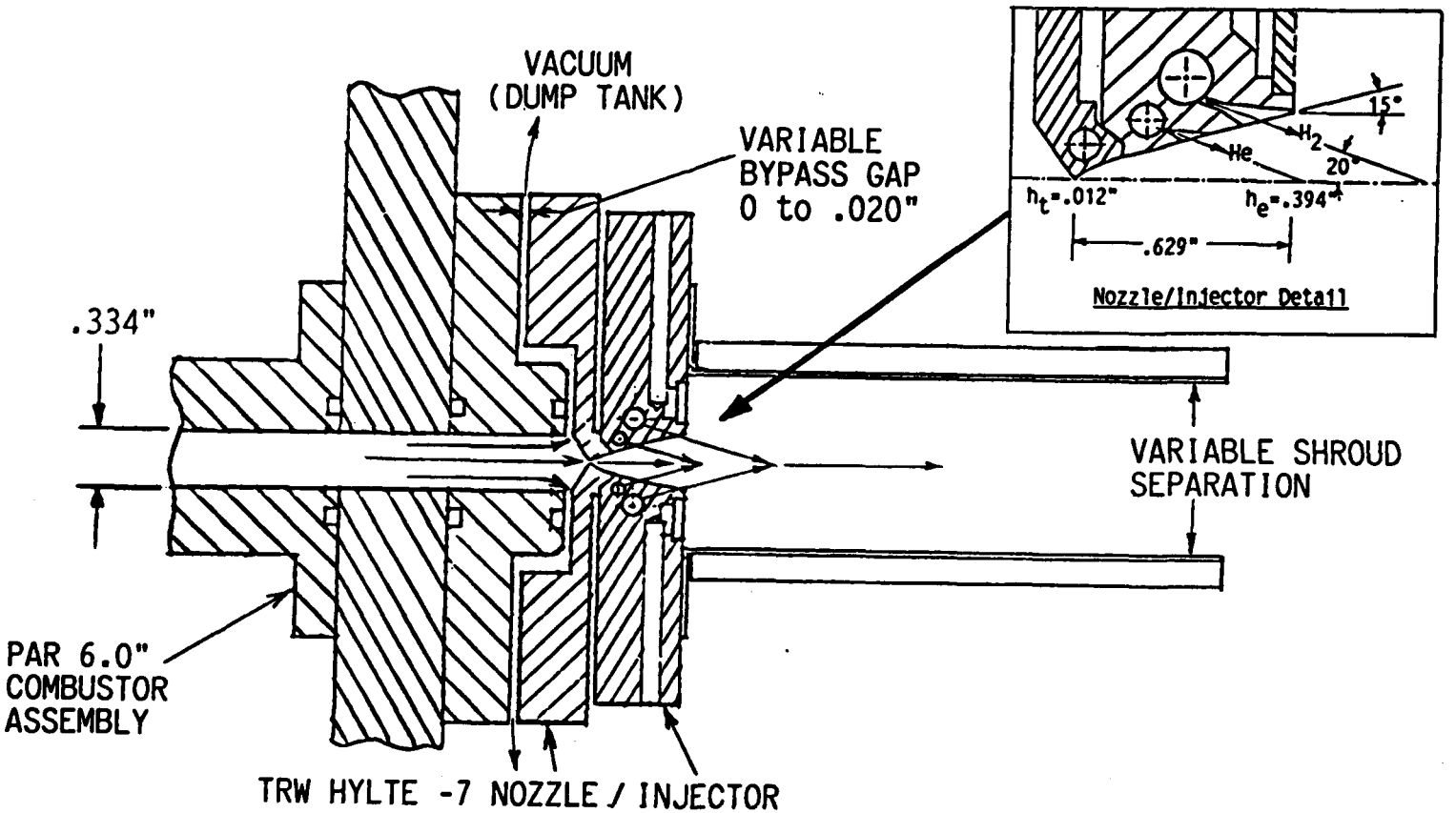

Note - The bypass concept dumps combustion products that have been cooled by the combustor walls and allows products from the relatively less disturbed center flow to exhaust through the nozzle to the lasing reaction zone.

Fig. 43

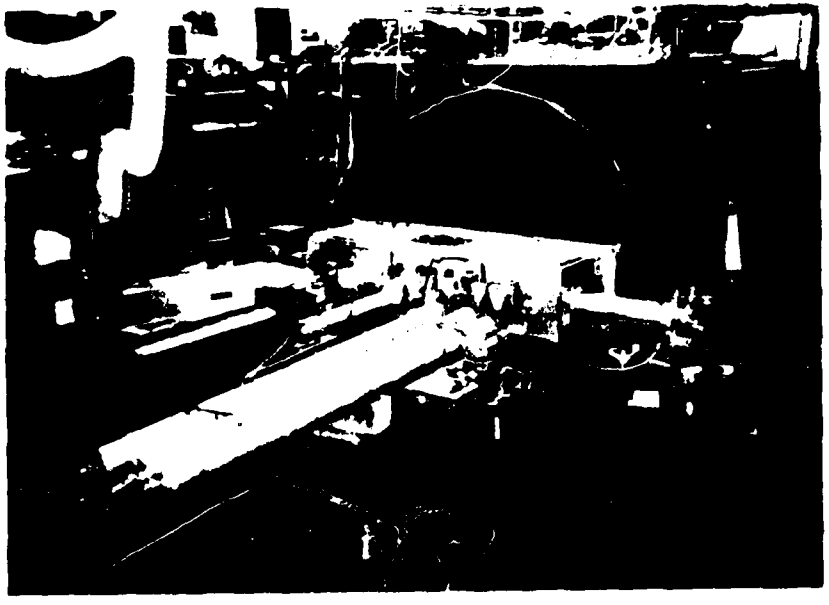

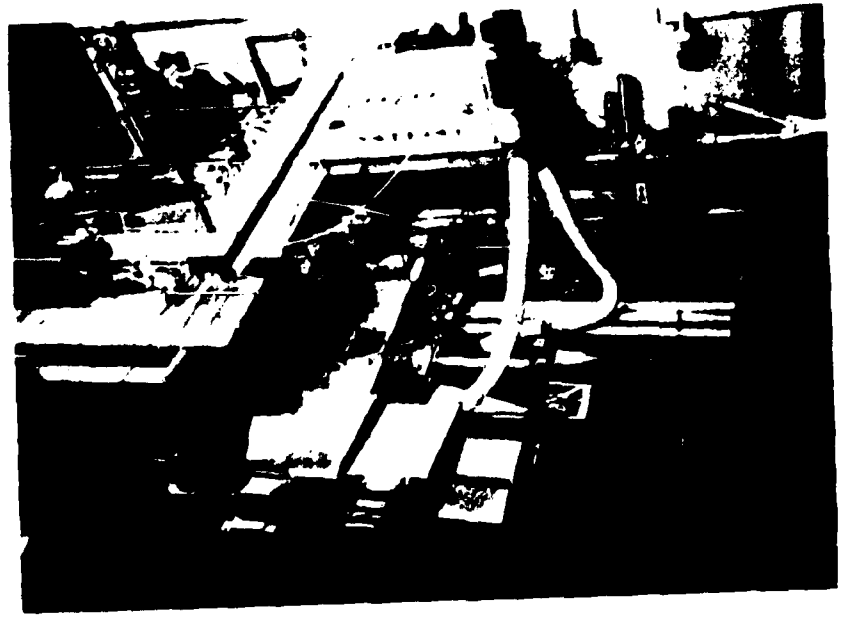

BLOWDOWN TEST FACILITY WITH
TRW HYLTE-07 NOZZLE INSTALLED

Fig. 44

Pacific Applied Research

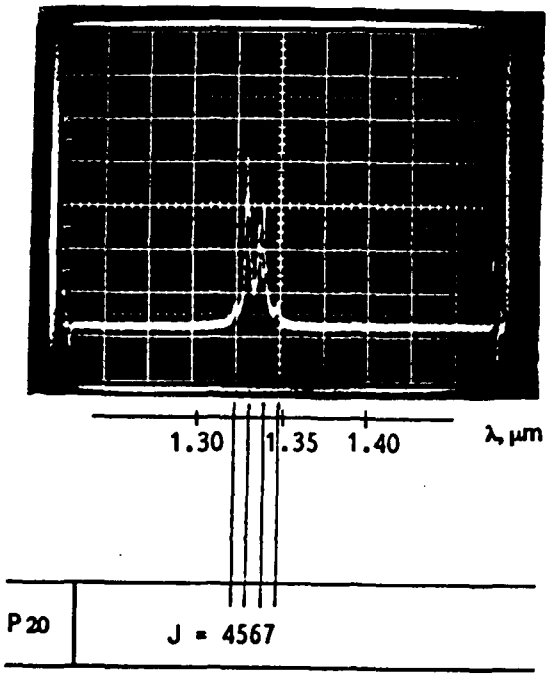

HF (ΔV = 2) OVERTONE LASING SPECTRA / HYLTE - 7 NOZZLE STUDY
TEST 12/4/92, #12
N_2F_4/D_2 BYPASS COMBUSTOR
A = 1.24 ; B = 0.90 ; ψ = 3.88 ; $\dot{m}_t$ = 3.64 g/s

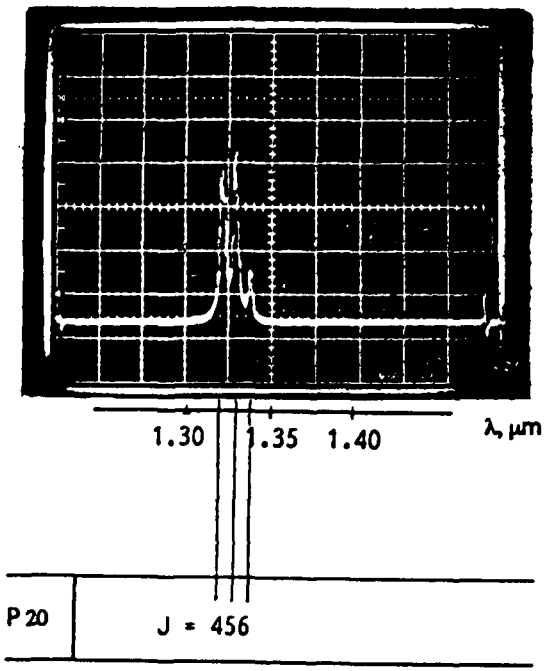

HF (ΔV = 2) OVERTONE LASING SPECTRA / HYLTE - 7 NOZZLE STUDY
TEST 12/3/92, #2
N_2F_4/D_2 BYPASS COMBUSTOR
A = 1.45 ; B = 0.97 ; ψ = 3.42 ; $\dot{m}_t$ = 3.74 g/s

Fig. 45

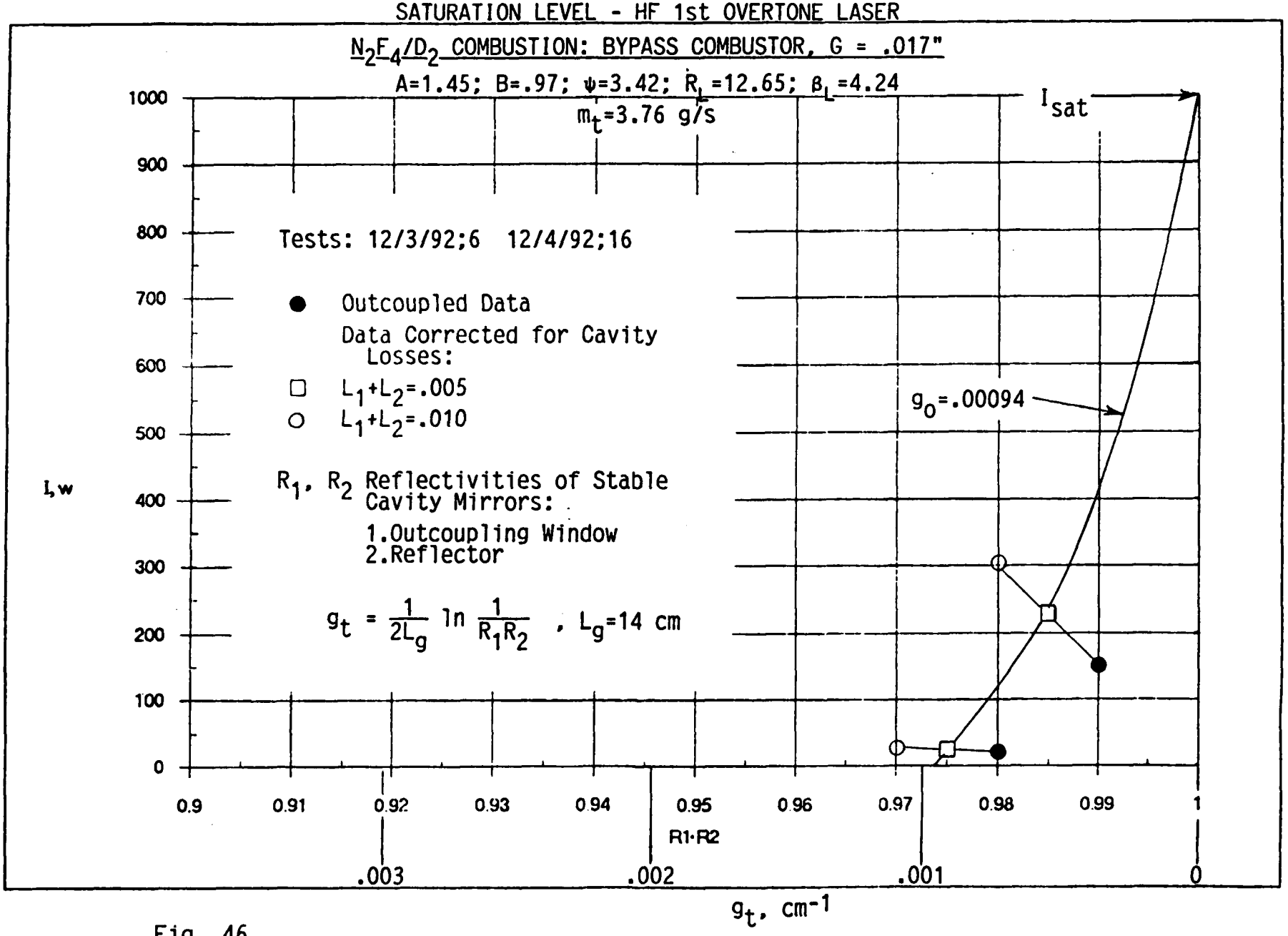
SATURATION LEVEL - HF 1st OVERTONE LASER
N_2F_4/D_2 COMBUSTION: BYPASS COMBUSTOR, G = .017"
A=1.45; B=.97; ψ=3.42; R_L=12.65; β_L=4.24
m_t=3.76 g/s
I_{sat}
Tests: 12/3/92;6 12/4/92;16
Outcoupled Data
Data Corrected for Cavity Losses:
L_1+L_2=.005
L_1+L_2=.010
R_1, R_2 Reflectivities of Stable Cavity Mirrors:
1.Outcoupling Window
2.Reflector
$g_t = \frac{1}{2L_g} \ln \frac{1}{R_1R_2}$, L_g=14 cm
g_0=.00094
I,w
1000
900
800
700
600
500
400
300
200
100
0
0.9
0.91
0.92
0.93
0.94
0.95
0.96
0.97
0.98
0.99
1
R1·R2
.003
.002
.001
0
g_t, cm^{-1}

Fig. 46

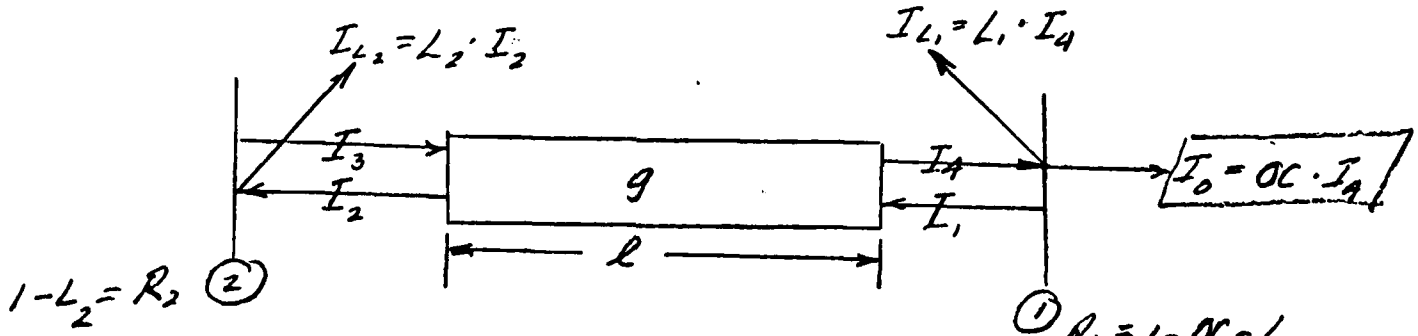

TOTAL LASING INT. $= I_C = I_o + I_{L_1} + I_{L_2}$

$= \alpha c \cdot I_4 + L_1 I_4 + L_2 \cdot I_2$

$= I_4 \left[\alpha c + L_1 + L_2 \frac{I_2}{I_4} \right]$

$$\boxed{\frac{I_C}{I_o} = \frac{\left[\alpha c + L_1 + L_2 \cdot (R_1/R_2)^{1/2} \right]}{\alpha c}}$$

$\frac{I_2}{I_1} = e^{g\ell}$; $\frac{I_4}{I_3} = e^{g\ell}$

$\therefore \frac{I_2}{I_4} = \frac{I_1}{I_3}$

$I_1 = R_1 \cdot I_4$; $I_3 = R_2 \cdot I_2$

$\therefore \frac{I_2}{I_4} = \frac{R_1 \cdot I_4}{R_2 \cdot I_2}$

OR $\boxed{\frac{I_2}{I_4} = \left(\frac{R_1}{R_2} \right)^{1/2}}$

DETERMINATION OF CORRECTED OUTPUT POWER, I_C, FROM MEASUREMENTS OF OUTCOUPLED POWER, I_o, AND WINDOW/MIRROR PROPERTIES

Fig. 47

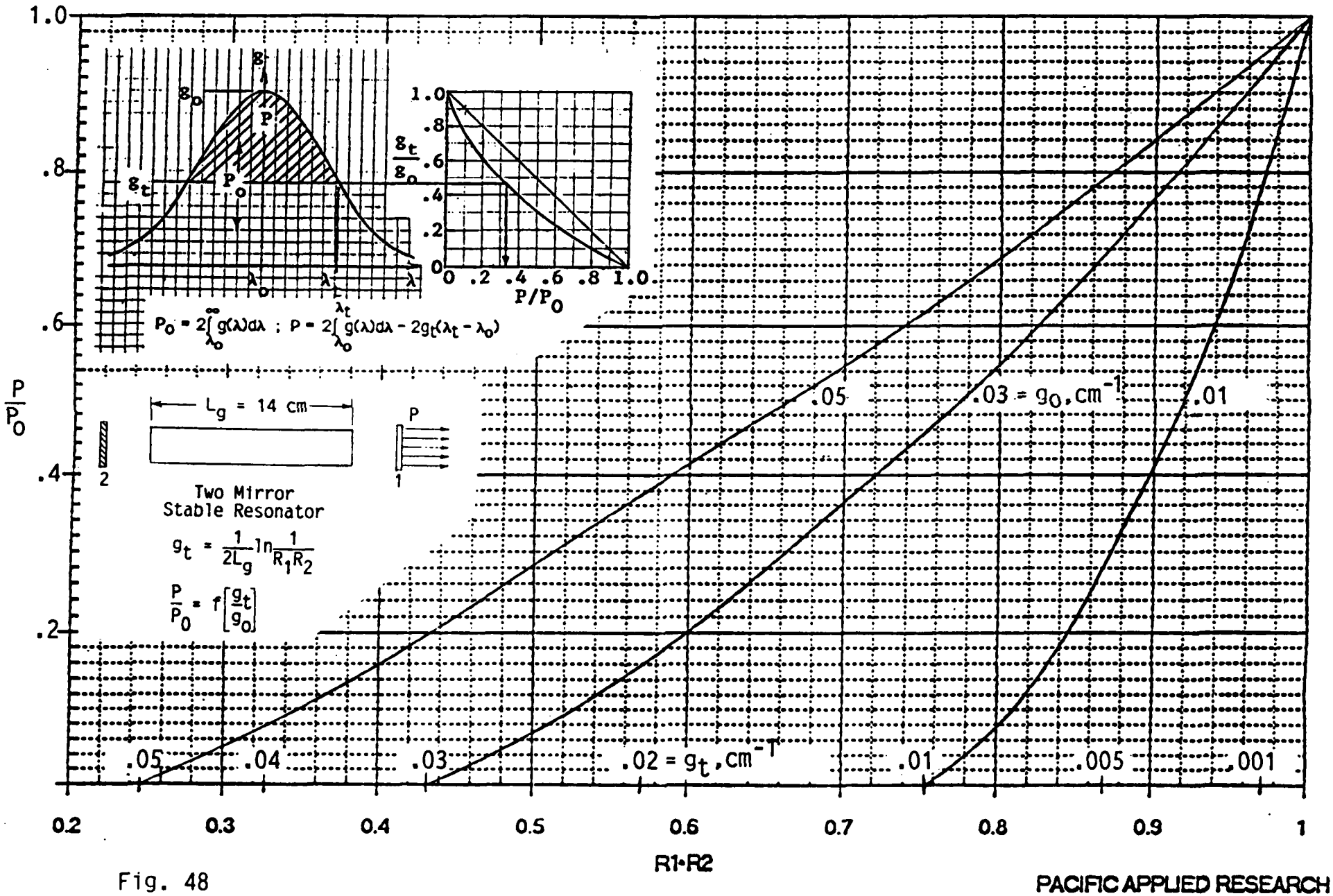

Fig. 48

PACIFIC APPLIED RESEARCH